In vitro Analysis of the Cytosolic Copper Metallochaperones in *Saccharomyces cerevisiae*

Kerrie Brusby

A Thesis Submitted for the Degree of Doctor of Philosophy

December 2016

Institute for Cell and Molecular Biosciences

Newcastle University

Declaration

I certify that this thesis contains my own work, except where acknowledged, and that no part of this work has been submitted in support of an application for other qualifications at this or any other institution.

Acknowledgements

I would like to thank Prof. Christopher Dennison for his supervision and support during my PhD, and for providing me with the opportunity to perform this research.

Many thanks also go to the BBSRC for funding this work with a BBSRC DTG Studentship.

I would also like to thank all of the lab members, past and present, who have worked alongside me for their encouragement and support. In particular, Stephen Allen, who kindly advised me during my initial research stage, and provided the Ccs1 mutant proteins used during my research.

I would also like to thank Dr. Helen Waller for her advice and assistance with performing Far-UV CD, and Dr. Joe Gray at Pinnacle for the analysis of proteins by mass spectrometry.

I would also like to thank the many friends I have made during my PhD, many of which have undertaken a similar journey.

Lastly, I would like to thank my family for their words of encouragement and belief in me.

Abstract

In yeast, Cu,Zn-superoxide dismutase (Sod1) is activated by the copper metallochaperone Ccs1, mainly in the cytosol. This involves the delivery of Cu^{1+} and the formation of a structurally important disulfide bond. Ccs1 consists of three domains, with domain 1 (D1) and domain 3 (D3) containing copper-binding CXXC and CXC motifs respectively. In human CCS1, D1 is the site of copper transfer and D3 is responsible for disulfide bond formation in SOD1. In yeast cells, D3 of Ccs1 is essential for Sod1 activation, whereas D1 is required only under copper-limiting conditions. The Cu^{1+}-binding ability of Ccs1 has been investigated using mutants in which the Cys residues in either the D1 (C17S/C20S-Ccs1) or D3 (C229S/C231S-Ccs1) copper-binding motif have been mutated to Ser residues, as well as a mutant lacking D3 (D1/2-Ccs1). Both D1 and D3 of Ccs1 are able to bind a single equivalent of Cu^{1+}, and dimerisation occurs upon Cu^{1+}-binding both via a copper mediated process as well as by disulfide bond formation. The Cu^{1+} affinity of D1 is $(2.6 \pm 0.5) \times 10^{18}$ M^{-1} at pH 7.5, while that of D3 is six times weaker. D1 of human CCS1 has a Cu^{1+} affinity which is over an order of magnitude greater than that of D3. Aerobic incubation of reduced E,Zn-Sod1 with all Cu^{1+}-loaded Ccs1 proteins produces catalytically active Cu,Zn-Sod1 containing the catalytically active disulfide bond. Activation with C17S/C20S-Ccs1 is slightly lower than with the wild type protein, however removal of the copper-binding site in D3 (C229S/C231S-Ccs1 and D1/2-Ccs1) has a much more marked effect. A second cytosolic metallochaperone, Atx1, delivers Cu^{1+} to the copper-transporting P-type ATPase Ccc2 for incorporation into the membrane protein Fet3p. The Cu^{1+} affinity of Atx1 is greater than those of the copper-binding motifs of Ccs1. Exchange of Cu^{1+} between D1 and D3 of Ccs1 and Atx1 occurs as expected on the basis of their Cu^{1+} affinities. Ccs1 and Atx1 may collect Cu^{1+} from the same source, and cross-talk between them and their copper-trafficking pathways could occur.

Units and Abbreviations

Measurements and Techniques:

M	mol dm^{-3}	Da	Daltons
L	litre	ε	Extinction coefficient (M^{-1} cm^{-1})
g	gram	nm	nanometre
µ	micro		
m	milli		
^{o}C	degrees celsius		
ppm	parts per million		

MALDI	matrix assisted laser desorption/ionization
MS	mass spectrometry
CD	circular dichroism
PCR	polymerase chain reaction
AAS	atomic force microscopy
SDS-PAGE	sodium dodecyl sulphate-polyacrylamide gel electrophoresis
ESI	electrospray ionization

Selected Chemicals:

DTT	dithiothreitol
BCA	bicinchoninic acid
BCS	bathocuproine disulfonic acid
DTNB	5,5'-dithiobis-(2-nitrobenzoic acid) (Ellman's reagent)
EDTA	ethylenediaminetetraacetic acid
Tris	tris(hydroxymethyl)aminoethane
Hepes	4-(2-Hydroxyethyl)piperazine-1-ethanesulfonic acid
Mes	2-(N-morpholino)ethanesulphonic acid

Selected Proteins:

Ccs1	Copper metallochaperone for Cu,Zn-superoxide dismutase
WT-Ccs1	Wild-type Ccs1 from *S. cerevisiae*
C17S/C20S-Ccs1	Cys-to-Ser Ccs1 mutant
C229S/C231S-Ccs1	Cys-to-Ser Ccs1 mutant
D1/2-Ccs1	Ccs1 amino acid residues 1 - 249
D2/3-Ccs1	Ccs1 amino acid residues 72 - 249
CCS	Ccs1 from *H. sapiens*
Atx1	Copper metallochaperone from *S. cerevisiae*
HAH1	Atx1 copper metallochaperone from *H. sapiens*
Sod1	Cu,Zn-superoxide dismutase from *S. cerevisiae*
SOD1	Sod1 from *H. sapiens*

Amino acids:

Alanine	Ala	A	Methionine	Met	M
Cysteine	Cys	C	Asparagine	Asn	N
Aspartic acid	Asp	D	Proline	Pro	P
Glutamic acid	Glu	E	Glutamine	Gln	Q
Phenylalanine	Phe	F	Arginine	Arg	R
Glycine	Gly	G	Serine	Ser	S
Histidine	His	H	Threonine	Thr	T
Isoleucine	Ile	I	Valine	Val	V
Lysine	Lys	K	Tyrptophan	Trp	W
Leucine	Leu	L	Tyrosine	Tyr	Y

Contents

Chapter 1: Introduction

1.1 The Chemistry of Copper

Copper is a member of the first row *d*-block metals with the electronic configuration [Ar] $3d^{10}\,4s^{1}$ and shares many of the characteristics particular to this group of elements. Copper metal is a good conductor of electricity and many copper compounds are coloured due to electronic transitions. Additionally, copper exhibits the prototypical transition metal ability to form compounds in many oxidation states due to a loss of d-electrons.

1.1.1 Oxidation States

Copper is the only first-row *d*-block metal to exhibit a stable +1 oxidation state, however in aqueous solution Cu^{1+} is disproportionated (simultaneously oxidised and reduced) to the solid metal and Cu^{2+} *(Reaction 1.3)*.

$Cu^{1+} \rightarrow Cu^{2+} + e^{-}$ E^{o} = - 0.153 V *Reaction 1.1*

$Cu^{1+} + e^{-} \rightarrow Cu_{(s)}$ E^{o} = + 0.521 V *Reaction 1.2*

$2Cu^{1+} \rightarrow Cu_{(s)} + Cu^{2+}$ E^{o}_{rcn} = + 0.368 V *Reaction 1.3*

The disproportionation of Cu^{1+} can be explained by the standard reduction potentials (E^{o}) of the half reactions that constitute the net *Reaction 1.3*. *Reaction 1.1* shows the oxidation of Cu^{1+} and *Reaction 1.2* shows the reduction of Cu^{1+}. The combination of the E^{o} for the two half reaction provides a positive E^{o}_{rcn} for the net reaction. The Nernst equation relates the E^{o} to the free Gibbs energy in an inverse relationship, therefore the Gibbs energy is negative *(Equation 1.1)*, indicating a spontaneous disproportionation.

$$\Delta G = -nFE \qquad \textit{Equation 1.1}$$

ΔG = Gibbs free energy
n = the number of electrons transferred in the half-reaction
F = Faraday constant
E = potential difference

Also, the completely filled 3d subshell of Cu^{1+} ([Ar] $3d^{10}$) would be expected to be energetically favoured over the incomplete subshell of Cu^{2+} ([Ar] $3d^{9}$), yet Cu^{1+} is larger and has a lower charge density than Cu^{2+} resulting in a much lower enthalpy of hydration for Cu^{1+}. Nevertheless, it is possible to stabilise Cu^{1+} ions in solution with appropriate ligands such as the cyanide ion (CN^-) as in *Method 2.17*.

Compared to the other first row *d*-block metals, the divalent copper ion has a high reduction potential of +0.157 E^O (V) for Cu^{2+}/Cu^{1+}, indicating that the release of an electron occurs less readily than hydrogen and Cu^{2+} is easily reduced to Cu^{1+}. This characteristic is exploited by biological systems through the interconversion of Cu^{2+} and Cu^{1+}, allowing enzymes to utilize copper as a cofactor for electron transfer catalysis by cycling between the two oxidation states.

A variety of Cu^{2+} compounds are coloured due to the incompletely filled 3*d* sub-shell which allows the promotion of an electron to a higher orbital upon interaction with a ligand. It is therefore consistent that Cu^{1+} cannot absorb energy for *d-d* transitions as there are no empty/partially-empty orbitals available to accept a promoted electron. This renders Cu^{1+} compounds colourless, except for when the counter ion is coloured or when charge transfer absorptions occur in the visible region.

1.1.2 Ligand Preference

The oxidation states of copper are also expected to have a preference for different ligands due to their allocation within the hard-soft acid base principle. Cu^{1+} is described as being a 'soft' Lewis acid on account of the low positive charge, electron pairs in the valence shell and a larger ionic radius than the divalent ion. It is therefore expected for Cu^{1+} to prefer 'soft' bases such as sulphur-containing amino acids as ligands such as cysteine and methionine, and the bonding of these complexes is considered to be highly covalent in character. Contrary to this, Cu^{2+} is described as being a 'hard' or borderline Lewis acid due to the higher positive charge and increased ionic radius. This ion is predicted to prefer 'hard' bases as ligands such as those containing nitrogen or oxygen donor atoms, including the amino acid histidine and those containing carboxylates, such as aspartate and glutamate acid. Consequently, the bonding of Cu^{2+} complexes is anticipated to be dominated by charge interactions and possess more ionic characteristics.

1.1.3 Coordination Geometry

Coordination geometries formed by Cu^{1+} are typical of ions with d^{10} configurations such as octahedral and tetrahedral. Octahedral complexes of d^9 ions, such as Cu^{2+}, results in a degenerate electronic state and the system undergoes Jahn-Teller distortions whereby the axial bonds are elongated. This has the effect of removing the degeneracy and lowering the overall energy, consequently Cu^{2+} complexes prefer distorted octahedral and square planar geometries.

1.1.4 Protein Modulation of Metal Ion

Isolated metal ions have particular properties, however incorporation into a metallo-protein often induces a modulation of these properties to increase the efficiency of a particular reaction. This can involve solvation patterns or the creation of specific electrostatic fields to enhance reactivity of the active site. Also, distinct coordination geometries enforced by the ligand sphere as described by the entatic state[1] and the induced rack hypotheses[2] have been suggested to explain the wide-ranging geometric and electronic characteristics of metal ions that are apparently adapted for function.

1.2 Cellular Toxicity of Copper

Copper is an essential micronutrient required for plant and animal health, however it is also associated with toxic effects. This toxicity has provided beneficial applications of copper, such as the creation of Bordeaux mixture to protect grapes from fungal infection,[3] to disinfect hospital drinking-water against *Legionella*,[4] and in 2008 became the first solid surface registered by the Environmental Protection Agency as an antimicrobial. Also, copper has also been linked to host defence mechanisms such as the antimicrobial function of macrophages within the immune system[5-10] and counteractive copper resistance mechanisms of pathogens.[5, 11] One explanation of copper toxicity arises from the ability of the ion to cycle between a +1 and +2 oxidation state, catalysing the formation of the highly reactive hydroxyl radical via Haber-Weiss *(Reaction 1.4)*[12] and Fenton-type reactions *(Reaction 1.5)*.[13]

$$O_2^- + H_2O_2 \rightarrow O_2 + {}^-OH + {}^{\cdot}OH \qquad \textit{Reaction 1.4}$$

$$Cu^+ + H_2O_2 \rightarrow Cu^{2+} + {}^-OH + {}^{\cdot}OH \qquad \textit{Reaction 1.5}$$

These radicals disrupt and damage cellular machinery through the oxidation of proteins, DNA and lipids, thereby inhibiting or altering normal cell function. Toxicity is also attributed to copper's ability to compete with other metal ions such as zinc, manganese and iron for protein binding sites. This is explained by the position of Cu^{2+} in the Irving-Williams series which describes copper as forming complexes with a higher relative stability than other divalent ions of the first-row *d*-block metals.[14] One example of damaging metal competition is inactivation of the dehydratase enzymes in *Escherichia coli* by copper due to disruption of the formation of iron-sulphur clusters via coordination of copper to the sulphur atoms and the displacement of iron.[15] It has been shown that this is avoided in cyanobacteria through compartmentalization of the location and metal ion environment where specific protein-folding takes place in the cell.[16] The toxicity of copper demonstrates the high level of importance in strictly controlling the transportation and use of this metal within cells. This is achieved through the use of metal chaperones which traffic copper to specific destinations. The chaperones also protect the metal ions from a highly chelating intracellular environment which in yeast was found to restrict the concentration of available copper to < 10^{-18} M.[17]

1.3 The Role of Cysteine Residues in Proteins

There are 20 naturally occurring amino acids which are the building blocks of proteins. They are linked by peptide bonds to form polypeptide chains and the side chain of each amino acid has different properties. These properties play an important role in influencing structure and allowing proteins to exhibit specific characteristics such as recognition by other biomolecules and the functioning of the active sites of enzymes.

The side chain of cysteine is a thiol group *(Figure 1.1)* whose sulphur atom is electron-rich, polarizable and quite nucleophilic (a tendency to donate electrons or to react at electron-poor sites). The nucleophilicity of cysteine is enhanced when it is in the deprotonated thiolate form.

Cysteine is present in many proteins and has been found to perform a range of biological functions. These include contributing to the folding and stability of proteins via the form of

disulphide bonds, participating in enzymatic active sites, undergoing post-translational modifications and of key importance for this thesis, the binding of metal ions.

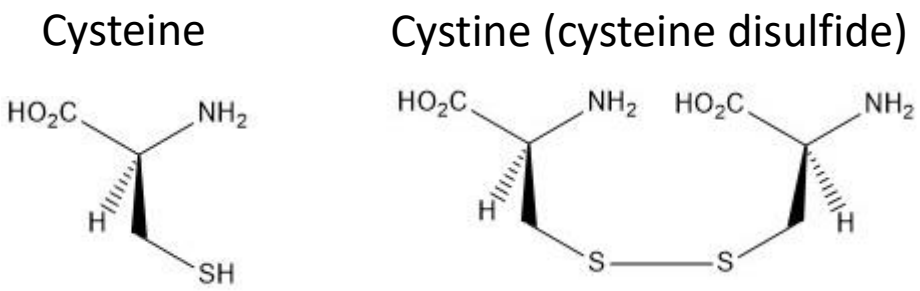

Figure 1.1. The structures of cysteine and cystine. The structure of the amino acid cysteine, and of cysteine in which the two thiol groups of cysteine residues have formed a disulphide bond. The structures were made in ChemBioDraw Ultra.

1.3.1 Cysteines and Protein Structure

A protein's structure is critically important for its function. Mis-folding can result in abhorrent behaviour or a detrimental lack of function *(see section 1.8.3)*. Cysteine residues play an important role in increasing the rigidity and stabilising the structure of many proteins through the formation of covalent disulfide bonds *(Reaction 1.6)*.

$$2(RSH) \rightarrow R\text{-}S\text{-}S\text{-}R + 2e^- + 2H^+ \qquad \textit{Reaction 1.6}$$

Disulfide bond formation results from the oxidation of cysteine residues. The cellular cytosol has long been regarded as a reducing environment due to the presence of glutathione (GSH) which is a low-molecular weight molecule with a thiol group.[18] Therefore, the reducing environment within the cytosol makes disulphide bond formation in proteins unlikely and production is usually localised to a specific cellular compartment. In eukaryotes this is mainly in the lumen of the endoplasmic reticulum whereas in Gram-negative bacteria it usually occurs in the periplasmic space.[19] In Gram-positive bacteria, which have an absence of traditional periplasmic compartments, the pathways of protein oxidation have not been fully explored however the identification of proteins similar to thiol-disulfide oxidoreductases has been reported.[20] Well documented examples of proteins that rely on disulphide bonds to stabilise their tertiary structure are insulin[21] and the human subclass of IgG2 antibodies.[22]

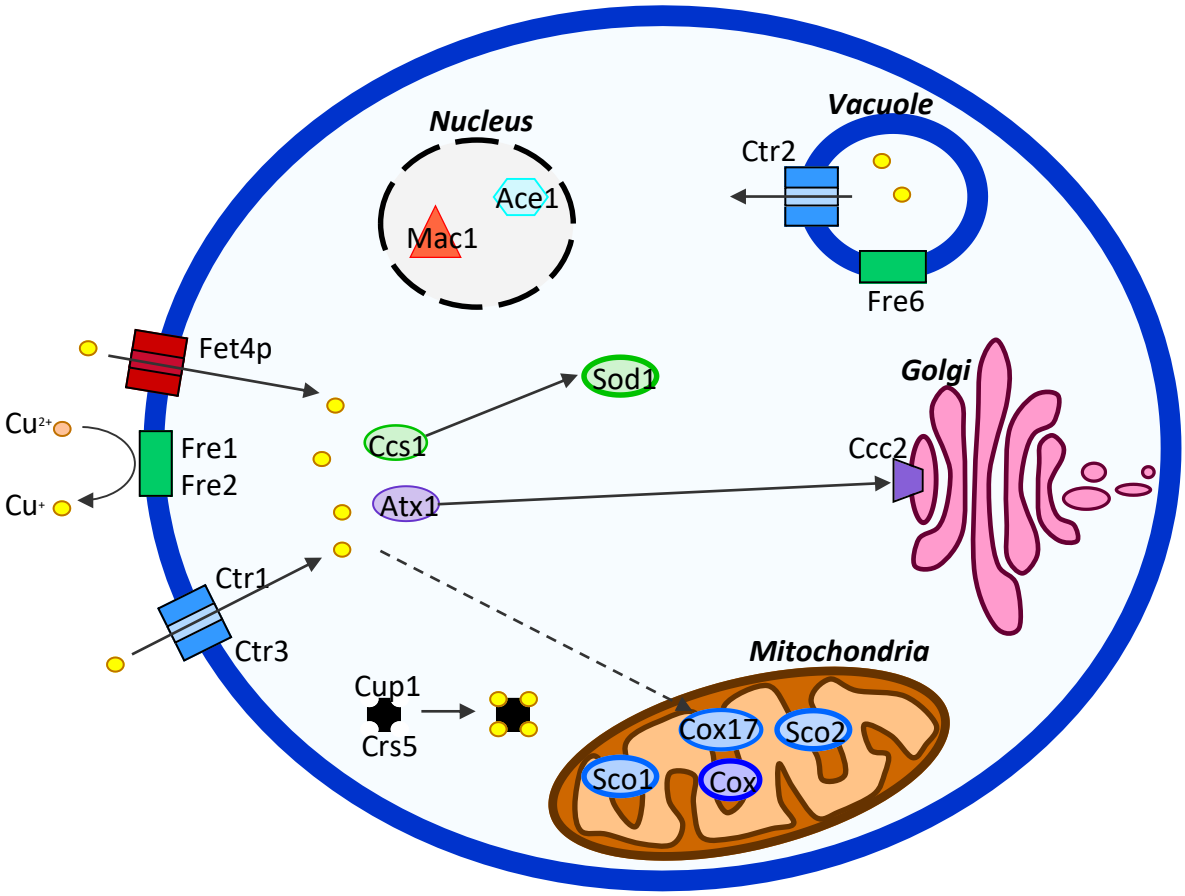

Figure 1.2. Copper homeostasis in *Sacharomyces cerevisiae*. The high affinity transporter proteins Ctr1 and Ctr3, surface metalloreductases Fre1 and Fre2, and low affinity transporter protein Fet4p are located at the cellular membrane. The high affinity transporter protein Ctr2 and metalloreductase Fre6 are located at the vacuole membrane. Cytochrome c oxidase (Cox) and copper chaperones for Cox (Cox17/Sco1/Sco2) are located in the mitochondria. The P-type ATPase Ccc2 is located at the Golgi body. The transcription factors Mac1 and Ace1 are located in the nucleus. The metallothioneins Cup1 and Crs5, Cu,Zn-superoxide dismutase (Sod1), copper chaperone for Sod1 (Ccs1) and copper chaperone for Ccc2 (Atx1) are located in the cytoplasm. Image created in Microsoft Publisher.

1.4 Copper Homeostasis in *Saccharomyces cerevisiae*

The limited resources within the environment of yeast cells requires a competitive mechanism for the acquisition of copper, and a regulatory system to evade potentially toxic accumulation of this ion (*Figure 1.2)*.

1.4.1 Copper Uptake

High affinity transporter proteins located at the plasma membrane have been identified to interact with and mediate the import of copper from the cell exterior to the cytosol. The primary uptake route is through the transporter protein Ctr1 which contains three trans-membrane domains arranged to form a central channel-like pore.[23, 24] Methionine-rich motifs at the extracellular surface and the second transmembrane domain, and cysteine residues of the carboxyl-terminal domain have been proposed as sites of copper binding during translocation. The lack of any features indicative of ATPase domains seen in active transporters leaves the question of how copper is driven across the membrane as unclear. It has been suggested that observation of a Cu^{2+}/K^{+} couple across the cellular membrane could be the driving force for an electrochemical gradient generating a Ctr1-mediated anti-port mechanism.[25] Alternatively, high-affinity copper ion uptake has been measured as a temperature and ATP-dependent process[26] which could indicate that Ctr1 forms higher order complexes that couple to ATPases. In addition to Ctr1, *S. cerevisiae* also contains a second high affinity copper transporter Ctr3,[27] a small cysteine-rich transmembrane protein reputed to have three domains similar to Ctr1. Interestingly, Ctr3 expression in the large majority of laboratory strains is absent due to the insertion of a transposable element at the promoter site. This is most probably due to domesticated strains having been derived from a common ancestor in which Ctr3 was silenced by a chance transpon event. Although Ctr1 and Ctr3 function interchangeably in high-affinity copper transport, there is little sequence homology between these two proteins. It has been observed that both transporters can function independently to provide high-affinity copper transport to yeast, although cells expressing both proteins have a distinct growth advantage over cells expressing either one of these transporters alone when copper is limiting.

The low-affinity transporter Fet4p functions as an Fe^{2+} permease which has been found to also facilitate Cu^{1+} transport across the cellular membrane.[28] Copper ions imported by Fet4p were found to be metabolised in a similar manner to those imported by Ctr1.[28] Copper also acts as a non-competitive inhibitor of iron uptake through Fet4p, indicating that binding of the two metal ions is not mutually exclusive and suggests that Fet4p has separate ligand sites for each substrate.

1.4.2 Copper Reductases

In aqueous solution, copper is found in the more stable Cu^{2+} oxidation state (Section 1.1.1), however copper transporters at the cell surface interact with the Cu^{1+} substrate. Metalloreductases at the plasma membrane have been identified which mobilize cytoplasmic electrons through the membrane and reduce Fe^{3+} to Fe^{2+}. It has also been shown that the metalloreductases Fre1 and Fre2[29, 30] implement the reduction of Cu^{2+} to Cu^{1+}.[23, 24] Considering that Cu^{1+} is easily oxidised to Cu^{2+} in the extracellular aerobic environment, it is feasible that a mechanism exists to protect Cu^{1+} in passage to the membrane transporters.

1.4.3 Cellular Destinations of Copper

Copper is required at three intracellular destinations, therefore, upon entry into the cell the metal is shuttled along one of three main intracellular transport pathways *(Figure 1.2)*. One route is transportation by the chaperone Atx1 to the membrane-bound P-type ATPase Ccc2 at the *trans*-Golgi network[31] for incorporation into the membrane-bound Fet3p oxidase, which participates in the uptake of iron at the cell surface.[32] Another destination for copper is the mitochondria where it is incorporated into the cytochrome c oxidase (Cox) which is involved in the respiratory chain process of ATP production. The role of the copper chaperone Cox17, originally thought to deliver copper to mitochondria, may actually be restricted to the delivery of copper to Cox within the intermembrane space.[33] The metallochaperones Sco1 and Sco2 have also been indicated as playing a role in the delivery of copper to Cox17 within mitochondria.[34] The third route is specific delivery to Cu,Zn-superoxide dismutase (Sod1) by the copper chaperone for Sod1 (Ccs1)[35] in both the cytoplasm, the mitochondrial intermembrane space and the nucleus, where it catalyses dismutation of the superoxide anion produced during aerobic respiration.

1.4.4 Copper Storage and Detoxification

Intracellular copper is also sequestered by low molecular weight cysteine-rich metallothioneins which function to detoxify the cell and provide copper resistance. In *S. cerevisiae*, the metallothioneins Cup1[20, 36] and Crs5[37] have been identified which tightly chelate the metal preventing solvent exposure and creating bound metal ions that are weakly exchangeable. Cup1 consists of a 53-amino acid polypeptide that binds 8 copper ions through 10 cysteine residues suggesting cluster formation of the metal ion.[18, 38] The metallothionein Crs5 was found to have a greater binding capacity for copper, 11-12 copper atoms ligated by ≤ 19 cysteine residues, and suggests that Csr5 may exhibit domain organisation as seen with mammalian metallothioneins.[39]

Cellular vacuoles are also used to regulate cytosolic metal ion concentrations. The process of accumulating alkali and transition metals, such as Ca^{2+}, K^{+}, Mn^{2+} and Fe^{2+}, into the vacuole are documented[40] whereas the process of copper import into the vacuole is yet to be identified. Nevertheless, the copper transporter protein Ctr2 has been established to localise at vacuolar membranes and exports copper into the cytoplasm in times of copper deficiency.[41]

1.4.5 Regulation of Copper Homeostasis

The intracellular copper pathways are controlled through copper-sensitive transcriptional regulators in order to maintain a steady-state balance of intracellular copper. When the extracellular copper concentration is in excess, the transcription factor Ace1 is activated to induce expression of the metallothioneins Csr5, Cup1 and the redox protein Sod1.[37, 42, 43] Copper activation occurs through the formation of polynuclear Cu^{1+} clusters by Ace1 cysteine residues[44] which stabilise a specific conformation enabling Ace1 to bind with a response element of its target gene.[45] The response element is a short DNA sequence within the promoter region of the gene and regulates the transcription of genes. The transcriptional activator Mac1 is associated with the copper uptake proteins Ctr1, Ctr2, Ctr3 and the metalloreductase Fre1. Structurally, Mac1 exhibits an amino-terminal DNA binding domain and a carboxyl-terminal that contains two cysteine-rich copper binding motifs which bind up to eight copper ions as a copper-thiolate cluster and are thought to function as direct copper sensors.[27, 46] Under low levels of copper, Mac1 surveys the intracellular copper milieu and regulates expression of associated proteins depending on cellular needs by interacting with

the promoters of target genes. When intracellular copper levels rise, copper binds to Mac1 stimulating an interaction between the DNA binding domain and the cysteine-rich terminus, thereby masking the activation domain and repressing its target genes.[29, 47-49] Mac1 also has an additional mode of regulation which is specific for copper in conditions of high intracellular copper concentration. In this circumstance the copper transporters are no longer useful to the cell and the transcription factor Mac1 undergoes proteolytic degradation.[50] This completely eliminates the expression of the copper transporters and serves as a defence mechanism to avoid excessive copper accumulation. In addition to transcriptional regulation, Mac1 has also been linked to a unique post-translational mechanism to control copper uptake by regulating the degradation of its target gene product.[51] Upon exposure to excess extracellular copper, the high-affinity transporter Ctr1 is rapidly and specifically degraded at the plasma membrane without internalisation or delivery to the vacuole.[52] Ctr1 degradation was found to occur only when Mac1 is expressed.[53, 54]Two possible roles of Mac1 have been proposed in Ctr1 degradation, the first proposes that Mac1 activates a gene that encodes the protease which degrades Ctr1. The second is that Mac1 recruits a protease or acts as a protease itself, however Mac1 is located in the nucleus[55] while Ctr1 degradation occurs at the membrane.[52] Nonetheless, truncated Mac1 has been found in the cytosol[55] and Mac1 itself undergoes degradation in response to high copper levels.

1.5 Mammalian Copper Homeostasis

In mammals, copper transport pathways require a higher order of coordination than yeast since transportation can occur through the blood, and specific areas such as the brain and heart have higher demands for copper.[56] The brain is one of the most energy-demanding tissues in the body[57] and the primary source of ATP is the electron transfer train in the mitochondria. The final complex in the chain is COX, whose subunits require copper.[58] Similarily, >95% of ATP production in the heart is produced by oxidative phosphorylation in the mitochondria.[59] The principal use of energy by the heart is to fuel contractions, followed by the operation of several ion pumps.[60, 61]

Although, on a cellular level the proteins associated with the human copper transfer pathways show a large degree of similarity to those of yeast. In humans, copper enters the cytosol through the same mechanism as that in yeast, through the high-affinity transporter

CTR1 at the plasma membrane. CTR1 is also located at intracellular vesicles and increased copper levels result in the re-localisation of CTR1 from the membrane to vesicles.[62] The same three intracellular destinations for copper exist in humans as in yeast. The chaperone HAH1 (yeast Atx1 homologue) transports copper to the ATPases ATP7A and ATP7B (equivalent to yeast Ccc2) at the *trans*-Golgi network for incorporation into cuproenzymes such as ceruloplasmin[63, 64] in the secretory pathway.[65] The importance of these transporters in copper homeostasis has been highlighted by genetic diseases, which are a result of incorrect protein function. Mutations associated with ATP7A results in Menkes disease whereas mutations of ATP7B result in Wilson's disease (see section 8.1.3).

In humans, copper is also required by COX in the mitochondria, and homologues of the yeast chaperones involved in copper delivery also exist; COX17, SCO1 and SCO2.[66] The route of copper delivery in humans to SOD1 corresponds to that in yeast and is achieved by CCS1.[35] Mutations and incorrect post-translational modifications of SOD1 have been linked to amyotrophic lateral sclerosis (see section 1.6.5).[67, 68]

1.6 Structure and Catalytic Action of Cu,Zn-Superoxide Dismutase

Cu,Zn-Sod1 plays an important role in antioxidant defence by scavenging superoxide radicals. The major source of intracellular superoxide is from ATP production in the mitochondria as a by-product of oxygen metabolism.[69]

1.6.1 Protein Structure of Cu,Zn-Superoxide Dismutase

Eukaryotic Sod1 proteins are highly conserved from primary to quarternary structure and are comprised of two identical subunits forming a dimeric protein. Each subunit consists of a β-barrel composed of eight antiparallel β-strands,[70] and contains one Cu^{2+} ion and a Zn^{2+} ion. Activity measurements have shown that there is no cooperativity between subunits, however monomeric Sod1 formed by disruption of the quarternary structure by residue mutations had a much lower activity than the native dimeric protein.[71]

1.6.2 Active site of Cu,Zn-Superoxide Dismutase

The zinc ion is completely buried in the Sod1 protein whereas the copper ion sits at the bottom of the active site channel.[72] The copper ion is solvent exposed and interacts with a water molecule at the axial position which is linked to the bulk solvent by a chain of well-ordered water molecules.[73] The edge of the active site channel is constituted by charged residues which provide a positive electrostatic field that drives the superoxide anion towards the copper ion. The copper ion is bound in a distorted square planar coordination by four histidine residues (His44, His46, His61, His118) and the zinc ion is coordinated by three histidine residues (His61, His69, His78) and an aspartic acid residue (Asp81) in a distorted tetrahedral geometry *(Figure 1.3)*.[74, 75] The distinguishing structural property of this active site is the bridge between the metal ions by the imidazolate group His61.

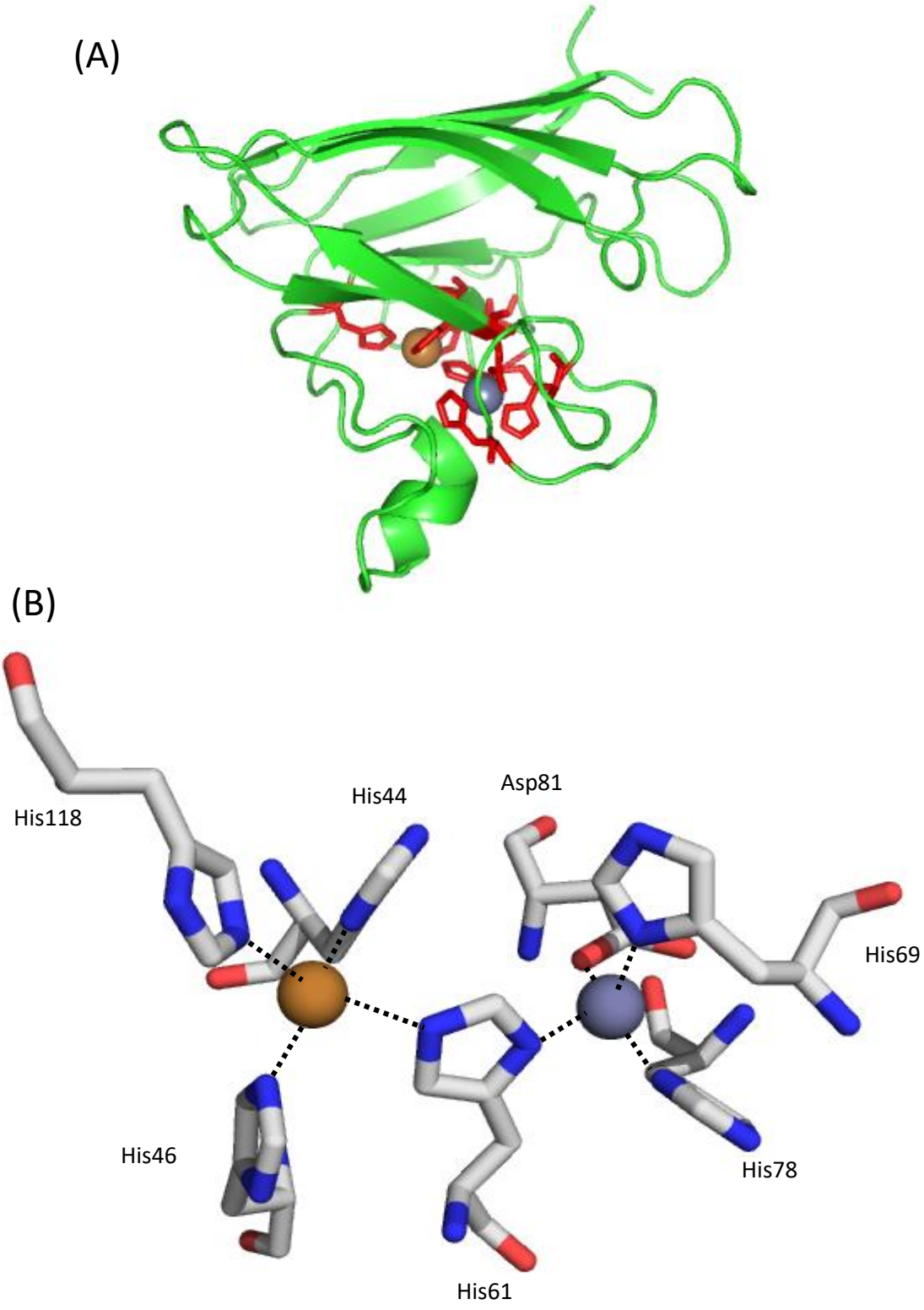

Figure 1.3. The structure of *S. cerevisiae* Cu,Zn-Sod1 and the active site with copper and zinc bound. (A) Crystal structure of Cu,Zn-Sod1, the metal-binding residues are shown in red and the Cu^{2+} (gold) and Zn^{2+} (blue) ions are shown as spheres. (B) The coordinating residues at the Cu^{2+} (gold sphere) and Zn^{2+} (blue sphere) ions are shown as sticks. Images created with PyMol v1.3 from the PDB file 1SDY.[74]

1.6.3 Catalysis Mechanism

The catalytic action of Sod1 involves the disproportionation of superoxide to molecular oxygen and hydrogen peroxide (Scheme 1.1). Kinetic studies have indicated that the copper ion of Sod1 is cyclically reduced and oxidised between the +1 and +2 oxidation states in two irreversible reactions *(Scheme 1.1)*.[76-78]

$$0_2^- + Cu^{2+} \rightarrow O_2 + Cu^+$$
$$2H^+ + O_2^- + Cu^+ \rightarrow H_2O_2 + Cu^{2+}$$

Scheme 1.1

Structures of Sod1 alone and in complex with the product H_2O_2 bound[4] and studies indicating an inner-sphere mechanism[79] have helped produce a unified general mechanism for Sod1 that takes into consideration steric restrictions at the copper site *(Figure 1.4)*.[4, 11]

Superoxide radicals have been shown to undergo spontaneous disproportionation to molecular oxygen and hydrogen peroxide in solution, however this requires the interaction of two superoxide molecules and is therefore second-order with respect to superoxide concentration. In contrast, catalysis of this reaction with Sod1 is first-order with respect to superoxide concentration and the reaction rate is only limited by the rate of diffusion.[6] It has been suggested that the rate of the enzymatic reaction is $\approx 10^4$ times faster than that of the spontaneous reaction.[79]

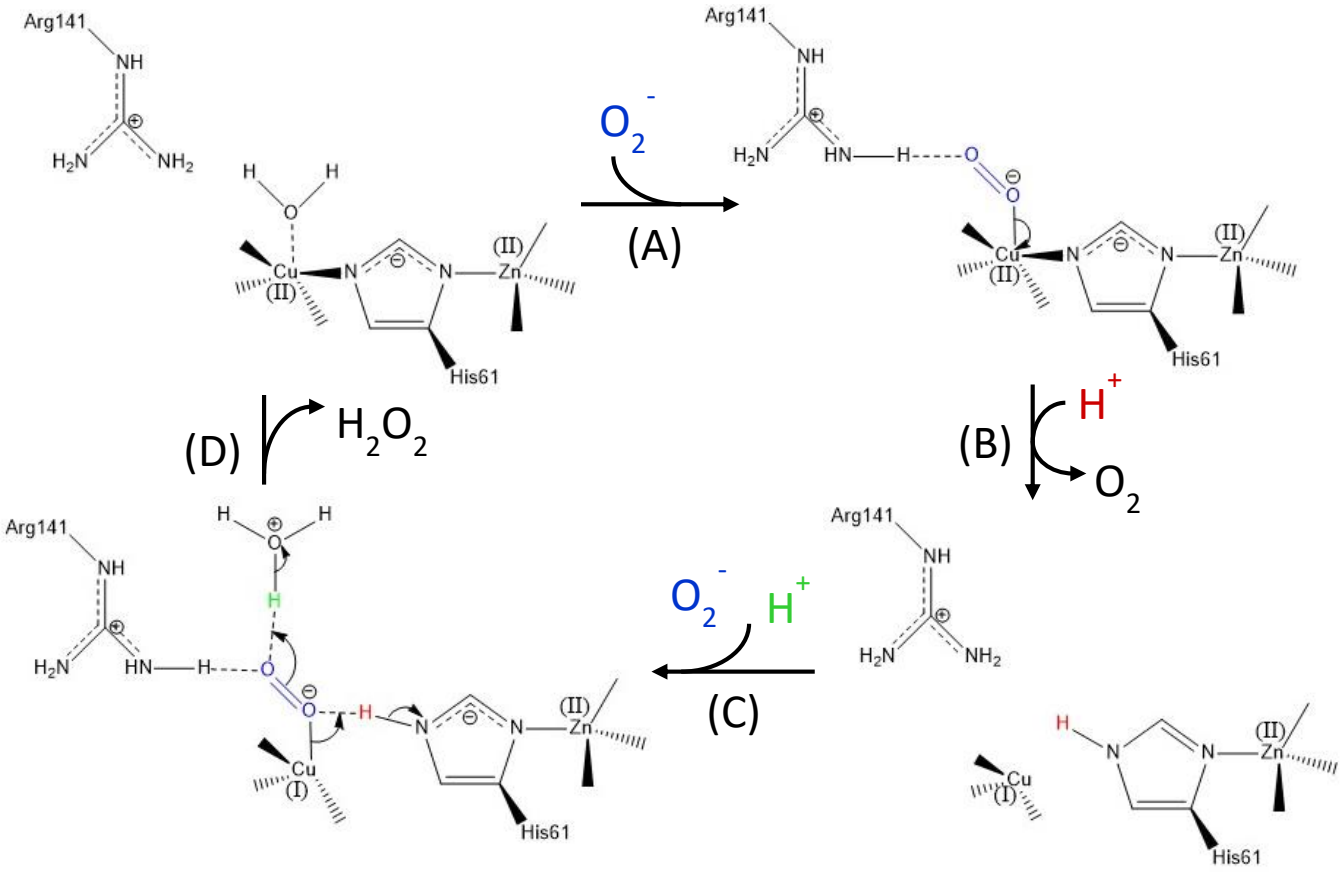

Figure 1.4. The mechanism showing how Sod1 catalyses the dismutation of superoxide into oxygen and hydrogen peroxide. (A) A superoxide anion displaces a water molecule in the axial position at the Cu^{2+} site of Sod1 and forms a hydrogen-bond with Arg141. (B) Superoxide is oxidised by Cu^{2+} via inner-sphere electron transfer resulting in 0_2 and Cu^{1+}-Sod1, cleavage of the Cu-N (His61) bond and protonation of His61. (C) A second superoxide anion binds to Cu^{1+} and is stabilised by hydrogen bonds to Arg141 and His61. (D) His61 donates a proton to superoxide prior to, or simultaneously with, inner-sphere electron transfer from Cu^{1+} and hydrogen peroxide is released following the addition of another proton (shown in green). The scheme is adapted from references [4, 11] and was made using ChemBioDraw Ultra.

1.6.4 Cu,Zn-Superoxide Dismutase Maturation

Maturation of Sod1 to an enzymatically active form requires the acquisition of both copper and zinc, and the formation of a structurally important disulfide bond between Cys57 and Cys146.[80] Exposure of apo-SOD1 to Zn^{2+} ions *in vitro* generates a mixture of E,Zn-Sod1 and Zn,Zn-SOD1 indicating that SOD1 is unable to site-selectively bind Zn^{2+} since a second ion is also bound to the Cu^{2+} site.[81] However, studies have shown that SOD1 is capable of site-specifically recruiting Zn^{2+} *in vivo.*[82] The copper chaperone for superoxide dismutase has been implicated in the formation of the disulphide bond in SOD1, and D3 of human CCS1 has been found responsible for this formation in SOD1 *in vitro*.[83] The stability of the structural disulphide in SOD1 is particularly interesting since the cytosol is a reducing environment due to the presence of excess reduced glutathione over the oxidised form.[84] These are important steps for the correct functioning of the enzyme and prevention of misfolding and aggregation of the protein.[80, 85]

1.6.5 Link to Amyotrophic Lateral Sclerosis

In humans, a link has been drawn between the neurodegenerative disorder familial amyotrophic lateral sclerosis (ALS) and the SOD1 protein. Symptoms include muscle atrophy due to the degeneration of motor neurons, and cognitive dysfunction such as language defects, repeating gestures and loss of inhibition. The clinical course of ALS is progressive and typically causes death within 3 – 5 years of onset, mostly due to respiratory failure.[86] The first causative mutations were found within the gene encoding SOD1,[87, 88] since then many more SOD1 mutations have been described, although pathogenicity has not been attributed to all. Initially, the loss of SOD1 activity found in patients with ALS and mutations throughout the SOD1 gene suggested a mechanism whereby a loss of function occurs, however, later research has shown that a toxic gain of function mechanism is the actual contributor to ALS.[89] The distinct lack of SOD1 activity in ALS patients has been associated with aggregation of the protein[90] and dissociation of the dimer due to oxidative stress.[91]

1.7 The Copper Chaperone for Cu,Zn-Superoxide Dismutase

The Sod1 copper chaperone Ccs1 is not only responsible for delivering copper directly to its target protein, but also activating Sod1 to its enzymatically active state.

1.7.1 The Structure of Ccs1

Structural studies with yeast Ccs1 have shown that the ≈ 30 kDa protein is comprised of three distinct domains which are thought to have specific functions. The N-terminal domain (D1) consists of 70 amino acid residues arranged in a βαββαβ fold and contains an MXCXXC (Cys17 and Cys20) copper binding site.[92] This domain is homologous to yeast Atx1, human HAH1 and bacterial CopZ since all feature the same βαββαβ fold and copper binding motif *(Figure 1.5)*. The central polypeptide domain (D2) of Ccs1 contains 123 residues arranged in β-barrel folds and is structurally homologous to Sod1, although the sub-loop which binds zinc in Sod1 is not present in Ccs1 *(Figure 1.6)*.[92] Human CCS1 contains the zinc-binding sub-loop seen in SOD1 however the primary function of this site is structural.[93] Interestingly, the most highly conserved sequences between D2 of Ccs1 and Sod1 are those known to be involved in facilitating Sod1 dimerisation, such as the residues whose peptide bonded backbone is involved in forming four hydrogen bonds at the Sod1 dimer interface (Ccs1 = Gly137 and Gly187, Sod1 = Gly52 and Gly115).[74] The same four hydrogen bonds seen in the Sod1 dimer are present in the Ccs1-Sod1 complex, however Leu152 involved in the Sod1 dimer is Arg217 of Ccs1 in the Ccs1-Sod1 complex *(Figure 1.7)*.[75] This suggests that the function of D2 is recognition and formation of a Ccs1-Sod1 complex preceding copper insertion. Although D2 is required for heterodimer formation, this domain alone is not sufficient and interactions with D3 have also been implicated.[94] The C-terminal domain (D3) of Ccs1 is a short random-coil polypeptide unique to this chaperone, and contains a CXC (Cys229 and Cys231) motif.[75] These structural domains are conserved across the majority of eukaryotic copper chaperones for Cu,Zn-superoxide dismutase *(Figure 1.8)*, however the CCS proteins of *Melanogaster drosophila*[95] and *Schizosaccharomyces pombe*[96] have been found to lack the CXXC motif of D1.

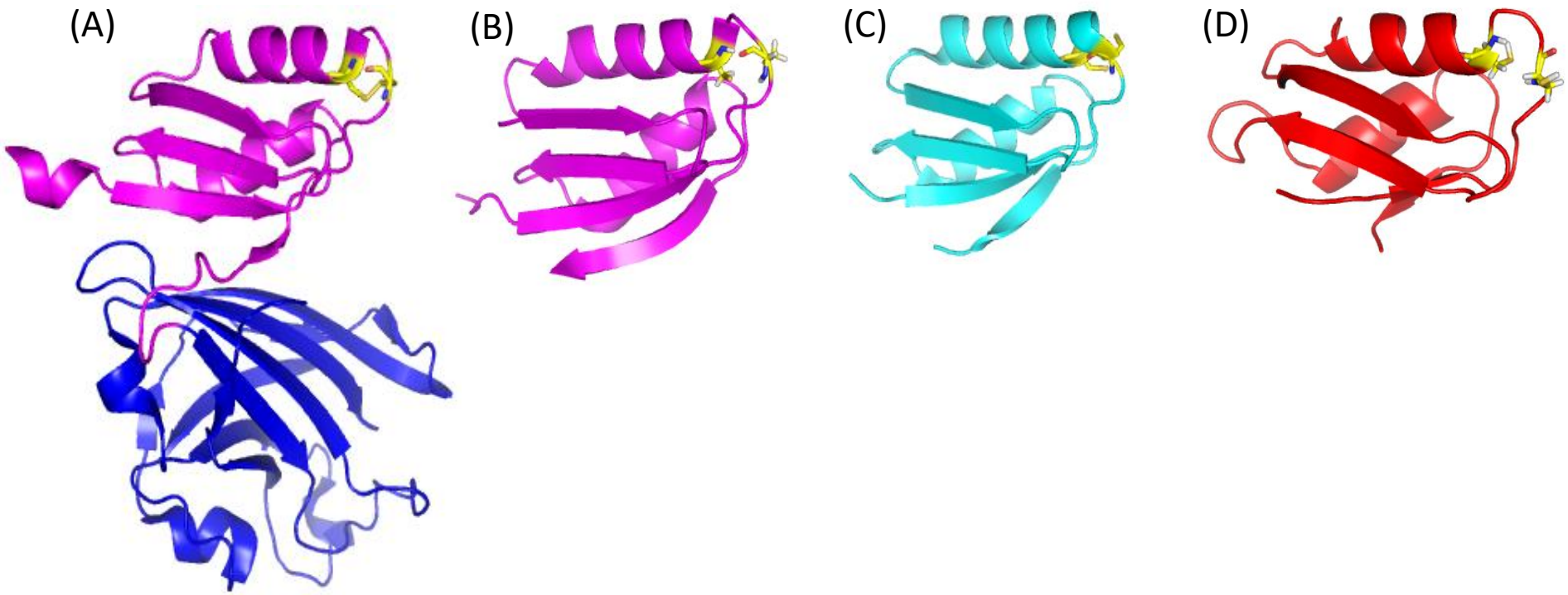

Figure 1.5. A comparison of the structure of domain 1 of Ccs1 to those of the Atx1-family of copper metallochaperones. The structures of *S. cerevisiae* Ccs1 (A) in which only D1 (magenta) and D2 (blue) are observed, *S. cerevisiae* Atx1 (B), *H. sapien* HAH1 (C) and *E. Hirae* CopZ (D). All proteins contain a $\beta\alpha\beta\beta\alpha\beta$-fold and MXCXXC sequence motif (D1 OF Ccs1). The metal-binding Cys residues are shown in yellow. Images created using PyMol v1.3 from the PDB files (A) 1QUP[92], (B) 1FD8[97], (C) 1FEE[26], (D) 1CPZ[24].

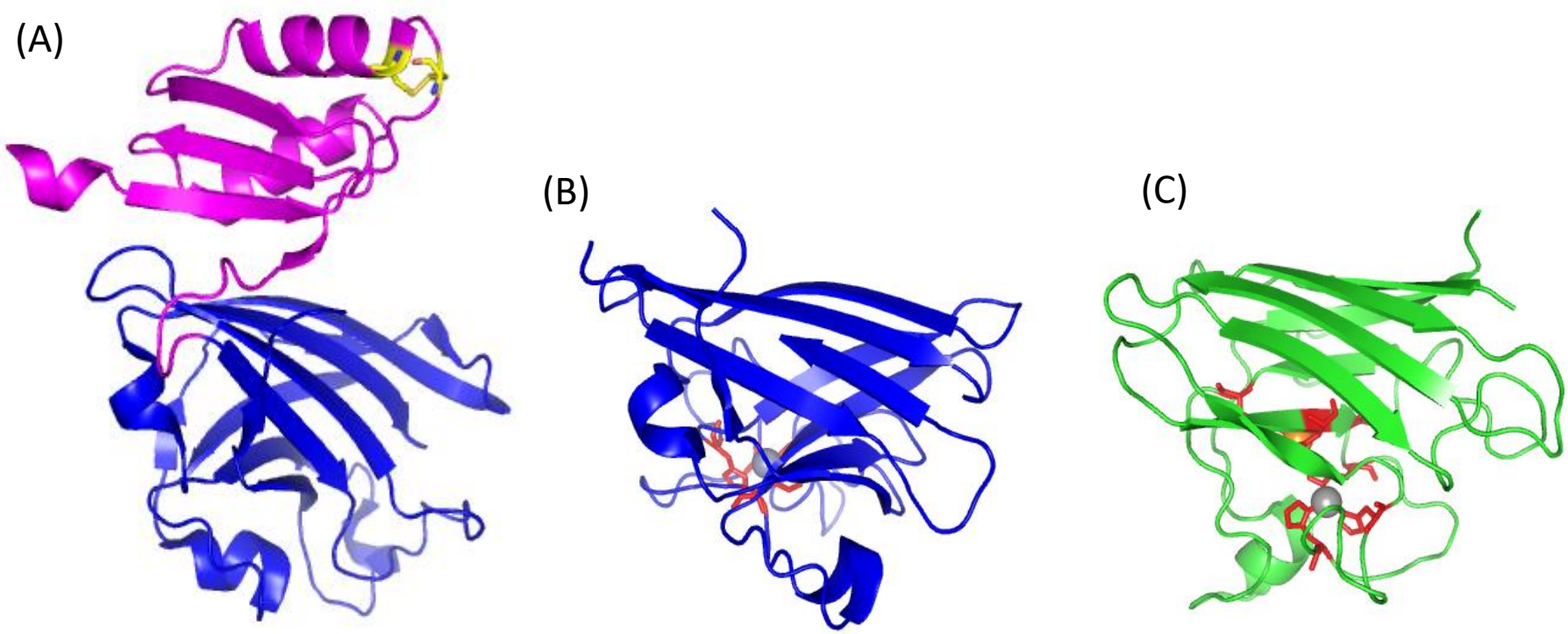

Figure 1.6. A comparison of the structure of domain 2 of Ccs1 to domain 2 of CCS1 and Sod1. Crystal structures of *S. cerevisiae* Ccs1 (A) in which only D1 (magenta) and D2 (blue) are observed, *H.sapien* CCS1 (B) in which only D2 is observed and *S. cerevisiae* Cu,Zn-Sod1 (C). The metal-binding Cys residues are shown in yellow, the His residues in red and the Cu^{2+} (gold) and Zn^{2+} (blue) ions are shown as spheres. Images created using PyMol v1.3 from the PDB files (A) 1QUP[92], (B) 1DO5[98], (C) 1SDY[99].

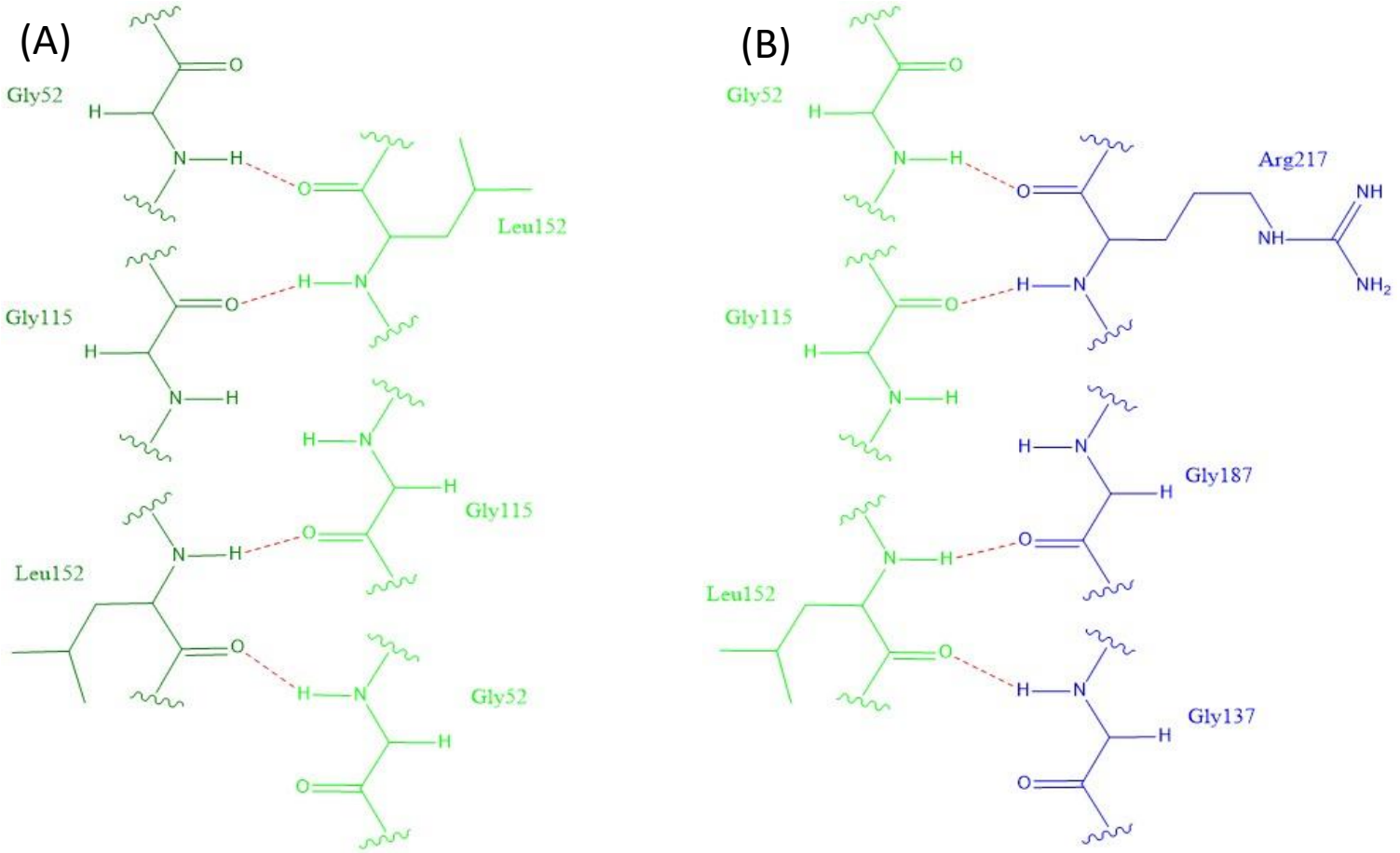

Figure 1.7. A comparison of the hydrogen bond interactions between the Sod1 homodimer and Sod1-Ccs1 heterodimer interfaces. The residues involved with hydrogen bonding of the (A) *S. cerevisiae* Sod1 homodimer (Sod1 monomer residues shown in dark or light green), and (B) the *S. cerevisiae* Sod1-Ccs1 heterodimer (Sod1 residues shown in light green and Ccs1 in blue).[75] Images created using ChemBioDraw Ultra.

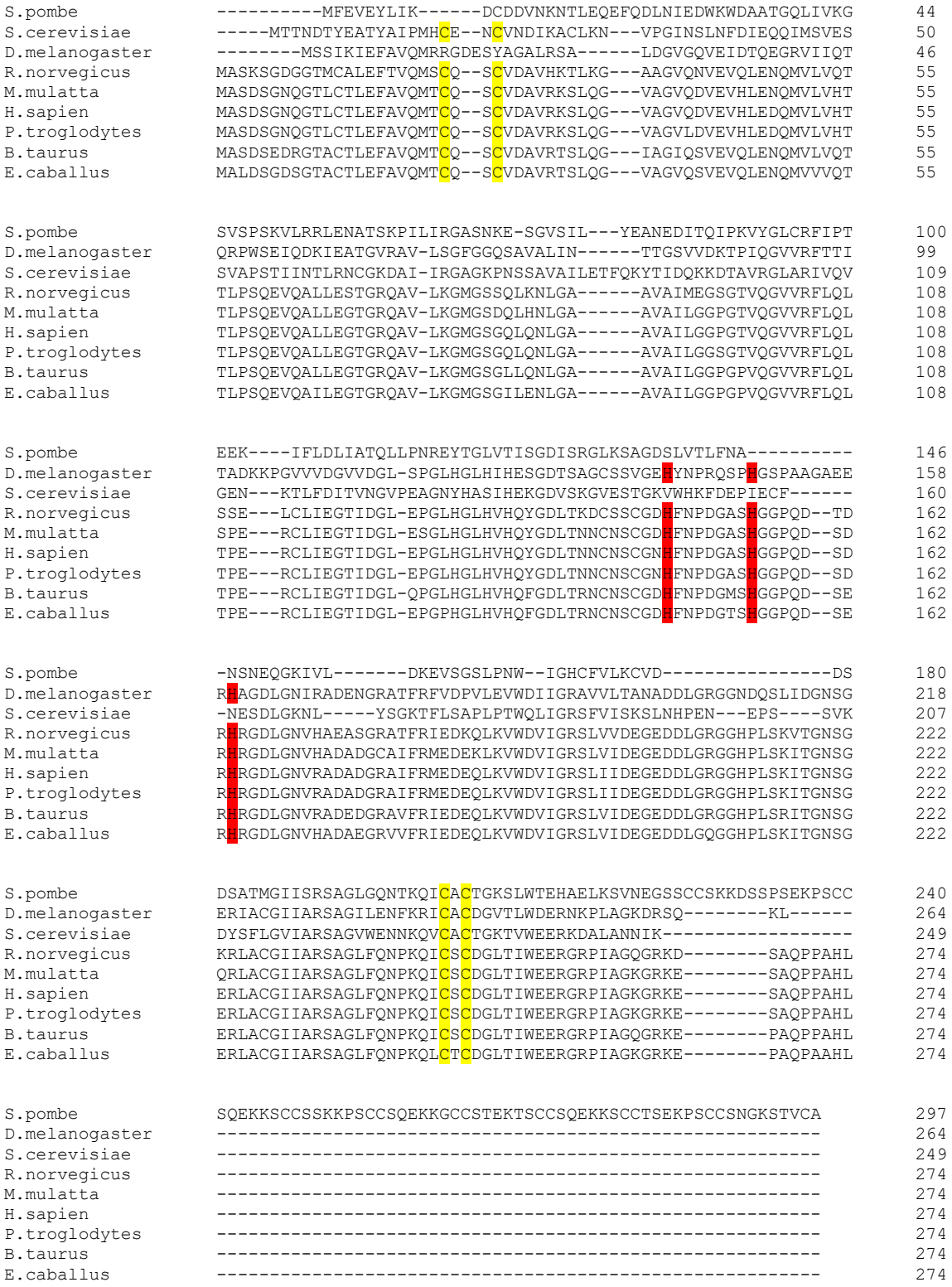

Figure 1.8. Sequence alignment of the copper metallochaperone for Cu,Zn-superoxide dismutases from a range of species. Cys residues which bind copper ions are highlighted in yellow and His residues which bind zinc ions are highlighted in red. Protein sequences sourced from UniProt[100] and aligned with Clustal Omega.[27, 101]
Protein sequence Accession Numbers: *Schizosaccharomyces pombe* Q10357, *Drosophila melanogaster* Q9BLY4, *S. cerevisiae* P40202, *Rattus norvegicus* Q9JK72, *Macaca mulatta* F7FL64 , *Homo sapien* O14618, *Pan troglodytes* H2Q473, *Bos taurus* E1BE86, *Equus caballus* F6UQH5.

1.7.2 The Mechanism of Sod1 Activation

The main focus of research has centred on the human and yeast chaperones, however there is major disagreement regarding the mechanism of Cu,Zn-superoxide dismutase activation. Studies performed *in vivo* with human CCS1 have shown that the CXXC motif of D1 is essential for SOD1 activation.[102] This is consistent with the higher affinity of the CXXC motif of D1 for copper compared to the CXC motif in D3.[103] However, investigations relying on SOD1 activity assays cannot identify the independent occurrence of copper insertion and disulphide formation. The use of nuclear magnetic resonance (NMR) and electrospray ionization mass spectrometry (ESI-MS) has allowed the actions of copper transfer and disulphide formation to be studied independently. These techniques have suggested that D1 of CCS1 is essential for copper insertion in humans, and D3 is responsible for the formation of the disulphide in SOD1.[83] The mechanism of human SOD1 activation by CCS1 has been suggested *(Figure 1.9)*.[83] Firstly, immature SOD1 (E,E-SOD1^{SH}, notation indicates empty metal sites and reduced disulfide) recruits zinc, then forms a heterodimeric complex with copper loaded CCS1. D1 of CCS1 then transfers the copper ion to SOD1 to form the fully metallated Cu,Zn-SOD1^{SH}, followed by disulphide isomerization from D3 to Cys57 and Cys146 of SOD1. Lastly, the heterodimeric complex dissociates releasing mature Cu,Zn-SOD1$^{S\text{-}S}$ and CCS1 which is able to activate further SOD1 molecules.

This mechanism is completely contradicted by investigations with yeast Ccs1. D1 of yeast Ccs1 was found to be necessary for Sod1 activation only under copper limiting conditions, and the cysteine residues of the CXC motif in D3 have been determined as crucial for Sod1 activation.[104] This is compatible with the position of D3 as adjacent to the active site of Sod1 in the crystal structure of the Ccs1-Sod1 complex, and is therefore ideally positioned for copper transfer *(Figure 1.10)*.[75] Also, in this structure the metal binding site of D1 is ≈ 35 Å from the SOD1 active site suggesting that D1 is not involved in direct copper insertion. A disulphide bond is also observed between Sod1 Cys57 and Ccs1 Cys229 which could indicate an intermediate in disulphide formation, or this could also simply be an artefact of crystallisation.

Due to the flexibility and only partial structural organization of D3 it has been proposed that D3 is able to obtain copper from D1.[105, 106] This has appeared feasible in both yeast Ccs1[75] and human CCS1,[107] and copper transfer has been observed between the human domains in partition experiments.[103] Therefore the role of D1 would be expected to involve Cu^{1+} acquisition and transfer to D3 for insertion into SOD1, however the increased affinity of D1 for Cu^{1+} compared to D3 would make this thermodynamically unfavourable.

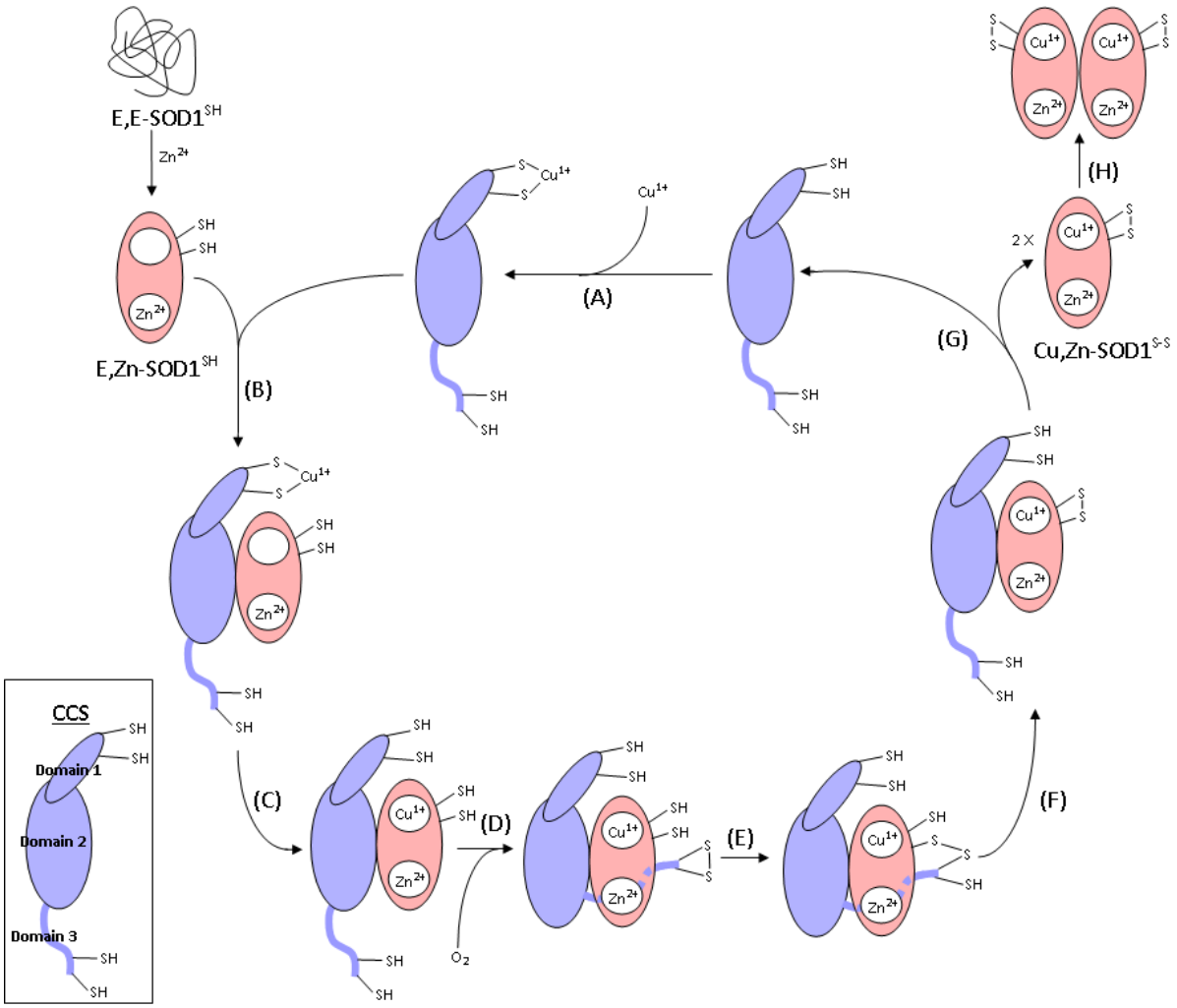

Figure 1.9. The activation of human SOD1 by CCS1, (A) CCS1 recruits Cu^{1+}. (B) E,Zn-$SOD1^{SH}$ forms a heterodimeric complex with Cu^{1+}-CCS1. (C) D1 of CCS1 transfers Cu^{1+} to E,Zn-$SOD1^{SH}$. (D) A disulfide bond is formed within the CXC motif in D3 of CCS1 and a conformational change moves D3 of CCS1 into the vicinity of the SOD1 Cys residues. (E and F) Disulfide isomerization from D3 of CCS1 to Cu,Zn-$SOD1^{SH}$. (G) The CCS1-SOD1 heterodimeric complex dissociates releasing Cu,Zn-$SOD1^{S-S}$ and CCS1. (H) Cu,Zn-$SOD1^{S-S}$ dimerization. The scheme is adapted from reference [83] and created in Microsoft Publisher.

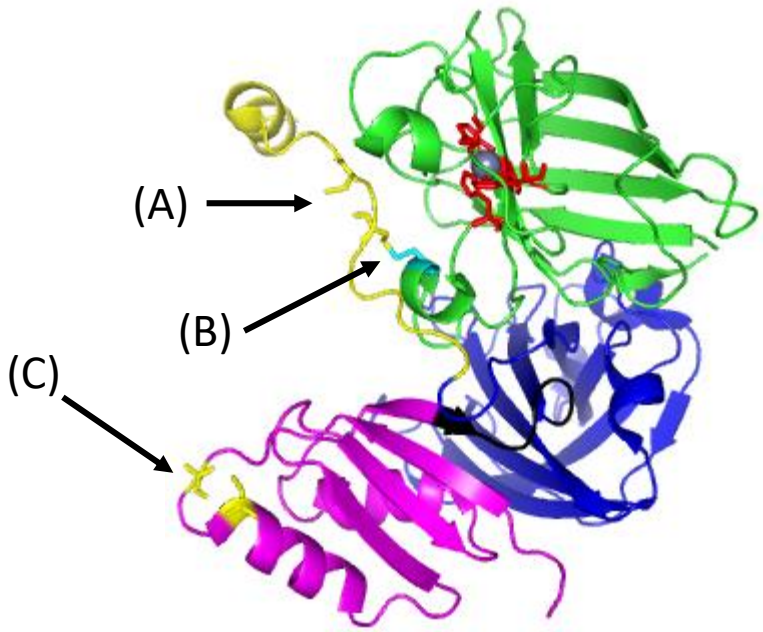

Figure 1.10. The crystal structure of the heterodimeric complex between *S. cerevisiae* Ccs1 and a mutant Sod1 (His48 mutated to Phe). (A) The location of Ccs1 copper-binding Cys229 and Cys231 in D3. (B) Disulfide bond between Cys229 of Ccs1 D3 and Cys57 of Sod1. (C) The location of Ccs1 D1 Cys17 and Cys20. The Sod1 monomer is shown in green, D1 of Ccs1 in magenta, D2 of Ccs1 in blue and D3 of Ccs1 in yellow. The metal-binding Cys residues are shown in yellow, the His residues in red and the Zn^{2+} (blue) ion is shown as a sphere. Image created using PyMol v1.3 from the PDB file 1JK9[75].

1.8 The Copper Chaperone Atx1 and its Target Protein Ccc2

The chaperone Atx1 is responsible for delivering copper to the ATPase cation transporter Ccc2 located at the membrane of the trans-Golgi network. Ccc2 facilitates the transport of copper into Golgi vesicles with the ultimate destination of the multicopper oxidase Fet3p which mediates high affinity iron uptake at the cell surface.[32]

1.8.1 Structure of Atx1 and Ccc2

Yeast Atx1 contains 72 residues arranged in a βαββαβ-fold, homologous to that seen in Ccs1 and ferredoxin proteins.[108] An MXCXXC motif (Cys15 and Cys18) is located at a comparable position to the one contained in Ccs1. The oxidation state of the copper bound to Atx1 has been measured as Cu^{1+} and is positioned within a trigonal geometry, most probably the two sulfurs of the MXCXXC motif and a third ligand, possibly O, N or S from another amino acid.[31]

The target protein of Atx1, the Ccc2 transporter, has an overall structure containing four cytoplasmic domains spread across eight membrane-spanning domains.[109] The majority of studies have focused on the amino terminal domain (Ccc2a) as this is the location of copper transfer from Atx1. Ccc2a contains 72 amino acid residues and shares the same βαββαβ-fold arrangement as Atx1.[110] Ccc2 is homologous to the ATP7A/ATP7B transporters in humans, although Ccc2a contains two MXCXXC metal binding motifs similar to that in Atx1, ATP7A/ATP7B both contain six of the same metal binding motifs.[111]

1.8.2 Copper Transfer to Ccc2

Specific residues along the surfaces of Atx1 and Ccc2a are thought to be the basis of recognition between these partner proteins. Atx1 has a number of basic lysine residues along its surface which complement the acidic glutamate and aspartate residues at the surface of Ccc2a.[108, 110] The electrostatic forces between these residues allow Atx1 to 'dock' with Ccc2a and provide the correct orientation of binding sites for direct copper transfer. This theory is backed up by a mutagenic study which showed that the loss of lysine residues at the surface of Atx1 caused decreased delivery of copper to Ccc2a.[112] NMR investigations and crystallography studies into the mechanism of Atx1 to Ccc2a copper transfer has

proposed the formation of copper bridged 2- and 3-coordinate intermediates between an Atx1-Ccc2 heterodimeric complex *(Figure 1.11)*.[31] A similar process has been suggested for the human homologues HAH1 and the transporters ATP7A and ATP7B.[113] Interestingly, it has been claimed that the thermodynamic gradient of copper transfer between Atx1 and Ccc2a is shallow, suggesting that this movement does not rely on a higher affinity of the target site.[114]

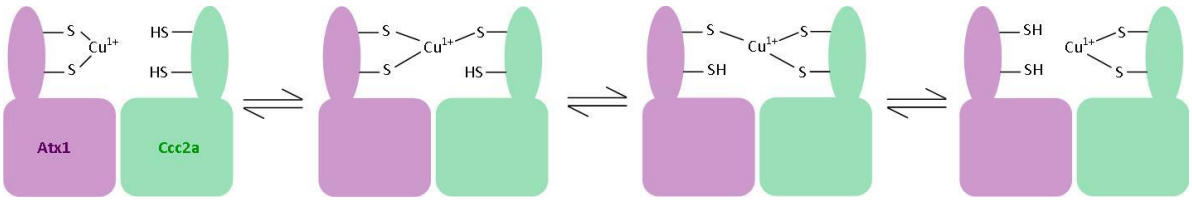

Figure 1.11. A proposed mechanism of Cu^{1+} transfer between Atx1 and Ccc2a in *S. cerevisiae*. The exchange of Cu^{1+} involves the stepwise formation of two- and three-coordinate Cu^{1+}-bridged intermediates. The scheme is adapted from reference [31] and created in Microsoft Publisher.

1.8.3 Associations with Human Diseases

The human homologues of the Atx1 target Ccc2 are ATP7A and ATP7B. A mutation in the ATP7A gene has been shown to cause the X-linked recessive Menkes disorder, of which onset typically begins in infancy and many affected newborns do not live past the age of 3 years. [115] The phenotypes of Menkes disease includes low muscle tone, seizures, progressive neurological deterioration, poor temperature regulation and characteristic kinky hair.[116,117] As a result of the mutation, copper distribution is disrupted resulting in accumulation in some tissues, whereas the brain and other tissues have unusually low levels. One important location of ATP7A is in the intestines where it is required for the absorption and transport of copper into the circulation. ATP7A is also located at the *trans*-Golgi network and is essential for transporting copper from the cytosol into the lumen for incorporation into secreted copper-requiring enzymes.[8-10, 115] The disease phenotypes are caused by mutational inactivation of ATP7A and inability of dietary copper to be absorbed and supplied to essential enzymes. The decreased supply of copper reduces the activity of copper-dependent proteins, reduced lysyl oxidase activity has been linked to hair and connective tissue abnormalities and neurological degeneration is suggested to be caused by reduced activity of neuronal cytochrome c oxidase.[118]

Mutations in the gene for ATP7B is linked to the autosomal recessive disorder Wilson's disease.[119] This is characterised by the accumulation of copper in the liver and brain[119] and a failure to excrete copper from the liver to bile. This results in toxic accumulation of the metal which kills hepatocytes and inadvertently releases copper into the central nervous system.[120] Symptoms present as liver disease and neurological or psychiatric issues such as parkinsonism, seizures and behavioural changes. Visible dark rings that circle the iris of the eye are often seen in affected patients, known as Kayser-Fleischer rings, and these are a diagnostic sign of the disease.

1.9 Bacterial Copper Homeostasis

It is currently thought that bacterial cells have a lower requirement for copper than eukaryotes. Understanding the routes of copper transport in bacteria is further complicated by the expectation of distinctive pathways and proteins between Gram-positive and Gram-negative organisms due to different cellular scaffolding. Nonetheless, there are three core

components involved in copper trafficking within Gram-positive and Gram-negative bacteria; a copper exporter, a copper chaperone and a copper-responsive transcriptional regulator.

The mechanism of copper import into Gram-positive bacteria is not fully understood. Several systems have been proposed, such as the action of YcnJ[121] and ZosA[23] as copper importers in *Bacillus subtilis*, however further evidence is required. The trafficking of copper to required destinations and the prevention of toxicity in the cytoplasm is undertaken by copper chaperones such as CopZ of *Enterococcus hirae*.[25] CopZ is an 8-kDa protein with a βαββαβ-fold and MXCXXC Cu^{1+}-binding motif that are both found in the yeast proteins Atx1 and Ccs1, and the human protein HAH1 *(Figure 1.5)*. Also, some methane-oxidising bacteria (methanotrophs) that oxidise methane to methanol secrete copper-binding peptides named methanobactins which mediate copper entry into the cell.[122, 123] In *E. coli* (Gram-negative), *c*opper resistance is attributed to two copper efflux systems, the Cue (copper efflux) and Cus (copper sensing) systems. The Cue system is the primary copper export route, whereas the Cus system is up-regulated under extreme levels of copper stress in order to transport copper across the cell envelope to the extracellular space.[124] The Cus system mediates the efflux of copper from the cytoplasm to the periplasm by the P-type ATPase CopA,[125] which shares similarities to the ATP7A and ATP7B transporters in humans, and Ccc2 in yeast. Further copper tolerance is attributed to a multi-copper oxidase, CueO, which oxidises Cu^{1+} to Cu^{2+} in the periplasm, thereby decreasing the rate of copper entry into the cytoplasm.[126] Both CopA and CueO are upregulated when cells are exposed to even low levels of copper.[124, 127] The Gram-positive bacteria *Bacillus subtilis* has also been shown to contain the metallochaperone CopZ which has a similar structure to yeast Atx1 and is thought to transfer copper to the transporter CopA.[128]

1.10 Cross-Talk Amongst Copper Pathways

Atx1 and Ccs1 are both cytosolic chaperones. The mechanism of how cells distribute copper between the various trafficking pathways is yet to be understood, the entry of copper into a cell is known but how the ions are then allocated along a particular route can only be theorized. Copper recruitment by the Ccs1 and Atx1 chaperones may occur from intracellular copper pools located in the mitochondrial matrix,[129] or in the cytoplasm. If this

is the case then the distribution of copper would depend on the specific affinity of the chaperones and their abundance within that location. Another possibility is that the chaperones actively collect copper from the Ctr1 transporter. In this scenario the distribution of copper would depend on preferential interactions at the chaperone-transporter interface, resulting in a competition between Atx1 and Ccs1 for copper. There is some evidence to support this mechanism as the exchange of copper between Ctr1 and Atx1 has been shown.[130] There are similarities between Ccs1 and Atx1 that are not limited to the copper binding motif, such as the βαββαβ-fold structure which is homologous to Atx1 and Ccs1 D1. This would suggest that they transfer or collect copper through a similar process, however, a study with chimeric genes have shown that Atx1 is unable to substitute for Ccs1 D1[104] and each mechanism of copper insertion seem to differ.

1.11 CCS-independent organisms

Certain eukaryotic organisms can activate SOD1 independently of the copper chaperone, such as the roundworm *Caenorhabditis elegans*, in a process thought to involve glutathione. This process may be explained by an ability of the cysteine residues involved in disulphide formation to undergo oxidation more readily.[131,132] In humans, it has been shown that SOD1 activation is achieved in cell lines that are unable to express CCS1 and that SOD1 can also receive copper via glutathione. In contrast, the Sod1 from yeast *S. cerevisiae* is unable to acquire copper independently of Ccs1, due to the presence of a proline residue near the C-terminal of the Sod1 protein.[133] This inability of *S. cerevisiae* to undergo Ccs1-independent activation of Sod1 makes it an ideal system for studying the intricate copper pathways involving Sod1 and Ccs1 because any alterations will not be masked by a basic level of activation independent of Ccs1.

1.12 The Use of Mutations to Investigate Cu^{1+} Affinities

The use of mutations to investigate the function of proteins has a long history in the biological sciences. One of the most direct ways to discover the function of a protein encoded by a particular gene is to observe what happens after the introduction of specific changes to its gene. Due to the interruption of cellular processes, mutations can be used to provide a means to understanding protein function. In studying the binding of Cu^{1+} to a

protein that has more than one binding site, as is the case with Ccs1, small changes can afford the ability to focus on a single binding-site in isolation. Such changes, such as to single amino acids, can be achieved with site-directed mutagenesis. By altering only selected amino acids using this technique, the effect on protein folding, interactions with other proteins and enzymatic function can be minimised if required.

In order to study the importance of the D1 Cys17 and Cys20, and D3 Cys229 and Cys231 residues in Ccs1, their mutation would be of great use. By removing the ability of the Cys-containng motif of one domain (D1 or D3) to bind Cu^{1+} or to form disulfide bonds, the remaining domain can be studied in isolation. Previously, the mutation of one or both of these cysteine residues in either D1 or D3 have been performed to study human CCS1 and *S. cerevisiae* Ccs1 *in vitro (Table 1.1)* with the most popular choice being to replace cysteine with serine.

Table 1.1. Mutations of Ccs1/CCS1 in the literature starting with the most recent. A range of single and double amino acid substitutions in the yeast and human proteins that have been studied previously.

Protein	**Mutation(s)**	**Year, Reference**
Human CCS1	Cys22 and Cys/25 to Ser in D1 Cys244 and Cys246 to Ser in D3	2012, [103]
Yeast *(S. cerevisiae)* Ccs1	Cys17 and Cys20 to Ser in D1 Cys229 and Cys231 to Ser in D3	2008, [95]
Human CCS1	Cys22 to Ala in D1 Cys244 to Ala in D3 Cys22 and Cys25 to Ala in D1 Cys244 and Cys246 to Ala in D3	2007, [134]
Human CCS1	Cys22 to Ser in D1 Cys244 to Ser in D3 Cys22 and Cys25 to Ser in D1 Cys244 and Cys246 to Ser in D3	2005, [135]

The side chain of serine is iso-structural to cysteine but includes a hydroxyl (OH) instead of a thiol (SH) group *(Figure 1.12)*. Serine is more hydrophilic than cysteine and is unable to form disulfide bonds. Also, due to the higher electronegativity and lower polarizability of serine compared to cysteine, the deprotonated hydroxyl group of serine is a 'hard' Lewis base and will bind very weakly, if at all to 'soft' Cu^{1+} ions *(see section 1.1.2)*. Therefore, the replacement of cysteine with serine in the CXXC (D1) and CXC (D3) motifs of Ccs1 could remove both the ability to form a disulfide bond and bind Cu^{1+} ions.

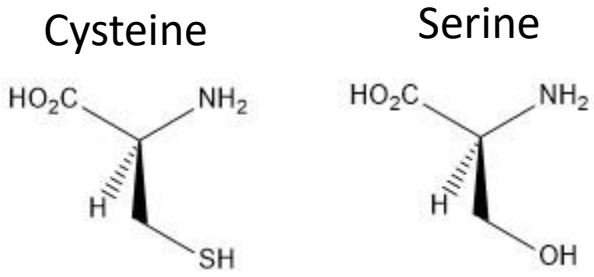

Figure 1.12. The structures of the amino acids cysteine and serine. The structures show the thiol group of cysteine and hydroxyl group of serine. The structures were drawn in ChemBioDraw Ultra.

1.13 The Affinity of Proteins for Metals

To develop a detailed understanding of how copper is driven along complex intracellular pathways the molecular basis of metal binding needs to be clarified. A fundamental property of metallo-proteins is their tendency to associate with specific metal ions. Known as the affinity of a protein *P* for a particular metal *M*, this is defined by the association constant K_b *(Equation 1.2)*.[136] Measurement of the affinity can provide a quantitative indication of metal selection and allows proteins to be compared by this characteristic.

$$M + P \rightleftharpoons MP \qquad K_b = \frac{[MP]}{[M][P]} \qquad \textit{(Equation 1.2)}$$

1.13.1 The Complications of Measuring Protein Affinity

The components of copper-trafficking systems present a variety of issues in a laboratory environment. Many copper-binding proteins, such as Ccs1 and Atx1, employ the amino acid cysteine to coordinate the metal ion, however the thiol side-chains of cysteines are readily oxidised to the disulfide which only binds metals very weakly. The thiol status of these proteins must be fully reduced in order to provide an accurate interaction with the metal. Also, Cu^{1+} is unstable in aqueous solution and prone to disproportionation to the more stable Cu^{2+} *(see section 1.1.1)*, thus it is crucial to review copper samples to determine the oxidation state of the metal in use. The use of specialist anaerobic equipment and sensitive analysis of each constituent can negate these issues, however experiments still require a highly vigilant mind-set even with these strategies in place.

Accurate estimation of Cu^{1+} protein affinities has proven difficult, which is highlighted by the range of values that been reported previously. For example, the affinity of HAH1 for Cu^{1+} has been reported as ranging from 10^5 to 10^{18} M^{-1} *(Table 1.2)*.

The problems with reliable evaluation are due to a variety of factors associated with particular methods and techniques that must be effectively considered. The lowest reported K_b value for HAH1 (10^5 M^{-1}, *Table 1.2*) was measured by the method of isothermal titration calorimetry (ITC). This is a direct method that measures the thermodynamics of interactions between two or more molecules in solution. It is viable that one ITC experiment can quantify the binding stoichiometry, affinity constant (K_b) and binding enthalpy (ΔH^o), and allow the calculation of the Gibbs energy change (ΔG^o) and entropy

change (ΔS^o) of a particular reaction. The ability to determine a complete thermodynamic picture of a binding event makes ITC a particularly useful technique, however major considerations are required to ensure careful analysis of experimental data since titration calorimeters measure the sum of the heat associated with all processes occurring upon titrant aliquots. Analysis of the data must include accurate corrections for precipitation, hydrolysis, redox reactions, metal ion competition with protons and interactions with the buffer.[21, 22] Also, adventitious binding of metal ions to the amino acid side-chains on protein surfaces is typical with K_b values as low as 10^6 M^{-1}, therefore it is improbable that proteins which specifically recruit a particular metal ion would have such a low affinity.

Table 1.2. Literature stated Cu^{1+} affinity *(K_b)* values of various metallo-proteins. The affinity values measured of human and yeast proteins for $Cu^{1+}$by a range of methods.

Protein	Cu^{1+} Affinity K_b (M^{-1})	pH	Reference	Method
HAH1 (Atox1) *Human*	2.5×10^5	6.5	100	ITC[a]
	3.5×10^{10}	7.5	96	Competition with BCA
	1.7×10^{16}	7.5	137	ESI-MS[b], competition with DTT
	3.9×10^{18}	7.0	138	Competition with BCS
	5.6×10^{17}	7.0	139	Competition with BCS
	4.3×10^{17}	7.0	140	Competition with BCS
Atx1 *Yeast*	2.1×10^{18}	7.0	138	Competition with BCS
	10^{19}	8.0	141	Competition with BCS
	10^{16}	6.0	19	Competition with BCS
	4.7×10^{17}	7.0	140	Competition with BCS
CCS1 *Human*	2.4×10^{15}	7.5	137	ESI-MS[b], competition with DTT
	5.5×10^{17}	7.5	103	Competition with BCS
Ccs1 *Yeast*	2.4×10^{17}	7.5	103	Competition with BCS

[a] Isothermal Titration Calorimetry
[b] Electrospray Ionization Mass Spectrometry

1.13.2 Indirect Competition Method

An alternative technique to measure a protein's affinity employs the competition between two ligands for metal ions, one ligand being the protein in question and the other a suitable small molecular ligand. This approach depends exclusively on the final equilibrium positions of the competition reaction, and is not affected by a lot of the issues associated with ITC. The process of complex formation does not affect the final equilibrium, the concentration of 'free' metal is considered negligible at equilibrium and the potential problems of metal hydrolysis and metal ions bound by buffers is prevented.

1.13.3 Ligand Choice

There are a variety of molecules that are able to bind Cu^{1+} however the selection of a suitable competitive ligand is crucial for successful competition. If the affinity of the ligand for Cu^{1+} is too low it will be unable to compete with the protein for the metal, similar problems arise if the ligand affinity is too high, therefore it is necessary to select a ligand with an affinity in the same region as the protein.

Dithiothreitol (DTT) is a small molecule *(Figure 1.13)* generally used as a reducing agent against thiolated DNA and protein disulfide bonds. The two sulfur donors are able to bind suitable metal ions such as Cu^{1+} with stoichiometries being dependent on the reaction conditions.[142] DTT has been used previously as a ligand for Cu^{1+} competition experiments,[137] however there are many problems associated with its use. Among these is the susceptibility of DTT oxidation in air and the requirement of accurate binding stoichiometries, resulting in DTT being designated as an unsatisfactory Cu^{1+} affinity reference.[138]

Two popular ligands used in this area are the bidentate bicinchoninic acid (BCA) and bathocuproine disulfonate (BCS) *(Figure 1.13)* which both bind Cu^{1+} in a 1 : 2 complex with Cu^{1+} and display intense absorption in the visible region. They have been proposed to buffer Cu^{1+} concentrations over the ranges $10^{12} – 10^{16}$ and $10^{15} – 10^{19}$ M^{-1} respectively,[136] making them ideal candidates for competing with higher-affinity proteins. It is important to note that BCA has a lower Cu^{1+} affinity than BCS and for many of the highly selective copper chaperones and target proteins within the affinity range 10^{17} - 10^{19} M^{-1}, BCA is not a suitable competitive ligand.

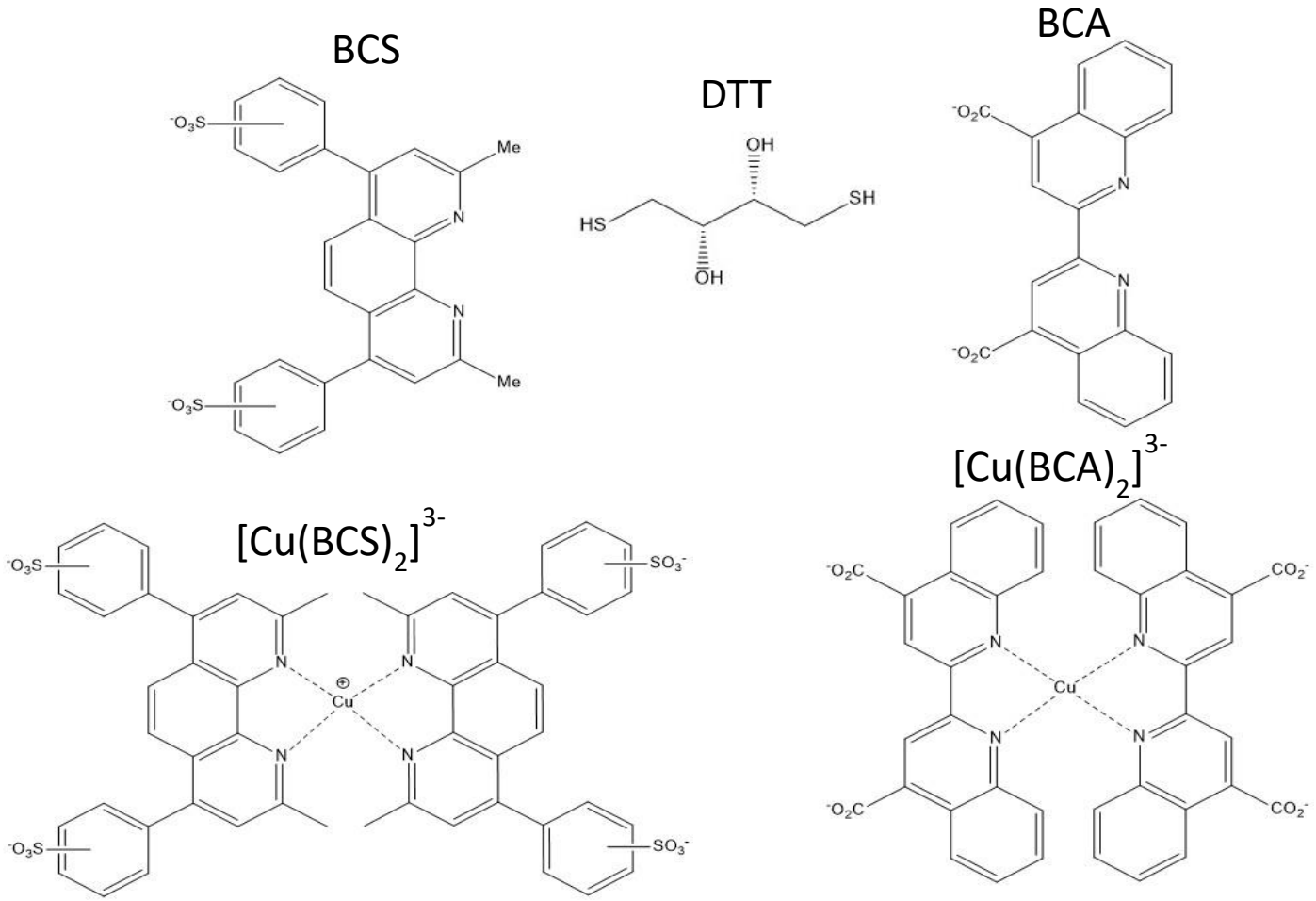

Figure 1.13. Molecular structure of Cu^{1+}-binding ligands. Structures of bathocuproinedisulfonic acid (BCS), bicinchoninic acid (BCA) and dithiothreitol (DTT). The structures were drawn in ChemBioDraw Ultra.

1.13.4 Overall Formation Constants

The competition method for calculation of a protein's affinity for Cu^{1+} requires an accurate affinity value of the probe ligand against which the protein affinity can be measured. In the case of the ligands *L* BCA/BCS which bind Cu^{1+} with a 2:1 stoichiometry, the affinity is defined as the overall formation constant β_2 *(Equation 1.3)*.

$$Cu^+ + 2L \leftrightarrow Cu^+L_2 \qquad \beta_2 = \frac{[Cu^+L_2]}{[Cu^+][L]^2} \qquad \textit{Equation 1.3}$$

Unfortunately, the affinities of the probes have been disputed, and similarly to the affinities, a range of values have been reported in the literature *(Table 1.2)*.

Discrepancies are highly significant when these values are being used to calculate protein affinities, because reliable affinities are required in order to draw conclusions regarding the movement of copper. For example, it has been suggested that copper is driven along particular routes due to affinity gradients,[137] therefore an accurate set of affinities is required to understand trends and mechanisms in copper homeostasis.

Table 1.3. Literature values of formation constant (β_2 values) of BCA and BCS for Cu^{1+}. A selection of the range of β_2 values of BCA and BCS for Cu^{1+} that have been calculated.

Ligand	Overall formation constant β_2 (M^{-2})	Reference
BCA	10^{14}	96
	$10^{11.4}$	19
	$10^{17.2}$	143
	$10^{17.3}$	138
	$10^{17.7}$	144
BCS	$10^{19.8}$	141
	$10^{22.1}$	19
	$10^{19.9}$	138
	$10^{20.8}$	144

Considering that both BCS and BCA both bind Cu^{1+} in a 1 : 2 complex with Cu^{1+} and display intense absorption in the visible region, the simplest method for determining the formation constant would be a direct titration with Cu^{1+}. However, direct addition of Cu^{1+} results in quantitative binding and the amount of complex formation should not exceed 90 % at equimolar concentrations of metal ion to avoid large errors during data analysis.[136]

One method for measuring the affinity of a ligand for a metal ion may be determined by potentiometric titration (Bjerrum titration) through competition with protons. Ligands can be considered as Lewis bases since they donate electron pairs, and the pK_a of a particular ligand atom at the site of copper binding is altered as the metal ion is bound. The proton concentration can be accurately measured by a pH electrode, therefore reliable formation constants can be determined providing that the ligand pK_a values are known. This method has been used to measure the affinity of BCS, although due to the instability of Cu^{1+} in solution, the β_2 of $[Cu^{2+}(BCS)_2]^{2-}$ was measured. This was then used alongside the reduction potential of the Cu^{2+}/Cu^{1+} couple and the Nernst equation to estimate the formation constant of $[Cu^{1+}(BCS)_2]^{3-}$.[138, 141] Unfortunately, uncertainties arise due to the ionic strength dependence of the reduction potentials and the structural differences between the mono- and divalent forms of the copper-BCS complexes. Furthermore, it is difficult to apply this approach to $[Cu^{2+}(BCA)_2]^{2-}$ due to the similar pK_a values of the carboxylate groups and the redox process of Cu^{2+}/Cu^{1+} couple being irreversible which prevents the use of the Nernst equation.

Alternative methods have utilised ITC to measure the β_2 of $[Cu^{I}(BCA)_2]^{2-}$,[96] or competition with other known ligands or proteins.[138, 143, 144] This competition method has also been applied to BCS and a variety of ligands and proteins have been employed to provide affinity standards.[19, 144] The use of cyanide as a competitive ligand has since been disapproved due to the presence of ternary complexes during the titration which prevent the derivation of a reliable formation constant.[144]

1.14 Hypotheses

The primary hypothesis of the work presented here is that the mechanism of copper transfer between the yeast Ccs1 and its target, Sod1, is fundamentally different from that of the human system. The foundation to the objectives used to test this hypothesis will be established via the expression of the full length wild-type Ccs1 protein and various Ccs1 mutant proteins. Double Cys-to-Ser mutations of the copper-binding motifs in D1 and D3 of Ccs1 will allow individual copper-binding sites to be scrutinized whilst also minimising any changes to the overall structure of the protein. Truncated proteins containing either D1/2 or D2/3 only of Ccs1 will also allow individual binding sites to be studied, as well as establish any possible structural contributions of D1 or D3.

The principal objectives to test this hypothesis are to determine the Cu^{1+} binding stoichiometries and affinity values for the copper binding motifs of D1 and D3 of Ccs1 using the Cu^{1+} ligands BCS and BCA. As these values have been determined for human CCS1, the measurement of these values in the yeast counterparts will enable a direct comparison. This will not only provide quantitative insight into the mechanism of copper transfer from Ccs1 to Sod1 in yeast, but also inform the proposed variation between the human and yeast copper-transfer process as suggested in the literature.

Another imperative objective is to investigate the activation of Sod1 by Ccs1 *in vitro* through the expression of Sod1 and the establishment of a Sod1 activity assay. This will identify the ability, if any, of the two distinct copper-binding sites of Ccs1 to activate Sod1 independently of each other and contribute to the overall discussion of the copper-transfer mechanism between Sod1 and Ccs1.

A supplement to these objectives is to investigate the factors that affect the oligomeric status of Ccs1 and the mutant Ccs1 proteins. This will allow direct comparison to the oligomeric status of the human CCS protein which has been extensively studied and designated as relevant to the mechanism of CCS function. The potential factors affecting the oligomerisation of the Ccs1 proteins which are to be investigated include the presence or lack of Cu^{1+}, loss of D1 or D3 and the disulphide status of the two copper binding sites.

An associated hypothesis also investigated in this work is that Ccs1 and another copper metallochaperone from a separate copper trafficking pathway in yeast, Atx1, can compete

for copper. This will be tested through determination of the affinity value for Axt1 using the same method as for Ccs1 and the Ccs1 mutants, which will provide a direct comparison between these proteins and acknowledge any potential interconnectivity between the Ccs1 and Atx1 pathways. Specifically, this could inform whether Ccs1 and Atx1 could compete for copper from the same pool within the cell or identify a method for controlling copper distribution along particular pathways. This investigation will be supplemented via copper exchange experiments between Ccs1 and Atx1 to demonstrate whether the transfer of copper between Atx1 and Ccs1 can occur *in vitro*.

1.15 References

1. H. C. Gasteiger E., Gattiker A., Duvaud S., Wilkins M.R., Appel R.D., Bairoch A., *Protein Identification and Analysis Tools on the ExPASy Server*, Humana Press, 2005.
2. W. C. Johnson, *Proteins: Structure, Function, and Bioinformatics*, 1990, **7**, 205-214.
3. J. F. Monty, R. M. Llanos, J. F. Mercer and D. R. Kramer, *The Journal of nutrition*, 2005, **135**, 2762-2766.
4. D. S. Shin, M. DiDonato, D. P. Barondeau, G. L. Hura, C. Hitomi, J. A. Berglund, E. D. Getzoff, S. C. Cary and J. A. Tainer, *Journal of Molecular Biology*, 2009, **385**, 1534-1555.
5. Maud E. S. Achard, Sian L. Stafford, Nilesh J. Bokil, J. Chartres, Paul V. Bernhardt, Mark A. Schembri, Matthew J. Sweet and Alastair G. McEwan, *Biochemical Journal*, 2012, **444**, 51-57.
6. C. White, J. Lee, T. Kambe, K. Fritsche and M. J. Petris, *Journal of Biological Chemistry*, 2009, **284**, 33949-33956.
7. D. Wagner, J. Maser, B. Lai, Z. Cai, C. E. Barry, K. Höner zu Bentrup, D. G. Russell and L. E. Bermudez, *The Journal of Immunology*, 2005, **174**, 1491-1500.
8. F. D'Amico, E. Skarmoutsou, S. Sanfilippo and J. Camakaris, *Acta histochemica*, 2005, **107**, 373-378.
9. M. J. Petris, D. Strausak and J. F. Mercer, *Human molecular genetics*, 2000, **9**, 2845-2851.
10. T. C. Steveson, G. D. Ciccotosto, X. M. Ma, G. P. Mueller, R. E. Mains and B. A. Eipper, *Endocrinology*, 2003, **144**, 188-200.
11. J. A. Tainer, E. D. Getzoff, J. S. Richardson and D. C. Richardson, *Nature*, 1983, **306**, 284.
12. F. Haber and J. Weiss, *Naturwissenschaften*, 1932, **20**, 948-950.
13. H. J. H. Fenton, *Journal of the Chemical Society, Transactions*, 1894, **65**, 899-910.
14. H. Irving and R. J. P. Williams, *Journal of the Chemical Society (Resumed)*, 1953, **0**, 3192-3210.
15. L. Macomber and J. A. Imlay, *Proceedings of the National Academy of Sciences*, 2009, **106**, 8344-8349.
16. S. Tottey, K. J. Waldron, S. J. Firbank, B. Reale, C. Bessant, K. Sato, T. R. Cheek, J. Gray, M. J. Banfield, C. Dennison and N. J. Robinson, *Nature*, 2008, **455**, 1138-1142.
17. T. D. Rae, P. J. Schmidt, R. A. Pufahl, V. C. Culotta and T. V. O'Halloran, *Science*, 1999, **284**, 805-808.
18. N. S. Kosower and E. M. Kosower, in *International Review of Cytology*, eds. G. H. Bourne, J. F. Danielli and K. W. Jeon, Academic Press, 1978, vol. 54, pp. 109-160.
19. C. S. Sevier and C. A. Kaiser, *Nature Reviews Molecular Cell Biology*, 2002, **3**, 836.
20. M. E. Reardon-Robinson and H. Ton-That, *Journal of Bacteriology*, 2016, **198**, 746-754.
21. C. Seung-Gu, C. Ki-Doo, J. Seung-Hwan and S. Hang-Cheol, *Mol. Cells*, 2003, **16**, 323-330.
22. J. Wypych, M. Li, A. Guo, Z. Zhang, T. Martinez, M. J. Allen, S. Fodor, D. N. Kelner, G. C. Flynn, Y. D. Liu, P. V. Bondarenko, M. S. Ricci, T. M. Dillon and A. Balland, *The Journal of Biological Chemistry*, 2008, **283**, 16194-16205.
23. T. Fukuhara, K. Kobayashi, Y. Kanayama, S. Enomoto, T. Kondo, N. Tsunekawa, M. Nemoto, N. Ogasawara, K. Inagaki and T. Tamura, *Bioscience, biotechnology, and biochemistry*, 2016, **80**, 600-609.
24. R. Wimmer, T. Herrmann, M. Solioz and K. Wuthrich, *J Biol Chem*, 1999, **274**, 22597-22603.
25. D. A. Capdevila, K. A. Edmonds and D. P. Giedroc, *Essays in biochemistry*, 2017, **61**, 177-200.
26. A. K. Wernimont, D. L. Huffman, A. L. Lamb, T. V. O'Halloran and A. C. Rosenzweig, *Nat Struct Biol*, 2000, **7**, 766-771.
27. M. Goujon, H. McWilliam, W. Li, F. Valentin, S. Squizzato, J. Paern and R. Lopez, *Nucleic Acids Research*, 2010, **38**, W695-W699.
28. R. Hassett, D. R. Dix, D. J. Eide and D. J. Kosman, *Biochemical Journal*, 2000, **351**, 477-484.
29. E. Georgatsou, L. A. Mavrogiannis, G. S. Fragiadakis and D. Alexandraki, *Journal of Biological Chemistry*, 1997, **272**, 13786-13792.
30. R. Hassett and D. J. Kosman, *Journal of Biological Chemistry*, 1995, **270**, 128-134.

31. R. A. Pufahl, C. P. Singer, K. L. Peariso, S. J. Lin, P. J. Schmidt, C. J. Fahrni, V. C. Culotta, J. E. Penner-Hahn and T. V. O'Halloran, *Science*, 1997, **278**, 853-856.
32. C. Askwith, D. Eide, A. Van Ho, P. S. Bernard, L. Li, S. Davis-Kaplan, D. M. Sipe and J. Kaplan, *Cell*, 1994, **76**, 403-410.
33. A. B. Maxfield, D. N. Heaton and D. R. Winge, *Journal of Biological Chemistry*, 2004, **279**, 5072-5080.
34. S. C. Leary, P. A. Cobine, B. A. Kaufman, G.-H. Guercin, A. Mattman, J. Palaty, G. Lockitch, D. R. Winge, P. Rustin, R. Horvath and E. A. Shoubridge, *Cell Metabolism*, 2007, **5**, 9-20.
35. V. C. Culotta, L. W. J. Klomp, J. Strain, R. L. B. Casareno, B. Krems and J. D. Gitlin, *Journal of Biological Chemistry*, 1997, **272**, 23469-23472.
36. J. L. Lopes, A. J. Miles, L. Whitmore and B. A. Wallace, *Protein science : a publication of the Protein Society*, 2014, **23**, 1765-1772.
37. V. C. Culotta, W. R. Howard and X. F. Liu, *Journal of Biological Chemistry*, 1994, **269**, 25295-25302.
38. S. S. Narula, D. R. Winge and I. M. Armitage, *Biochemistry*, 1993, **32**, 6773-6787.
39. L. T. Jensen, W. R. Howard, J. J. Strain, D. R. Winge and V. C. Culotta, *Journal of Biological Chemistry*, 1996, **271**, 18514-18519.
40. M. S. Cyert and C. C. Philpott, *Genetics*, 2013, **193**, 677-713.
41. E. M. Rees, J. Lee and D. J. Thiele, *Journal of Biological Chemistry*, 2004, **279**, 54221-54229.
42. D. H. Hamer, D. J. Thiele and J. E. Lemontt, *Science*, 1985, **228**, 685-690.
43. E. B. Gralla, D. J. Thiele, P. Silar and J. S. Valentine, *Proc Natl Acad Sci U S A*, 1991, **88**, 8558-8562.
44. C. T. Dameron, D. R. Winge, G. N. George, M. Sansone, S. Hu and D. Hamer, *Proceedings of the National Academy of Sciences of the United States of America*, 1991, **88**, 6127-6131.
45. A. Dobi, C. T. Dameron, S. Hu, D. Hamer and D. R. Winge, *J Biol Chem*, 1995, **270**, 10171-10178.
46. L. T. Jensen and D. R. Winge, *European Molecular Biology Organization Journal*, 1998, **17**, 5400-5408.
47. M. M. Pena, K. A. Koch and D. J. Thiele, *Mol Cell Biol*, 1998, **18**, 2514-2523.
48. Y. Yamaguchi-Iwai, M. Serpe, D. Haile, W. Yang, D. J. Kosman, R. D. Klausner and A. Dancis, *J Biol Chem*, 1997, **272**, 17711-17718.
49. S. Labbe, Z. Zhu and D. J. Thiele, *J Biol Chem*, 1997, **272**, 15951-15958.
50. Z. Zhu, S. Labbe, M. M. Pena and D. J. Thiele, *J Biol Chem*, 1998, **273**, 1277-1280.
51. J. Yonkovich, R. McKenndry, X. Shi and Z. Zhu, *J Biol Chem*, 2002, **277**, 23981-23984.
52. C. E. Ooi, E. Rabinovich, A. Dancis, J. S. Bonifacino and R. D. Klausner, *The EMBO Journal*, 1996, **15**, 3515-3523.
53. Y. Yamaguchi-Iwai, M. Serpe, D. Haile, W. Yang, D. J. Kosman, R. D. Klausner and A. Dancis, *Journal of Biological Chemistry*, 1997, **272**, 17711-17718.
54. S. Labbé, Z. Zhu and D. J. Thiele, *Journal of Biological Chemistry*, 1997, **272**, 15951-15958.
55. A. Joshi, M. Serpe and D. J. Kosman, *Journal of Biological Chemistry*, 1999, **274**, 218-226.
56. M. Yukawa, K. Amano, M. Suzuki-Yasumoto and M. Terai, *Archives of environmental health*, 1980, **35**, 36-44.
57. L. Rossi, M. F. Lombardo, M. R. Ciriolo and G. Rotilio, *Neurochemical Research*, 2004, **29**, 493-504.
58. T. Tsukihara, H. Aoyama, E. Yamashita, T. Tomizaki, H. Yamaguchi, K. Shinzawa-Itoh, R. Nakashima, R. Yaono and S. Yoshikawa, *Science*, 1996, **272**, 1136-1144.
59. J. S. Ingwall, *ATP and the Heart*, Springer US, 2012.
60. H. Suga, *Physiological Reviews*, 1990, **70**, 247-277.
61. C. L. Gibbs, *Physiological Reviews*, 1978, **58**, 174-254.
62. S. A. Molloy and J. H. Kaplan, *Journal of Biological Chemistry*, 2009, **284**, 29704-29713.
63. K. Terada, Y. Kawarada, N. Miura, O. Yasui, K. Koyama and T. Sugiyama, *Biochimica et Biophysica Acta (BBA) - Molecular Basis of Disease*, 1995, **1270**, 58-62.

64. M. Sato and J. D. Gitlin, *Journal of Biological Chemistry*, 1991, **266**, 5128-5134.
65. I. Hamza, M. Schaefer, L. W. J. Klomp and J. D. Gitlin, *Proceedings of the National Academy of Sciences*, 1999, **96**, 13363-13368.
66. C. Oswald, U. Krause-Buchholz and G. Rödel, *Journal of Molecular Biology*, 2009, **389**, 470-479.
67. R. Rakhit and A. Chakrabartty, *Biochimica et Biophysica Acta (BBA) - Molecular Basis of Disease*, 2006, **1762**, 1025-1037.
68. Y. Furukawa and T. V. O'Halloran, *Antioxidants & redox signaling*, 2006, **8**, 847-867.
69. J. F. Turrens, *Bioscience Reports*, 1997, **17**, 3-8.
70. N. L. Ogihara, H. E. Parge, P. J. Hart, M. S. Weiss, J. J. Goto, B. R. Crane, J. Tsang, K. Slater, J. A. Roe, J. S. Valentine, D. Eisenberg and J. A. Tainer, *Biochemistry*, 1996, **35**, 2316-2321.
71. I. Bertini, M. Piccioli, M. S. Viezzoli, C. Y. Chiu and G. T. Mullenbach, *European Biophysics Journal*, 1994, **23**, 167-176.
72. H. X. Deng, A. Hentati, J. A. Tainer, Z. Iqbal, A. Cayabyab, W. Y. Hung, E. D. Getzoff, P. Hu, B. Herzfeldt, R. P. Roos and a. et, *Science*, 1993, **261**, 1047-1051.
73. L. M. Murphy, R. W. Strange and S. S. Hasnain, *Structure*, 1997, **5**, 371-379.
74. K. Djinovic, G. Gatti, A. Coda, L. Antolini, G. Pelosi, A. Desideri, M. Falconi, F. Marmocchi, G. Rotilio and M. Bolognesi, *Journal of Molecular Biology*, 1992, **225**, 791-809.
75. A. L. Lamb, A. S. Torres, T. V. O'Halloran and A. C. Rosenzweig, *Nature Structural & Molecular Biology*, 2001, **8**, 751-755.
76. E. M. Fielden, P. B. Roberts, R. C. Bray, D. J. Lowe, G. N. Mautner, G. Rotilio and L. Calabrese, *Biochem J*, 1974, **139**, 49-60.
77. D. Klug-Roth, I. Fridovich and J. Rabani, *Journal of the American Chemical Society*, 1973, **95**, 2786-2790.
78. J. Rabani, D. Klug and I. Fridovich, *Israel Journal of Chemistry*, 1972, **10**, 1095-1106.
79. V. V. Smirnov and J. P. Roth, *Journal of the American Chemical Society*, 2006, **128**, 16424-16425.
80. F. Arnesano, L. Banci, I. Bertini, M. Martinelli, Y. Furukawa and T. V. O'Halloran, *Journal of Biological Chemistry*, 2004, **279**, 47998-48003.
81. L. Banci, L. Barbieri, I. Bertini, F. Cantini and E. Luchinat, *PLoS ONE*, 2011, **6**, e23561.
82. L. Banci, L. Barbieri, I. Bertini, E. Luchinat, E. Secci, Y. Zhao and A. R. Aricescu, *Nature Chemical Biology*, 2013, **9**, 297-299.
83. L. Banci, I. Bertini, F. Cantini, T. Kozyreva, C. Massagni, P. Palumaa, J. T. Rubino and K. Zovo, *Proceedings of the National Academy of Sciences*, 2012, **109**, 13555-13560.
84. C. Hwang, A. J. Sinskey and H. F. Lodish, *Science*, 1992, **257**, 1496-1502.
85. Y. Furukawa, A. S. Torres and T. V. O'Halloran, *European Molecular Biology Organization Journal*, 2004, **23**, 2872-2881.
86. L. J. Haverkamp, V. Appel and S. H. Appel, *Brain : a journal of neurology*, 1995, **118 (Pt 3)**, 707-719.
87. D. R. Rosen, T. Siddique, D. Patterson, D. A. Figlewicz, P. Sapp, A. Hentati, D. Donaldson, J. Goto, J. P. O'Regan, H. X. Deng and et al., *Nature*, 1993, **362**, 59-62.
88. H. X. Deng, A. Hentati, J. A. Tainer, Z. Iqbal, A. Cayabyab, W. Y. Hung, E. D. Getzoff, P. Hu, B. Herzfeldt, R. P. Roos and et al., *Science*, 1993, **261**, 1047-1051.
89. L. I. Bruijn, M. K. Houseweart, S. Kato, K. L. Anderson, S. D. Anderson, E. Ohama, A. G. Reaume, R. W. Scott and D. W. Cleveland, *Science*, 1998, **281**, 1851-1854.
90. E. J. Yoon, H. J. Park, G. Y. Kim, H. M. Cho, J. H. Choi, H. Y. Park, J. Y. Jang, H. S. Rhim and S. M. Kang, *Experimental & molecular medicine*, 2009, **41**, 611-617.
91. S. A. Ezzi, M. Urushitani and J. P. Julien, *J Neurochem*, 2007, **102**, 170-178.
92. A. L. Lamb, A. K. Wernimont, R. A. Pufahl, V. C. Culotta, T. V. O'Halloran and A. C. Rosenzweig, *Nature Structural & Molecular Biology*, 1999, **6**, 724-729.
93. T. Endo, T. Fujii, K. Sato, N. Taniguchi and J. Fujii, *Biochemical and Biophysical Research Communications*, 2000, **276**, 999-1004.

94. P. J. Schmidt, C. Kunst and V. C. Culotta, *Journal of Biological Chemistry*, 2000, **275**, 33771-33776.
95. K. Kirby, L. T. Jensen, J. Binnington, A. J. Hilliker, J. Ulloa, V. C. Culotta and J. P. Phillips, *Journal of Biological Chemistry*, 2008, **283**, 35393-35401.
96. J. Laliberté, L. J. Whitson, J. Beaudoin, S. P. Holloway, P. J. Hart and S. Labbé, *Journal of Biological Chemistry*, 2004, **279**, 28744-28755.
97. F. Arnesano, L. Banci, I. Bertini, D. L. Huffman and T. V. O'Halloran, *Biochemistry*, 2001, **40**, 1528-1539.
98. A. L. Lamb, A. K. Wernimont, R. A. Pufahl, T. V. O'Halloran and A. C. Rosenzweig, *Biochemistry*, 2000, **39**, 1589-1595.
99. K. Djinovic, G. Gatti, A. Coda, L. Antolini, G. Pelosi, A. Desideri, M. Falconi, F. Marmocchi, G. Rolilio and M. Bolognesi, *Acta crystallographica. Section B, Structural science*, 1991, **47 (Pt 6)**, 918-927.
100. The UniProt Consortium, *Nucleic Acids Research*, 2017, **45**, D158-D169.
101. F. Sievers, A. Wilm, D. Dineen, T. J. Gibson, K. Karplus, W. Li, R. Lopez, H. McWilliam, M. Remmert, J. Söding, J. D. Thompson and D. G. Higgins, *Molecular Systems Biology*, 2011, **7**.
102. A. L. Caruano-Yzermans, T. B. Bartnikas and J. D. Gitlin, *Journal of Biological Chemistry*, 2006, **281**, 13581-13587.
103. S. Allen, A. Badarau and C. Dennison, *Biochemistry*, 2012, **51**, 1439-1448.
104. P. J. Schmidt, T. D. Rae, R. A. Pufahl, T. Hamma, J. Strain, T. V. O'Halloran and V. C. Culotta, *Journal of Biological Chemistry*, 1999, **274**, 23719-23725.
105. A. C. Rosenzweig, *Accounts of Chemical Research*, 2000, **34**, 119-128.
106. T. D. Rae, A. S. Torres, R. A. Pufahl and T. V. O'Halloran, *Journal of Biological Chemistry*, 2001, **276**, 5166-5176.
107. G. S. A. Wright, S. S. Hasnain and J. G. Grossmann, *Biochemical Journal*, 2011, **439**, 39-44.
108. A. C. Rosenzweig, D. L. Huffman, M. Y. Hou, A. K. Wernimont, R. A. Pufahl and T. V. O'Halloran, *Structure*, 1999, **7**, 605-617.
109. D. Fu, T. J. Beeler and T. M. Dunn, *Yeast*, 1995, **11**, 283-292.
110. L. Banci, I. Bertini, S. Ciofi-Baffoni, D. L. Huffman and T. V. O'Halloran, *Journal of Biological Chemistry*, 2001, **276**, 8415-8426.
111. F. Arnesano, L. Banci, I. Bertini, S. Ciofi-Baffoni, E. Molteni, D. L. Huffman and T. V. O'Halloran, *Genome Research*, 2002, **12**, 255-271.
112. M. E. Portnoy, A. C. Rosenzweig, T. Rae, D. L. Huffman, T. V. O'Halloran and V. C. Culotta, *Journal of Biological Chemistry*, 1999, **274**, 15041-15045.
113. A. K. Wernimont, D. L. Huffman, A. L. Lamb, T. V. O'Halloran and A. C. Rosenzweig, *Nature Structural Molecular Biology*, 2000, **7**, 766-771.
114. D. L. Huffman and T. V. O'Halloran, *Journal of Biological Chemistry*, 2000, **275**, 18611-18614.
115. C. Vulpe, B. Levinson, S. Whitney, S. Packman and J. Gitschier, *Nature Genetics*, 1993, **3**, 7-13.
116. L. B. Moller, M. Mogensen and N. Horn, *Biochimie*, 2009, **91**, 1273-1277.
117. J. H. Menkes, M. Alter, G. K. Steigleder, D. R. Weakley and J. H. Sung, *Pediatrics*, 1962, **29**, 764-779.
118. S. G. Kaler, *Advances in pediatrics*, 1994, **41**, 263-304.
119. P. C. Bull, G. R. Thomas, J. M. Rommens, J. R. Forbes and D. W. Cox, *Nature Genetics*, 1993, **5**, 327-337.
120. A. Ala, A. P. Walker, K. Ashkan, J. S. Dooley and M. L. Schilsky, *The Lancet*, 2007, **369**, 397-408.
121. S. Chillappagari, M. Miethke, H. Trip, O. P. Kuipers and M. A. Marahiel, *Journal of Bacteriology*, 2009, **191**, 2362-2370.
122. A. El Ghazouani, A. Baslé, S. J. Firbank, C. W. Knapp, J. Gray, D. W. Graham and C. Dennison, *Inorganic Chemistry*, 2011, **50**, 1378-1391.
123. H. J. Kim, D. W. Graham, A. A. DiSpirito, M. A. Alterman, N. Galeva, C. K. Larive, D. Asunskis and P. M. A. Sherwood, *Science*, 2004, **305**, 1612-1615.

124. F. W. Outten, D. L. Huffman, J. A. Hale and T. V. O'Halloran, *Journal of Biological Chemistry*, 2001, **276**, 30670-30677.
125. C. Rensing, B. Fan, R. Sharma, B. Mitra and B. P. Rosen, *Proceedings of the National Academy of Sciences*, 2000, **97**, 652-656.
126. G. Grass and C. Rensing, *Biochemical and Biophysical Research Communications*, 2001, **286**, 902-908.
127. J. V. Stoyanov, J. L. Hobman and N. L. Brown, *Molecular Microbiology*, 2001, **39**, 502-512.
128. L. Banci, I. Bertini, R. Del Conte, J. Markey and F. J. Ruiz-Dueñas, *Biochemistry*, 2001, **40**, 15660-15668.
129. P. A. Cobine, L. D. Ojeda, K. M. Rigby and D. R. Winge, *Journal of Biological Chemistry*, 2004, **279**, 14447-14455.
130. Z. Xiao and A. G. Wedd, *Chemical Communications*, 2002, **0**, 588-589.
131. L. T. Jensen and V. C. Culotta, *Journal of Biological Chemistry*, 2005, **280**, 41373-41379.
132. J. M. Leitch, L. T. Jensen, S. D. Bouldin, C. E. Outten, P. J. Hart and V. C. Culotta, *Journal of Biological Chemistry*, 2009, **284**, 21863-21871.
133. M. C. Carroll, J. B. Girouard, J. L. Ulloa, J. R. Subramaniam, P. C. Wong, J. S. Valentine and V. C. Culotta, *Proceedings of the National Academy of Sciences of the United States of America*, 2004, **101**, 5964-5969.
134. J. P. Stasser, G. S. Siluvai, A. N. Barry and N. J. Blackburn, *Biochemistry*, 2007, **46**, 11845-11856.
135. J. P. Stasser, J. F. Eisses, A. N. Barry, J. H. Kaplan and N. J. Blackburn, *Biochemistry*, 2005, **44**, 3143-3152.
136. Z. Xiao and A. G. Wedd, *Natural Product Reports*, 2010, **27**, 768-789.
137. L. Banci, I. Bertini, S. Ciofi-Baffoni, T. Kozyreva, K. Zovo and P. Palumaa, *Nature*, 2010, **465**, 645-648.
138. Z. Xiao, J. Brose, S. Schimo, S. M. Ackland, S. La Fontaine and A. G. Wedd, *Journal of Biological Chemistry*, 2011, **286**, 11047-11055.
139. A. Badarau and C. Dennison, *Journal of the American Chemical Society*, 2011, **133**, 2983-2988.
140. S. Allen, A. Badarau and C. Dennison, *Dalton Transactions*, 2013, **42**, 3233-3239.
141. Z. Xiao, F. Loughlin, G. N. George, G. J. Howlett and A. G. Wedd, *Journal of the American Chemical Society*, 2004, **126**, 3081-3090.
142. A. Kr zel, W. Lesniak, M. Jezowska-Bojczuk, P. Mlynarz, J. Brasun, H. Kozlowski and W. Bal, *J Inorg Biochem*, 2001, **84**, 77-88.
143. Z. Xiao, P. S. Donnelly, M. Zimmermann and A. G. Wedd, *Inorganic Chemistry*, 2008, **47**, 4338-4347.
144. P. Bagchi, M. T. Morgan, J. Bacsa and C. J. Fahrni, *Journal of the American Chemical Society*, 2013, **135**, 18549-18559.

Chapter 2: Methods

2.1 Buffer solutions

All buffer solutions were prepared using Milli-Q grade water (Millipore 'Simplicity' water purification system) with a rated resisitivity of ≥ 18M Ωcm. For all solutions, the pH was adjusted by addition of either HCl (BDH, AnalR) or NaOH (Sigma).

2.1.1 Tris(hydroxymethyl)aminomethane Buffer

Tris(hydroxymethyl)aminoethane (Tris) (Sigma) buffer was used primarily in the pH range of 7.0 to 7.5. This buffer was mainly used for the isolation, purification and storage of proteins.

2.1.2 Sodium Acetate Buffer

Sodium acetate (NaOAc) (BDH) buffer was used to buffer solutions in the pH range 3.0 to 6.0. This buffer was primarily used for the dialysis procedure.

2.1.3 4-(2-Hydroxyethyl)piperazine-1-ethanesulfonic Acid Buffer

4-(2-Hydroxyethyl)piperazine-1-ethanesulfonic acid (Hepes) buffer was used to buffer solutions in the pH range 7.0 to 7.5. This buffer was primarily used for copper binding experiments, exchange experiments and Sod1 activation experiments.

2.1.4 2-(N-morpholino)ethanesulphonic Buffer

2-(N-morpholino)ethanesulphonic (Mes) (Sigma) buffer was used to buffer solutions in the pH range 5.5-6.5. This buffer was used primarily for protein purification.

2.1.5 Phosphate buffer

Phosphate buffer was primarily used for the Ellman's thiol assay *(Method 2.15)*. Buffers were prepared by mixing stock solutions of 1 M dibasic and monobasic potassium phosphate, K_2HPO_4 and KH_2PO_4, respectively (Fluka). Dibasic and monobasic phosphates were combined in the proportions shown in Table 2.1 for a particular pH. Small adjustments to the pH were achieved by addition of either HCl or NaOH as required.

K_2HPO_4 (mL)	KH_2PO_4 (mL)	pH
13.2	86.8	6.0
19.2	80.8	6.2
27.8	72.2	6.4
38.1	61.9	6.6
49.7	50.3	6.8
61.5	38.5	7.0
71.7	28.3	7.2
80.2	19.8	7.4
86.6	13.4	7.6
90.8	9.2	7.8
94.0	6.0	8.0

Table 2.1. Volumes of 1 M stocks of K_2HPO_4 and KH_2PO_4 required to prepare 1 L of 0.1 M potassium phosphate buffer solutions in the pH range 6.0 – 8.0.

2.2 Measurement of pH values

Measurement of pH values for buffer solutions were made using an Orion 420A pH meter connected to a Russell glass pH electrode (Thermo, type KCMAW11). The pH meter was calibrated prior to use with two standard buffer solutions of either pH 4.0 and 7.0 or 7.0 and 10.0 (Sigma) depending on the pH range measured.

2.3 DNA Cloning

2.3.1 Isolation of Plasmid DNA from Escherichia coli

Plasmid DNA was isolated and purified from *Escherichia coli* (*E. coli*) using the GenElute Plasmid Miniprep Kit (Sigma). A single colony of the fresh *E. coli* transformant containing the required plasmid were grown in 10 mL fresh LB with 100 μg/mL ampicillin or 100 μg/mL kanamycin, overnight at 37 °C and 250 rpm. A 3-5 mL volume of the overnight culture was used to purify plasmid DNA. The purity of plasmid DNA was judged by measuring the UV spectrum and using the relative absorbances at 260 and 280 nm, where an A_{260}/A_{280} ratio of 1.5-1.8 usually indicated a suitably pure DNA sample with little RNA contamination.

2.3.2 Determination of Plasmid DNA Concentration

The concentration of plasmid DNA was determined by measuring the absorbance of a sample at 260 nm and using the relationship that 1 OD_{260} unit is equal to 50 μg/mL of double

stranded DNA. The concentration of primers purchased from Sigma was based on the DNA synthesis report provided by the companies.

2.3.3 Plasmid DNA Digestion

The digestion of plasmid DNA was carried out using restriction enzymes (BamH1 and Nde1, New England Biolabs) according to the manufacturer's instructions to provide restriction sites for ligation reactions. Typically ≈ 1000-3000 ng of plasmid DNA to be digested in a 50 μL solution containing the required restriction enzymes was incubated at 37 °C for 2 hours followed by heating at 80 °C to inactivate the restriction enzymes. Digested plasmid was then loaded onto an agarose gel for DNA size determination and excision where required.

2.3.4 Ligation Reactions of Plasmid and Insert DNA

Ligation of digested plasmid DNA (pGEMT, Promega) and insert DNA was achieved using the T4 DNA ligase kit (Promega) according to the manufacturer's instructions. Required amounts of plasmid and insert DNA in 10 μL of T4 DNA ligase buffer with the appropriate amount of T4 DNA ligase were typically incubated at 4 °C overnight for ligation reaction. The ligation reaction sample was then transformed into fresh *E. coli* (JM101) competent cells.

2.3.5 Gene amplification

The polymerase chain reaction (PCR) was used to amplify the gene sequence for D1/2-Ccs1 and D2/3-Ccs1 from pGEMT_WT_Ccs1 to incorporate Nde1/BamH1 restriction sites for ligation into pET29a vector. The gene sequence for Sod1 was amplified from S. cerevisiae genomic DNA. The PCR reaction contained 2 ng of template plasmid DNA, 0.4 mM deoxyribonucleotide triphosphates (dNTPs) mix (Promega), 125 ng of each primer (forward and reverse), 1 unit of Q5 polymerase (NEB) and 1 μL of 10x Q5 buffer made up to 10 μL.

2.3.6 Cloning

The plasmids pET29a_yCCS_WT, pET29a_yCCS_SC17-20S and pET29a_yCCS_SC229-231S were created previously by Stephen Allen and Adriana Badarau. The DNA coding for residues 1-222 and 72 - 249 of Ccs1, corresponding to D1/2 and D2/3 respectively, were cloned (primers listed in Table 2.2) incorporating Nde1/BamH1 restriction sites and using the plasmid pGEMT_WT_Ccs1 to amplify the sequence. The DNA coding for wild-type Sod1 were cloned (primers listed in Table 2.2) incorporating Nde1/BamH1 restriction sites and using *S. cerevisiae* genomic DNA obtained from Dr Claudia Schneider. Inserts were ligated

into the Nde1 and EcoR1 restriction sites of pET29a giving pET29a_D1/2_Ccs1, pET29a_D2/3_Ccs1 and pET29a_ySod1

Construct	Primer Sequence 5' → 3'
pET29a_D1/2_Ccs1	GAACATATGACCACGAACGATACATACGAGGC (forward) GAAGGATCCCTACCACACACCAGCGC (reverse)
pET29a_D2/3_Ccs1	GAACATATGGCCGGGAAGCCG (forward) GAAGGATCCCTATTTGATGTTGTTGGCCAAGGC (reverse)
pET29a_ySod1	GAACATATGGTTCAAGCAGTCGC (forward) GAAGGATCCTTAGTTGGTTAGACC (reverse)

Table 2.2. Primers used for making the D1/2-Ccs1 and D2/3-Ccs1 mutants, and cloning Sod1.

2.3.7 DNA Sequencing

DNA sequencing was used to verify truncated and amplified genes in plasmid DNA. Size and purity of DNA was typically assessed by agarose gel electrophoresis and measurement of absorbance of samples at 260 and 280 nm. DNA sequence analysis was then commissioned to Lark Technology (Beckman Coulter).

2.4 Growing of *E.coli*

All growth media was prepared in deionised water and sterilised by autoclaving at 121 ^{o}C for 30 mins.

2.4.1 Growth media LB

Luria-Bertani (LB) medium consisted of 10 g/L tryptone (Melford), 10 g/l NaCl (Melford) and 5 g/l yeast extract (Melford). The LB-agar solid medium consisted of LB supplemented with 15 g/l agar (Melford). The medium was used to grow E. coli strains JM101 for molecular cloning and BL21 for protein expression, typically in the presence of the appropriate antibiotic (100 µg/mL ampicillin or 100 µg/mL kanamycin).

2.4.2 Preparation of Competent E. coli cells

LB was inoculated with a single colony of *E. coli* and incubated overnight at 37 ^{o}C with shaking (250 rpm). The overnight culture was then diluted 100-fold into fresh LB (10ml) and grown for a further 2 hours under the same conditions. Cells were then spun down at 1500 × g for 10 mins and the cell pellet resuspended in ice cold TSS (1ml of a solution of 85% LB, 10% PEG, 5% DMSO and 50 mM MgCl).[145]

2.4.3 Transformation of E. coli

To 100 µL of competent cells 1-3 µL of plasmid DNA was added and incubated on ice for 20 minutes before heat shocking at 42 °C for ≈ 1 min. The solution was incubated on ice for a further 2 mins before adding 1 mL of LB and incubating at 37 °C with shaking (250rpm) for 1 hour. After incubation, dilutions were made with LB and culture was plated onto freshly prepared LB-Agar plates with appropriate antibiotics (100µg/mL ampicillin or 50µg/mL kanamycin). Plates were incubated overnight at 37 °C.[145]

2.4.4 Expression studies: Total and Soluble Cell Protein

In order to determine the growing period for optimal protein expression (as judged by SDS-PAGE) small-scale trials were carried out with the pET29a expression plasmid, containing the required protein gene insert, transformed into *E.coli* strain BL21. LB (10 ml containing 100 µg/mL kanamycin for Ccs1 variants and Sod1) was inoculated with a single colony containing the expression plasmid and grown overnight at 37 °C with shaking (250 rpm). The next day a 100-fold dilution of each culture into LB (50 ml containing 100 µg/mL kanamycin) was made and incubated for 2 hours at 37 °C with shaking (i.e. until the OD_{600} had reached ≈ 0.6-0.8). Isopropyl β-D-1-thiogalactopyranoside (IPTG) was then added to an effective concentration of 1 mM. Samples (5 ml) of the cultures were taken at times of 0, 2, 4, 6 hours and overnight after induction with IPTG. The samples were spun down at 12,000 rpm in a desktop centrifuge for ≈ 5 mins, the supernatant removed and the cell pellet and resuspended in buffer. Samples from cultures were sonicated and 100µl was removed for total protein content. The remaining solution was pelleted at ≈ 12,000 g in a desktop centrifuge for ≈ 5 minutes and 100µl of the supernatant removed for soluble protein content. Samples were then analysed by SDS-PAGE to judge an optimal cell harvesting time after protein induction.

2.5 Overexpression and Purification of Proteins from *E.coli* BL21

2.5.1 Overexpression of WT-Ccs1, the Cys-to-Ser mutants, D2/3-Ccs1, Atx1 and Sod1

Escherichia coli BL21 transformed with either pET29a_yCCS_WT, pET29a_yCCS_SC17-20S, pET29a_yCCS_SC229-231S, pET29a_yD2_3_Ccs1, Atx1 and pET29a_ySod1 was grown in LB medium at 37 °C until an OD_{600} 0.6 - 0.8 was reached. Protein expression was induced by the addition of 1 mM Isopropyl β-D-thiogalactopyranoside, and cells were incubated for a further 6 hours before being harvested, with pellets stored at -30 °C.

2.5.2 Overexpression of D1/2-Ccs1

Escherichia coli BL21 transformed with pET29a_yD1_2_Ccs1 were grown in LB medium at 37 ^{o}C until an OD_{600} 0.6 - 0.8 was reached. Protein expression was induced by the addition of 1 mM Isopropyl β-D-thiogalactopyranoside, and cells were incubated overnight at 16 ^{o}C before being harvested, with pellets stored at -30 ^{o}C.

2.5.3 Purification of WT-Ccs1, Cys-to-Ser Mutants and Truncated Mutant D1/2-Ccs1

Cells were resuspended in 20 mM tris(hydroxymethyl)aminomethane (Tris) pH 8.0, sonicated and centrifuged at 35,000 g for 20 min (+4^{o}C). The supernatant was diluted 4-fold with Milli-Q water prior to being loaded onto a self-packed DEAE-Sepharose column (50 mL, GE Healthcare). Protein was eluted with a linear NaCl gradient (0 – 500 mM) in 5 mM Tris (pH 8.0). Fractions containing Ccs1 [identified by sodium dodecyl sulphate-polyacrylamide gel electrophoresis (SDS-PAGE)] were combined and exchanged via ultrafiltration (Amicon stirred cell with a 10 kDa molecular mass cutoff membrane) into 5 mM Mes (pH 6.5). The final purification step included a HiTrap SP column (5 mL, GE Healthcare) with a 0 – 300 mM NaCl gradient, and fractions containing pure protein (≥ 90 % as judged by SDS-PAGE) were combined.

2.5.4 Purification of Atx1

Cells were resuspended in 20 mM tris(hydroxymethyl)aminomethane (Tris) pH 8.0, sonicated and centrifuged at 35,000 g for 20 min (+4 ^{o}C). The supernatant was diluted 4-fold with Milli-Q water prior to being loaded onto a self-packed DEAE-Sepharose column (50 mL, GE Healthcare). Protein was eluted with cuts of buffer containing 0, 0.2, 0.4 and 1 M NaCl and fractions containing Atx1 were identified by sodium dodecyl sulphate-polyacrylamide gel electrophoresis (SDS-PAGE). Protein fractions were combined and exchanged using ultrafiltration (Amicon stirred cell with a 5 kDa molecular mass cut-off membrane) into 10 mM **2- (*N*-Morpholino) ethanesulfonic acid hydrate** (Mes) pH 6.0. The next purification step used a HiTrap SP column (5 mL, GE Healthcare) with a 0 – 300 mM NaCl gradient, and fractions containing Atx1 (as judged by SDS-PAGE) were combined and reduced to < 10 mL using ultrafiltration and 2 mM DTT added. The final purification step used an S75 gel filtration column equilibrated with 20 mM Hepes, 200 mM NaCl ph 7.5 and injections containing ≤ 10 mg Atx1 were monitored at 280 nm. Fractions containing monomeric Atx1 were combined.

2.5.5 Purification of Sod1

Cells were resuspended in 20 mM tris(hydroxymethyl)aminomethane (Tris) pH 8.0, sonicated and centrifuged at 35,000 g for 20 min (+4^{o}C). The supernatant was diluted 4-fold with Milli-Q water prior to being loaded onto a self-packed DEAE-Sepharose column (50 mL, GE Healthcare). Protein was eluted with a linear NaCl gradient (0 – 500 mM) in 5 mM Tris (pH 8.0). Fractions containing Sod1 [identified by sodium dodecyl sulphate-polyacrylamide gel electrophoresis (SDS-PAGE)] were combined and exchanged via ultrafiltration (Amicon stirred cell with a 10 kDa molecular mass cutoff membrane) into 5 mM Mes (pH 5.0). The final purification step included a HiTrap SP column (5 mL, GE Healthcare) with a 0 – 300 mM NaCl gradient, and fractions containing pure protein (≥ 90 % as judged by SDS-PAGE) were combined.

2.6 Ion exchange chromatography

Ion-exchange chromatography was used for purification of proteins. Diethylaminoethyl (DEAE) sepharose (GE Healthcare) fast flow (FF) column material was used to prepare anion exchange columns for the purification of WT-Ccs1, C17S/C20S-Ccs1, C229S/C231S-Ccs1, D1/2-Ccs1, Atx1 and Sod1. Hitrap SP (5 mL) columns (GE Healthcare) were used for purification of WT-Ccs1, C17S/C20S-Ccs1, C229S/C231S-Ccs1, D1/2-Ccs1 and Sod1. HiTrap Q HP (1 mL) columns (GE Healthcare) were used for copper exchange experiments with Atx1.

2.6.1 Equilibration of Ion-Exchange Column Material

Ion-exchange column material (DEAE-Sepharose) was washed with 2 L of buffer solution prior to use of column for protein purification. The pH of the eluate was checked to ensure equilibration of column. All columns were ran and stored at 4 ^{o}C.

2.6.2 Loading and elution of protein on Ion-Exchange Column Material

Proteins were loaded onto DEAE sepharose column material in the same buffer as that of the column material. Elution of proteins was achieved by increasing the ionic strength of the buffer by providing a NaCl gradient between 0-500 mM NaCl by mixing two buffers with and without the salt.

2.6.3 Regeneration of Ion-Exchange Column Material

DEAE and SP sepharose FF column material was regenerated by washing with 500 ml of 2 M NaCl (contact time ≈ 30 mins) to remove bound proteins. The column material was then

washed with 1 L of distilled water followed by 500 ml of 1 M NaOH (contact time ≈ 30 mins). The material was then washed with distilled water until the pH was neutral. Column materials were stored in 20 % ethanol at 4 ^{o}C.

2.6.4 Ion-exchange using HiTrap Q Column

Protein loading was achieved by syringe, and protein elution was achieved by applying buffer solutions with and without 200 mM NaCl through a peristaltic pump for separation of proteins in an anaerobic chamber for Cu^{1+} exchange experiments.

2.7 Gel Filtration Chromatography

Preparative gel filtration chromatography was used for the purification of proteins whilst analytical gel filtration chromatography was used to determine the oligomeric state of proteins. Masses of proteins, determined on preparative and analytical gel filtration chromatography columns, were deduced by comparison of elution volumes against a set of protein standards of known molecular weight *(Method 2.7.2)*.

2.7.1 Preparative Gel Filtration Chromatography

A Supderdex 75 (10/300 GL GE Healthcare, 24 mL) column attached to an AKTA prime (GE Healthcare) was used for purification of proteins by gel filtration chromatography. A buffer of 20 mM Tris pH 7.5 containing 200 mM NaCl was used as the column buffer. Injection volumes were typically ≤ 2 % of the column volume and eluted at a flow rate of 1 mL/min. Elution of proteins was typically monitored at 280 nm and 215 nm (AKTA prime) or 280 nm (AKTA purifier).

2.7.2 Analytical Gel Filtration Chromatography

Analytical gel filtration chromatography was routinely performed on a Superex 75 column (10/300 GL GE Healthcare, 24 mL) column attached to an AKTA prime. The column was equilibriated in 20 mm Hepes with 200 mM NaCl at pH 7.5 or 20 mm Hepes with 200 mM NaCl plus 250 μM DTT at pH 7.5 at a flow rate of 0.8 mL/min. Absorbance was measured at 280 nm and the typical injection volume of samples (10 – 200 μM) was 200 μL. Buffer without DTT was routinely bubbled with nitrogen for 4 hrs and left in the anaerobic chamber overnight prior to use, and nitrogen was bubbled through during use. The column was calibrated using a low molecular weight calibration kit (GE Healthcare) containing: blue dextran (2000 kDa), conalbumin (75 kDa), ovalbumin (43 kDa), carbonic anhydrase (29 kDa), ribonuclease A (13.7 kDa) and aprotinin (6.5 kDa).

2.8 Ultrafiltration

2.8.1 Centrifugal Ultrafiltration

Amicon ultra 4 (10 kDa MWCO (molecular weight cut-off), Millipore) and Vivaspin 500 (5 kDa and 10 kDa MWCO, Sartorius) centrifugal concentrators were used to concentrate protein solutions and remove adventitiously bound metals through buffer exchange. Exchanging buffer involved concentrating the protein solution and then diluting the sample 10-fold in the concentrator and repeating this process 3 times. A fixed angle rotor operating at ≈ 12,000 g was used to centrifuge samples.

2.8.2 Amicon Stirred Cell Ultrafiltration

An Amicon stirred cell (200 mL cell, Amicon) fitted with an appropriate regenerated cellulose membrane (5-10 kDa MWCO, Millipore) was used to perform buffer exchanges during the purification of proteins. A pressure of approximately 3-4 bar supplied from an N_2 oxygen-free cylinder was applied during operation of the stirred cell.

2.9 Dialysis of protein solutions

2.9.1 Preparation of dialysis tubing

Dialysis tubing (14 kDa MWCO, Sigma) was prepared by soaking the tubing for 1 hour in an aqueous solution of 1 % acetic acid followed by exchange into distilled water and stirring for several minutes. The tubing was then placed into a solution of 1mM ethylenediaminetetraacetic acid (EDTA) and 1 % sodium carbonate and stirred for a further ~3 minutes. The solution was then refreshed and the dialysis tubing heated to ~60 oC and then allowed to cool to room temperature over a period of 30 minutes. The above heating process was repeated once more and dialysis tubing exchanged into Milli-Q water and heated again to 60 ^{o}C and allowed to cool before storing in fresh Milli-Q water (at 4^{o}C).(*2*)

2.9.2 Dialysis of Sod1 Protein Solutions

Dialysis was used for buffer exchange during the preparation of Zn-depleted WT-CCS. Dialysis tubing was washed thoroughly prior to use in buffer to be used during dialysis.

Purified Sod1 was diluted four-fold with 50 mM sodium acetate at pH 3.8 and dialysed against 50 mM sodium acetate at pH 3.8 plus 10 mM EDTA at 4 ^{o}C with stirring for ≈ 5 hrs. The dialysis buffer was then refreshed to 50 mMm sodium acetate at pH 3.8 for 2 hrs, then

refreshed again with the same buffer and stirred overnight. The dialysis buffer was refreshed to 50 mM sodium acetate at pH 5.5 and stirred for a minimum of 3 hrs. The buffer solution was typically 50-100 X sample volume.

2.10 Electrophoresis

2.10.1 Sodium Dodecyl Sulfate-Polyacrylamide Gel Electrophoresis (SDS-PAGE)

A 12 % or 15 % acrylamide/bis-acrylamide (BioRAD) running gel containing 100 mM Tris pH 8.8, 0.1 % SDS, 0.1 % ammonium persulfate (APS, Aldrich) and 0.05 % N,N,N',N'-tetramethylene diamine (TEMED, Aldrich) was prepared in deionised water and allowed to set for 30 mins. The stacking gel, 5 % acrylamide/bis-acrylamide containing 100 mM Tris pH 6.8, 0.1 % SDS, and 0.1 % APS and 0.1 % TEMED in deionised water, was poured directly on top of the running gel. A comb containing 10/15 ridges was inserted into the stacking gel to produce wells for sample loading. The stacking gel was allowed to set for 45 mins. Protein samples for electrophoresis were prepared in cracking buffer [50 mM Tris pH 6.8, 1 % SDS (Aldrich), 15 % glycerol (Sigma), 2 % DTT and 0.025 % bromophenol blue (BDH) in water. Protein samples in cracking buffer were heated at 95 ^{o}C for 5 mins. Typically 10 µL of this protein in cracking buffer was loaded into the wells of the gel. Broad range molecular weight marker (BioRAD) was loaded onto most gels as a reference. The SDS-PAGE buffer was 5 mM Tris pH 8.8 containing 200 mM glycine (Sigma) and 0.1 % SDS. All electrophoresis experiments were performed using a Mini-Protean II Cell from BioRAD with a constant voltage of 150-200 V applied from a powerpack.

2.10.2 Non-Denaturing Polyacrylamide Gel Electrophoresis (NATIVE-PAGE)

Gels prepared and ran as with SDS-PAGE gels *(Method 2.10.1)* without the use of SDS or a molecular weight marker.

2.10.3 Agarose Gel Electrophoresis

Agarose (0.8-1.5 %) (Melford) in electrophoresis buffer, Tris-acetate-EDTA (TAE: 40 mM Tris, 40 mM acetate and 1mM EDTA pH 8.0) was heated in a microwave oven until all of the agarose dissolved. This was then cooled and poured into a tray with a comb with 8 or 15 fingers. After ≈ 60 min the set agarose was transferred to an electrophoresis tank and covered with TAE buffer. DNA samples were mixed with 5X loading buffer and applied to a well in the agarose gel. A voltage of 100 V was applied and electrophoresis was carried out

until the bromophenol blue approached the edge of the agarose gel. The Agarose gel was then stained by incubation in a solution of with GelRed Nucleic Acid Gel Stain (Biotium) diluted 10,000X in water for ≈ 20 mins. DNA in agarose gels was detected using an ultraviolet trans-illuminator (UV Tec). When DNA fragments in the agarose gel were required they were excised using a scalpel and purified from the agarose gel using the GeneElute Miniprep Kit (Sigma).

2.11 Determination of the molecular weights of proteins

Protein molecular weights were determined by either matrix assisted laser desorption ionisation time-of-flight (MALDI-TOF) or electrospray ionization mass spectrometry by Dr J. Gray (Pinnacle, Newcastle University, UK).

2.12 UV/vis Spectroscopy

All UV/Vis spectra were acquired on a Perkin-Elmer λ35 spectrophotometer. Measurements were made using 10 mm path length quartz cuvette (anaerobic cuvettes were used when anaerobic conditions required).

2.13 Far-UV Circular Dichroism Spectroscopy

Far-UV circular dichroism (CD) spectra (180-250 nm) of proteins were obtained on a Jasco J-810 spectrometer using a 0.2 mm path length quartz cuvette. The cuvette compartment was maintained at a temperature of 20 ^{o}C during all measurements and 10 scans were accumulated per for both blank and protein sample spectra.

2.14 Atomic Absorption Spectroscopy (AAS)

Copper concentrations were determined by AAS using an M Series spectrometer (Thermo Electron Corp.) with a calibration range of 0.2 – 2 ppm copper in 2 % HNO_3. Protein samples were diluted to produce a concentration of copper at ≈ 1 ppm, assuming that the binding site(s) of the protein is saturated with copper (2 equivalents of copper for WT-Ccs1 and Sod1, 1 equivalent of copper for C17S/C20S-Ccs1, C229S/C231S-Ccs1, D1/2-Ccs1, Atx1). A calibration range of 0.1 – 1 ppm was used for zinc and protein samples were diluted to

produce a concentration of zinc at ≈ 0.5 ppm, assuming that the binding sites of the proteins are saturated with zinc (2 equivalents of copper for WT-Ccs1 and Sod1, 1 equivalent of copper for C17S/C20S-Ccs1, C229S/C231S-Ccs1, D1/2-Ccs1, Atx1).

2.15 Protein Reduction

Protein samples (80 – 250 μM) were reduced by overnight incubation with 5 mM DTT at +4 ^{o}C. The samples were desalted and exchanged into the required buffer using a PD10 column (GE Healthcare) in an anaerobic chamber (Belle Technology, <2 ppm O_2). Protein reduction was confirmed by thiol quantification using 5,5 Dithiobis(2-nitrobenzoic acid) (DTNB, Ellman's reagent). The molar absorption coefficient ε = 14150 M^{-1} cm^{-1} was used for determining the number of free thiols per protein monomer.[146]

2.16 Protein Quantification

WT-Ccs1, C229S/C231S-Ccs1 and C17S/C20S-Ccs1 were quantified using the absorbance at 280 nm and the calculated extinction coefficients (ε_{280}) of 31315 M^{-1} cm^{-1} for WT-Ccs1 and 31190 M^{-1} cm^{-1} for the mutants. D1/2-Ccs1 was also quantified using the absorbance at 280 nm and a ε_{280} of 25690 M^{-1} cm^{-1}. The ε_{280} for Sod1 (1615 M^{-1} cm^{-1}) is too low to provide an accurate method of quantification from the absorbance at 280 nm. Therefore concentrations determined from Bradford assays with D1/2-Ccs1 (quantified by absorbance at 280 nm) used for the standard curve provided protein concentrations. Concentrations of Atx1 were routinely quantified for reduced apo-protein using the Ellman's assay and considering two cysteines.

2.17 Spectroscopic Determination of Cu^{1+} Binding

A Cu^{1+} stock solution (50 mM $[Cu(CH_3CN)_4]PF_6$ in 100 % acetonitrile) was diluted 50-fold into the appropriate buffer and added to proteins using a gastight syringe (Hamilton). Copper concentrations were determined using either bathocuproine disulphonate (BCS) or bicinchoninic acid (BCA). For measurements using BCS and BCA, ε_{483} and ε_{562} values of 12500 and 7700 M^{-1} cm^{-1} for $[Cu(BCS)_2]^{3-}$ and $[Cu(BCA)_2]^{3-}$ were used.

2.17.1 Protein Cu^{1+} Binding Stoichiometries

Cu^{1+} binding stoichiometries were determined by measuring the competition between proteins and BCA for Cu^{1+}. Titrations of Cu^{1+} into protein samples (10 μM) in the presence of 150-500 μM BCA were performed with measurement of the increase in absorbance at 562 nm due to the formation of $[Cu(BCA)_2]^{3-}$. Titrations were performed in 20 mM Hepes with 200 mM NaCl at pH 7.5.

2.17.3 Protein Cu^{1+} affinity determinations

Protein Cu^{1+} affinities (K_b values) were determined by competition assays with BCS and BCA using an approach described previously.[103, 139, 147] Titrations were performed by adding BCS (50 mM) or BCA (1 - 15 mM) into a solution of Cu^{1+}-protein (10 μM) containing an excess of apo-protein (10 μM) with 0.5 equivalents of Cu^{1+} in all cases. Apo-protein (500 – 1000 μM) was also titrated into a solution of $[Cu(BCS)_2]^{3-}$ or $[Cu(BCA)_2]^{3-}$ (10 μM) with an excess of BCS or BCA (50 – 700 μM). After each addition of BCS/BCA or protein the absorbance at 483 or 562 nm was measured, for determination of the concentrations of $[Cu(BCS)_2]^{3-}$ or $[Cu(BCA)_2]^{3-}$ respectively, after equilibration (typically 10-25 mins). All titration data were fit using Origin 7 to a 1:1 Cu^{1+}:protein binding model using equations (2.1) and (2.2) below.

$$[L] = 2[CuL_2] + \sqrt{\frac{K_b([P] - [Cu] + [CuL_2])[CuL_2]}{([Cu] - [CuL_2])\beta}} \qquad \textit{Equation 2.1}$$

$$[P] = \frac{([Cu] - [CuL_2])([L] - 2[CuL_2])^2\beta}{K_b[CuL_2]} + [Cu - [CuL_2] \qquad \textit{Equation 2.2}$$

In equations (2.1) and (2.2), [L] is the total concentration of BCS or BCA, $[CuL_2]$ is the concentration of $[Cu(BCS)_2]^{3-}$ or $[Cu(BCS)_2]^{3-}$, [P] is the total protein concentration, [Cu] is total Cu^{1+} concentration, K_b is the proteins Cu^{1+} affinity constant and β is the overall affinity constant for formation of $[Cu(BCS)_2]^{3-}$ or $[Cu(BCA)_2]^{3-}$. $[Cu(BCS)_2]^{3-}$ has an overall stability constant (β_{max} value) of 6.3×10^{19} M^{-2} (at pH ≥ 8.0),(*12*) and alterations in the β_{max} value with pH were calculated assuming a pK_a of 5.7(*12*) according to equation (5.3).(*7*)

$$\beta = \frac{\beta_{max}}{\left(1 + \frac{[H^+]}{K_a}\right)^2}$$ *Equation 2.3*

In which β is the overall affinity constant for $[Cu(BCS)_2]^{3-}$ for a specified pH, β_{max} is the maximal overall stability constant of $[Cu(BCS)_2]^{3-}$, K_a is the acid dissociation constant of BCS and $[H^+]$ is the proton concentration. A β value for $[Cu(BCA)_2]^{3-}$ of 5 x 10^{17} M^{-2} was used and a β value for $[Cu(BCS)_2]^{3-}$ of 6.3 x 10^{20} M^{-2} was used at pH 7.5. No significant difference was found at pH 7.0 and therefore the same β value has been used at these pH values.

2.18 Cu^{1+} Exchange Experiments

Cu^{1+} exchange between Atx1 and C17S/C20S-Ccs1 and C229S/C231S-Ccs1 was performed by mixing Cu^{1+}-loaded protein with the partner apo-protein in 20 mM Hepes pH 7.5 (total volume 1 mL). The mixtures were incubated for 1 – 24 hrs and loaded onto a HiTrap Q HP anion exchange column pre-equilibriated in the same buffer. Atx1 did not bind to the column and was eluted with salt-free buffer (20 mM Hepes pH 7.5). The Ccs1 mutants were eluted with 20 mM Hepes, 200 mM NaCl, pH 7.5 (1 mL fractions). Protein concentrations in the fractions were determined using Bradford assays using D1/2-Ccs1 as the standard and Cu^{1+} concentrations were measured with BCS. The equilibrium concentrations were used for each set of partner proteins to calculate K_{ex} from Equation 2.

$$K_{theo} = \frac{K_b^{Ccs1}}{K_b^{Atx1}}$$ *Equation 2.3*

2.19 Activation of Sod1 by Ccs1 Variants

The ability of Cu^{1+}-loaded Ccs1 variants to activate E,Zn-Sod1 was assayed using a Sod1 nitro-blue tetrazolium (NBT) assay. This assay utilises NBT which produces NBT-diformazan upon

interaction with superoxide. Superoxide ions are produced photochemically by the reduction of riboflavin. Sod1 catalyses the dismutation of superoxide therefore the presence of achromatic zones on an otherwise purple/blue gel is a reduction in the appearance of NBT-diformazan and a measure of Sod1 activity present in the sample.

Reaction mixtures typically consisted of 5 μM E,Zn-Sod1, 5 μM Cu^{1+}-Ccs1, 100 μM EDTA and 100 μM BCS. E,Zn-Sod1 and Cu,Zn-Sod1 was prepared by the addition of equal quantities of E,E-Sod1, $ZnSO_4$ and/or $Cu^{2+}(NO_3)_2$. Cu^{1+}-Ccs1 proteins were incubated for 30 mins prior to being mixed with E,Zn-Sod1, EDTA and BCS. Once combined, samples were exposed to air, incubated at 37 ^{o}C for 1 hr and loaded onto a NATIVE-PAGE gel. Gels were stained with a solution containing 100 mM sodium phosphate at pH 7.0, 4.3 % *N,N,N',N'*-tetramethylethylenediamine and 2.8 mM μM riboflavin for 20 mins with shaking. Exposure of the gel to bright light for 5 mins initiated the formation of superoxide and the gel gradually darkened to a purple/blue colour.

2.20 References

1. C. T. Chung, S. L. Niemela and R. H. Miller, *Proceedings of the National Academy of Sciences*, 1989, **86**, 2172-2175.

2. P. W. Riddles, R. L. Blakeley and B. Zerner, *Analytical Biochemistry*, 1979, **94**, 75-81.
3. S. Allen, A. Badarau and C. Dennison, *Biochemistry*, 2012, **51**, 1439-1448.
4. A. Badarau and C. Dennison, *Journal of the American Chemical Society*, 2011, **133**, 2983-2988.
5. A. Badarau and C. Dennison, *Proceedings of the National Academy of Sciences*, 2011, **108**, 13007-13012.

Chapter 3: Results

3.1 Purification and Initial Characterisation of Proteins

All of the proteins expressed and purified in this project were determined by SDS-PAGE to be > 90 % pure. The molecular weights of WT-Ccs1, C17S/C20S-Ccs1, C229S/C231S-Ccs1, D1/2-Ccs1 and Sod1 were determined to be within 7 Da of expected values *(Table 3.1)*. All of the proteins are mixtures of protein comprised of the full amino acid sequence or lacking the N-terminal methionine due to removal of the N-terminal methionine by methionine aminopeptidase (MetAP).[148] However, Sod1 was measured only as protein lacking the N-terminal methionine, both with and without a water adduct, and a peak with a mass 117 Da less than the expected value was present. Furthermore, D2/3-Ccs1 has a mass 191 Da less than expected value (60 Da less than expected for protein lacking N-terminal methionine) and appeared as a mixture of monomer and dimer. These discrepancies in the measured masses of the D2/3-Ccs1 and Sod1 proteins are not easily explained. All Ccs1 variants and Atx1 were purified with negligible amounts of copper and zinc. Sod1 was purified with negligible amounts of copper and ≈ 0.7 zinc equivalents per protein monomer.

Reduced apo-protein samples provided the numbers of free thiols per monomer, determined using the Ellman's assay *(Method 2.15)* and protein concentrations. The concentration of proteins were determined using the absorbance at 280 nm and calculated ε_{280} values (Methods 2.16) from the online ExPASy ProtParam tool.[1] Values of 4.7 ± 0.4, 2.7 ± 0.5 and 3.0 ± 0.5 (n = 10) thiols per monomer were obtained for apo-WT-Ccs1, C17S/C20S-Ccs1 and C229S/C231S-Ccs1 *(Table 3.2)*. The D1/2-Ccs1 mutant which lacks D3, gave 2.9 ± 0.1 (n = 10) thiols per monomer *(Table 3.2)*. WT-Ccs1 contains 7 cysteine residues therefore the expected thiol count is 7, the C17S/C20S-Ccs1, C229S/231S-Ccs1 and D1/2-Ccs1 variants contain 5 cysteine residues therefore the expected thiol is 5. The calculated ε_{280} of Sod1 (1615 M^{-1} cm^{-1}) is too low to provide an accurate method of quantification from the absorbance at 280 nm. Therefore concentrations determined from Bradford assays with D1/2-Ccs1 (quantified by absorbance at 280 nm) were used for the standard curve provided protein concentrations. A comparison to the thiol concentration determined using the Ellman's assay gave 1.8 ± 0.2 (n = 10) thiols per monomer *(Table 3.2)*.

Concentrations of Atx1 determined from the absorbance at 280 nm and the calculated ε_{280} of 4470 M^{-1} cm^{-1} gave values ≈ 200 % higher than those from the Ellman's assay. Also, the Bradford assay (BSA as standard) gave concentrations ≈ 300 % higher. Consequently,

concentrations of Atx1 were routinely quantified for reduced apo-protein using the Ellman's assay *(Method 2.15)* and considering two cysteines.

3.2 Far-UV Circular Dichroism (CD) Spectra

CD spectroscopy is a form of light absorption spectroscopy that measures the difference in absorbance of right- and left-handed polarized light by a substance. It has been shown that CD spectra between 260 - 180 nm can be analyzed for the different secondary structural content such as alpha helices, parallel and antiparallel beta sheets.[2, 149]

CD spectroscopy was performed on WT-Ccs1 and the Ccs1 variants in order to determine if the Cys-to-Ser mutations of C17S/C20S-Ccs1 and C229S/C231S-Ccs1, or loss of domain in D1/2-Ccs1 and D2/3-Ccs1 caused any structural disruption. Far-UV CD spectra show that the Cys-to-Ser mutations in C17S/C20S-Ccs1 and C229S/C231S-Ccs1, as well as the loss of D3 in D1/2-Ccs1 do not alter the overall secondary structure relative to WT-Ccs1 *(Figure 3.1).* All Ccs1 spectra contain a main positive peak at ≈ 187 nm which is indicative of α-helical content, and a minor positive peak at ≈ 200 nm which is indicative of β-sheet content, which correspond to the spectrum previously reported for Ccs1.[103] In contrast, the CD spectrum for the D2/3-Ccs1 mutant, which lacks D1, contains a large negative peak at 195 nm indicating that the protein is significantly unfolded, existing mainly as a an irregular structure.[150] The similarities of CD spectra between unfolded polypeptides and those containing polyproline II (PPII) helix-like confirmations, which are characterised by a distinct negative peak at < 200, have suggested that Iirregular structures may actually have some organisational structure such as PPII confirmations.[36] Due to this dramatic loss of secondary structure as compared to WT-Ccs1, the D2/3-Ccs1 protein was therefore not used for any further experiments.

Subtraction of the far-UV CD spectrum of D1/2-Ccs1 from that of WT-Ccs1 provides a spectrum for D3-Ccs1 *(Figure 3.2)*. The presence of a negative peak at 200 nm is characteristic of small unstructured peptides.[151]

The Far-UV CD spectrum of Atx1 partly resembles that of WT-Ccs1 due to a positive peak at ≈ 190 nm, however the minor positive peak at ≈ 200 nm of the Ccs1 proteins is lacking in the Atx1 spectrum *(Figure 3.3)*. The CD spectrum also includes a single broad negative peak at ≈

210 nm which is identical to that measured previously for Atx1 of *S. cerevisiae*.[140] In the literature, two negative peaks at ≈ 108 and 220 nm characteristic of α-helical content are observed for Atx1 of *S. cerevisiae*,[7] and the cyanobacterium *Synechocystis*.[140, 147]

The secondary structure of Sod1 was monitored at each stage of a dialysis procedure *(Method 2.9.2)* for zinc removal from the purified E,Zn-Sod1 *(Results 3.1)*. The copper and zinc content of Sod1 was measured by Atomic Absorption Spectroscopy (AAS) at each stage of the dialysis procedure. After incubation at pH 3.8 and treatment with EDTA, which removes zinc to form E,E-Sod1 undergoes significant unfolding indicated by a large negative peak at 200 nm *(Figure 3.4)*. Transfer to pH 5.5 shows that E,E-Sod1, begins to refold and regain some secondary structure, indicated by the small positive peak at 195 nm. Incubation of E,E-Sod1 at pH 7.5 shows further secondary structure organisation, however, the complete folded protein form is only achieved upon the addition of zinc. Further addition of copper to E,Zn-Sod1 does not affect the overall structure *(Figure 3.4)*.

3.3 Analytical Gel Filtration Chromatography

Analytical gel filtration chromatography was used to determine the oligomeric state of Ccs1 in the apo-form and when Cu^{+} is bound *(Method 2.7.2)*.

In the absence of Cu^{1+}, WT-Ccs1, C229S/C231S-Ccs1 and D1/2-Ccs1 are predominately monomeric *(Figure 3.5 A, B & C)* with a small proportion of dimer (11, 4, 3 % dimer respectively). C17S/C20S-Ccs1 is shown to form equal proportions of monomer and dimer indicating that this mutant is more readily prone to dimerization *(Figure 3.5 D)* than WT-Ccs1 and the other Ccs1 mutants. The presence of DTT in the buffer reduces the amount of dimer present with WT-Ccs1 and C17S/C231S-Ccs1 (from 11 to 8 % and 3 to 2 peak shift % dimer respectively), and eliminates dimer formation in C229S/C231S-Ccs1 and D1/2-Ccs1. This shift in monomer : dimer ratio in the presence of the reducing agent DTT indicates that dimerization is most probably due to inter-molecular disulfide bonds.

Upon the binding of Cu^{1+}, both dimeric and monomeric species of WT-Ccs1 are observed *(Figure 3.6 A)* which persist in the presence of DTT *(Figure 3.6 B*). The occurrence of dimerization in the presence of a reducing agent and increasing dimer formation observed with higher concentrations of Cu^{1+} suggests that dimerization is due to interactions with Cu^{1+}

and not disulfide formation. Dimerization upon the addition of Cu^{1+} is also observed for C229S/C231S-Ccs1 and D1/2-Ccs1 *(Figure 3.7 A & C)*. The presence of dimer increases with Cu^{1+} concentration from 4 % for apo-C229S/C231S-Ccs1 to 16 and 34 % for 0.5 and 1.0 equivalents of Cu^{1+} bound respectively. The presence of dimer increases with Cu^{1+} concentration from 4 % for apo-D1/2-Ccs1 to 13 and 33 % for 0.5 and 1.0 equivalents of Cu^{1+} bound respectively. However, this dimerization is eliminated in the presence of DTT *(Figure 3.7 B & D).* C17S/C20S-Ccs1 shows the highest proportion of dimer formed with the addition of copper *(Figure 3.7 E)*, increasing from 49 % for apo-C17S/C20S-Ccs1 to 61 and 77 % for 0.5 and 1.0 equivalents of Cu^{1+} bound respectively. Dimer formation is reduced in the presence of DTT *(Figure 3.7 F)*, yet the dimer remains a major form in presence of DTT (5 % for apo-C17S/C20S-Ccs1 to 49 and 59 % for 0.5 and 1.0 equivalents of Cu^{1+} bound respectively) suggesting that dimerization is not disulfide linked and is related to the binding of Cu^{1+}.

Copper is found to associate with both the monomeric and dimeric forms of WT-Ccs1 *(Figure 3.8).* At 0.5 and 1.0 equivalents of Cu^{1+}, the copper is found to associate almost equally between the monomeric and dimeric protein forms *(Figure 3.8 A & B)*. At Cu^{1+} concentrations over 1.0 equivalent, copper is found to preferentially bind to the monomer *(Figure 3.8 C & D)*. In the presence of DTT the resolution of the peaks is diminished, although Cu^{1+} appears to preferentially bind to the dimeric protein up to 1.0 equivalent of copper *(Figure 3.9 A & B)*. At higher Cu^{1+} concentrations it is not possible to distinguish monomer/dimer peaks *(Figure 3.9 C & D)*.

Copper also binds to both the monomer and dimer of C229S/C231S-Ccs1 *(Figure 3.10 A & B)*. In the presence of DTT only monomeric protein is present therefore Cu^{1+} is only found to associate with the monomer *(Figure 3.10 C & D)*. Copper association with D1/2-Ccs1 is identical to C229S/C231S-Ccs1, *(Figure 3.11)*. The corresponding Cu^{1+} binding oligomerisation of C229S/C231S-Ccs1 and D1/2-Ccs1 is expected since both proteins only contain the copper binding site in D1 of Ccs1.

The addition of Cu^{1+} to C17S/C20S-Ccs1 shows that Cu^{1+} favours association with the dimeric protein *(Figure 3.12 A & B)*, which could be due to preferential binding interactions or the higher majority of dimer present over monomer. Interestingly, in the presence of DTT at the Cu^{1+} concentration of 0.5 equivalents, Cu^{1+} also preferentially binds to the dimeric protein

(Figure 3.12 C). At the Cu^{1+} concentration of 1.0 equivalent the protein peaks are not resolved therefore the exact location of Cu^{1+} cannot be distinguished *(Figure 3.12 D)*.

Analytical gel filtration chromatography was also used to determine the oligomeric form of apo-Atx1 and the Cu^{1+}-bound form. In the absence of Cu^{1+}, 67 % of apo-Atx1 is dimeric in the absence of DTT and 59 % is dimeric in the presence of DTT *(Figure 3.13)*. Upon the addition of Cu^{1+} the monomer : dimer ratio shifts to favour the monomer and Cu^{1+} is found to be associated with the monomer *(Figure 3.14)*. Previously, the major form of Atx1 was found to be the monomer regardless of the presence or absence of copper.[31]

Purified Sod1 was shown by analytical gel filtration to be dimeric in the presence of DTT (Figure 3.15), and monomeric protein was only observed after incubation of Sod1 with DTT overnight.[80, 152, 153]

3.4 Cu^{1+} Binding Stoichiometries of Ccs1 variants

Cu^{1+} binding stoichiometries were determined by titrating Cu^{1+} into apo-protein in the presence of BCA *(Method 2.17.1)*. C229S/C231S-Ccs1 and D1/2-Ccs1 bind $\approx$ 1 equivalent of Cu^{1+} in the presence of 500 μM BCA *(Figure 3.16 B & D)*, whereas WT-Ccs1 is shown to bind beyond one equivalent of Cu^{1+} due to weak competition with BCA *(Figure 3.16 A)*. Similarly, C17S/C20S-Ccs1 shows weak competition with BCA, therefore the binding stoichiometry cannot be determined *(Figure 3.16 C)*. Reduction of the BCA concentration to 150 μM shows that WT-Ccs1 is able to bind two equivalents of Cu^{1+}, and C17S/C20S-Ccs1 binds one equivalent of Cu^{1+} *(Figure 3.17)*. WT-Ccs1 and the Ccs1 mutants show identical Cu^{1+} binding stoichiometry as the human homologues.[103]

3.5 Cu^{1+} Binding Affinities of Ccs1 variants

The K_b values of the two Cu^{1+} binding sites of Ccs1, located in D1 and D3, have been measured individually by competition titrations with Ccs1 mutants containing only one of the two copper-binding sites of Ccs1 and BCS/BCA *(Method 2.17.3)*. Since WT-Ccs1 contains two copper-binding sites, 0.5 equivalents of Cu^{1+} was used in all affinity titrations. The Cu^{1+} affinity of WT-Ccs1, C229S/C231S-Ccs1 and D1/2-Ccs1 for Cu^{1+} have been measured as almost identical as $(2.6 \pm 1.1) \times 10^{18}$, $(2.6 \pm 0.5) \times 10^{18}$ and $(2.7 \pm 1.0) \times 10^{18}$ M^{-1} respectively

(Figure 3.18 and Table 3.4). The agreement between the affinity of WT-Ccs1 and those of the Ccs1 variants containing the copper-binding site of D1 only indicates that the 0.5 equivalent of Cu^{1+} used in the affinity titrations was bound to D1 of WT-Ccs1. Titrations of apo-protein into $[Cu(BCS)_2]^{3-}$ provided comparable values which confirm that equilibrium conditions were reached in the experiments and therefore validate the determined values and the methods used *(Figure 3.19)*.

The addition of a relatively low concentration of BCS to Cu^{1+}-C17S/C20S-Ccs1 resulted in the removal of ≈ 70 % Cu^{1+} by BCA over the course of 5 hours *(Figure 3.20)*. As suggested from the stoichiometry titrations, this removal of Cu^{1+} suggests a lower affinity of the D3 copper-binding site for Cu^{1+}. Therefore, experiments with BCA were performed to measure the Cu^{1+} affinity of C17S/C20S-Ccs1 as done previously with the equivalent human CCS1 mutant *(Method 2.17.3)*.[103] Experiments performed under the previous conditions involved the incubation of several samples of C17S/C20S-Ccs1 plus 0.5 equivalents of Cu^{1+} with a range of BCA concentrations for a period of 48 hrs. This resulted in plots *(Figure 3.21 A)* which lacked the typical trend of the affinity plots for WT-Ccs1 and C229S/C231S-Ccs1, and the Cu^{1+} affinity measured is an order of magnitude higher than that measured by titrations of apo-C17S/C20S-Ccs1 into $[Cu(BCA)_2]^{3-}$ *(Figure 3.21 B)*. The extension of the affinity experiments after the experimental time frame of 48 hrs showed the prolonged and eventual complete removal of Cu^{1+} from C17S/C20S-Ccs1 by BCA *(Figure 3.22).* This renders the Cu^{1+} affinity values obtained by these conditions as invalid. Monitoring of the free thiol count of C17S/C20S-Ccs1 over time in the presence of Cu^{1+} and BCA shows that these components do not affect the oxidation state of the cysteine residues, therefore the prolonged loss of Cu^{1+} is not due to oxidation of the protein. Similarly, monitoring of the thiol state of WT-Ccs1 shows that the presence of BCA does not cause oxidation of the cysteine residues *(Figure 3.23)*. In order to check the stability of WT-Ccs1 during the affinity experiments, several points of the titration were monitored over time and remained stable, showing that Cu^{1+} removal by BCS was completed within the time frame of each titration addition (≈ 15 min) *(Figure 3.24)*.

The continuation of Cu^{1+} removal from C17S/C20S-Ccs1 by BCA outside of the experimental time frame suggested that this may also occur in experiments consisting of titrating apo-C17S/C20S-Ccs1 into $[Cu(BCA)_2]^{3-}$. Investigations into the stability of these titrations showed

that Cu^{1+} removal from $[Cu(BCA)_2]^{3-}$ by C17S/C20S-Ccs1 occurred within the time frame of each titration addition (≈ 15 min) and remained stable *(Figure 3.25)*. This method and conditions were therefore approved to measure the affinity value of C17S/C20S-Ccs1 for Cu^{1+}, and the K_b value has been measured as (4.1 ± 0.9) x 10^{17} M^{-1} which is less than three times lower than WT-Ccs1 *(Figure 3.21 B and Table 3.4)*.

3.6 Cu^{1+} Binding Affinities of Atx1

The K_b value for Cu^{1+} binding to Atx1 were determined from competition titrations with BCS at pH 7.0 and 7.5 *(Method 2.18)*. Measurement of the Cu^{1+} affinity at pH 7.5 allows a direct comparison to the Ccs1 affinities measured here, whereas an affinity at pH 7.0 can be used to compare with previous literature values.[139] The affinity of Cu^{1+} binding to Atx1 measured by titration of BCS into Cu^{1+}-Atx1 at pH 7.0 is (4.2 ± 1.4) x 10^{18} M^{-1} *(Figure 3.26 A and Table 3.4)*. This is consistent with measurements provided by titrations of apo-Atx1 into $[Cu(BCS)_2]^{3-}$ *(Figure 3.26 B)* which indicate that equilibrium has been reached and therefore validate the determined values and the methods used. Experiments performed at pH 7.5 provided a K_b value greater than three times higher than the value at pH 7.0, and also provide consistent measurements from titrations of BCS into Cu^{1+}-Atx1 and apo-Atx1 into $[Cu(BCS)_2]^{3-}$ *(Figure 3.26 and Table 3.4)*.

3.7 Cu^{1+} Transfer between Atx1 and Ccs1 variants

Copper transfer between Atx1 and either C17S/C20S-Ccs1 or C229S/C231S-Ccs1 at pH 7.5 was performed with Cu^{1+}-loaded Atx1 with an apo-Ccs1 variant, and apo-Atx1 with a Cu^{1+}-loaded Ccs1 variant. The K_{ex} values were determined and compared to the K_{theo} values calculated from the Cu^{1+} affinities measured *(Method 2.18)*. Atx1 and Ccs1 were separated using an anionic Hitrap Q column at pH 7.5. Atx1 did not bind whereas the Ccs1 proteins were eluted with buffer plus 200 mM NaCl *(Figure 3.28)*.

The transfer of Cu^{1+} between Atx1 and C229S/C231S-Ccs1, in both experiments where Cu^{1+} originated with one of the partner proteins, was found to be complete within the timeframe of the experiment (≈ 1 hr). The K_{ex} values vary between the two experiments *(Table 3.5)*,

which is due to a difference in the equivalent equilibrium protein concentrations by only 1 µM.

The Cu^{1+}-transfer between Atx1 and C17S/C20S-Ccs1 within the same timeframe (≈ 1 hr) provided K_{ex} values which are not consistent *(Table 3.6)* due to differences of the equivalent equilibrium protein concentrations which signifies that equilibrium was not reached. A significantly longer incubation period (≈ 24 hr) provided identical equivalent equilibrium protein concentrations and K_{ex} values which demonstrates that equilibrium was achieved, and shows that the reaction with C17S/C20S-Ccs1 is slower but completed within the allotted timeframe *(Table 3.7)*. The K_{ex} values show a similar trend to the calculated K_{theo} values *(Table 3.6)* indicating that a greater level of exchange is possible between C229S/C231S-Ccs1 and Atx1 than C17S/C20S-Ccs1 and Atx1.

3.8 Activation of Sod1 by Ccs1

The activity of Sod1 was determined by the proteins ability to catalyse the dismutation of superoxide and visualised by means of an NBT assay *(Method 2.19)* in which the formation of NBT-diformazan by superoxide is diminished by the presence of catalytically active Cu,Zn-Sod1. The dismutation of superoxide by Cu,Zn-Sod1 causes achromatic areas at its location on an otherwise purple/blue gel.

Cu,Zn-Sod1 formed from incubation with the salts $ZnSO_4$ and $Cu^{2+}(NO_3)_2$ was shown to be enzymatically active using the NBT assay *(Method 2.19)* and yeast Sod1 was shown to run at a similar level to bovine erythrocyte SOD1 by native-PAGE *(Figure 3.30)*. These experiments were performed aerobically with E,E-Sod1 which was not reduced therefore the catalytically important disulphide bond remained intact. Furthermore, no activity was observed with E,Zn-Sod1. Achromatic bands on the native-PAGE gels indicating activity of Sod1 were observed to be very intense at relatively low concentrations of protein therefore the optimum concentration of Sod1 to be loaded onto native-PAGE gels for the NBT assay was determined as 100 ng *(Figure 3.29)*.

None of the isolated Cu^{1+}-Ccs1 variants show achromatic bands in the NBT assay compared to Cu,Zn-Sod1 *(Figure 3.31)* at the same concentration of 100 ng. Sod1 activity is observed after incubation with all Cu^{1+}-Ccs1 variants *(Figure 3.32)*. WT-Ccs1 provides a level of Sod1

activation similar to that observed from E,Zn-Sod1 plus $Cu^{2+}(NO_3)_2$. All of the Ccs1 variants (C17S/C20S-Ccs1, C229S/C231S-Ccs1 and D1/2-Ccs1) provide lower activity levels of Sod1 compared to WT-Ccs1. However, the activity of Sod1 observed after incubation with Cu^{1+}-C17S/C20S-Ccs1 is higher than with the Ccs1 variants which contain the D1 copper-binding site only (C229S/C231S-Ccs1 and D1/2-Ccs1). Comparison of the Sod1 activity produced after incubation with Cu^{1+}-WT-Ccs1 and Cu^{1+}-C17S/C20S-Ccs1 over a range of decreasing concentrations *(Figure 3.33)* definitively shows that WT-Ccs1 produces a greater level of activation than C17S/C20S-Ccs1. Sod1 activity is equally lower after incubation with Cu^{1+}-C229S/C231S-Ccs1 and Cu^{1+}-D1/2-Ccs1 as compared to WT-Ccs1.

Table 3.1. Experimental and calculated masses of Ccs1 proteins and Sod1 determined by mass spectrometry.

Protein	Technique	Experimental mass (Da)	Theoretical mass (Da)	Mass Difference (Da)[c]
WT-Ccs1	MALDI-MS[a]	27330 ±27 27195 ±27[b]	27330 27199[b]	0 -4
C17S/C20S-Ccs1	MALDI-MS[a]	27293 ±27 27160 ±27[b]	27298 27167[b]	-5 -7
C229S/C231S-Ccs1	MALDI-MS[a]	27292 ±27 27159 ±27[b]	27298 27167[b]	-6 -2
D1/2-Ccs1	ESI-MS[d]	24282 ±1 24149[b] ±1	24284 24153[b]	-2 -4
D2/3-Ccs1	ESI-MS[d]	19453 ±1 38906 ±1	19644 19513[b]	+9 -60
Sod1	ESI-MS[d]	15738[b] ±1 15721[b] ±1	15855 15723[b]	-117 -2

[a] Matrix assisted laser desorption/ionization mass spectrometry
[b] Values for proteins without the N-terminal methionine
[c] Difference values calculated from [experimental mass – theoretical mass]
[d] Electrospray mass spectrometry

Table 3.2. Experimental and expected free thiol count for Ccs1 proteins and Sod1 as determined by the Ellman's assay.

Protein	Experimental free thiol count[a]	Expected free thiol count[b]
WT-Ccs1	4.7 ± 0.4	7
C17S/C20S-Ccs1	2.7 ± 0.5	5
C229S/C231S-Ccs1	3.0 ± 0.5	5
D1/2-Ccs1	2.9 ± 0.2	5
Sod1	1.8 ± 0.2	2

[a] Calculated from the Ellman's assay and protein concentration *(Methods 2.15)* and Average values from ten independent determinations.
[b] Number of cysteine residues in protein amino acid sequence.

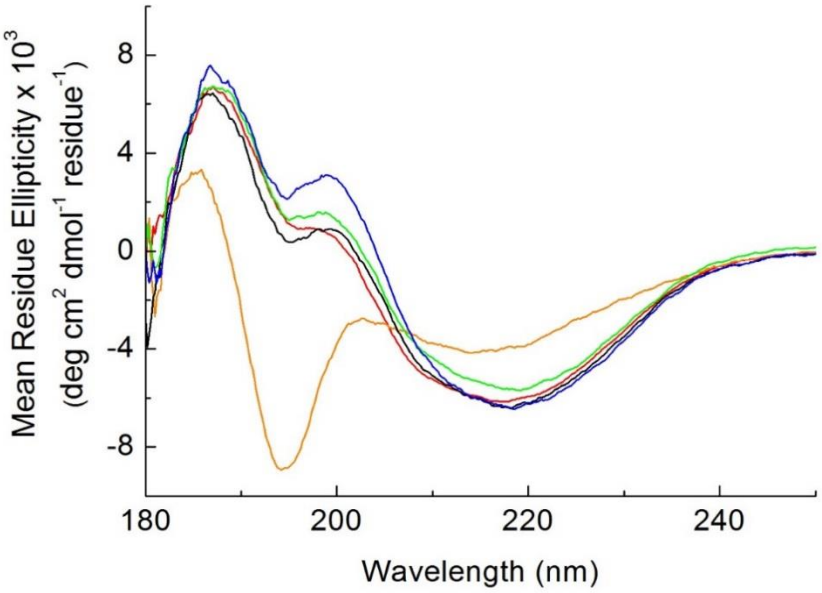

Figure 3.1. Far-UV CD spectra of WT-Ccs1 and Cys-to-Ser apo-Ccs1 variants indicating the secondary structure of the proteins. Apo-WT-Ccs1 (black), apo-C17S/C20S-Ccs1 (red), apo-C229S/C231S-Ccs1 (green), apo-D1/2-Ccs1 (blue) and apo-D2/3-Ccs1 (orange) in 100 mM potassium phosphate at pH 8.0, and protein concentrations 0.50 mg/mL, 20^{o}C. The D2/3-Ccs1 mutant gives a spectrum indicative of an unfolded protein.

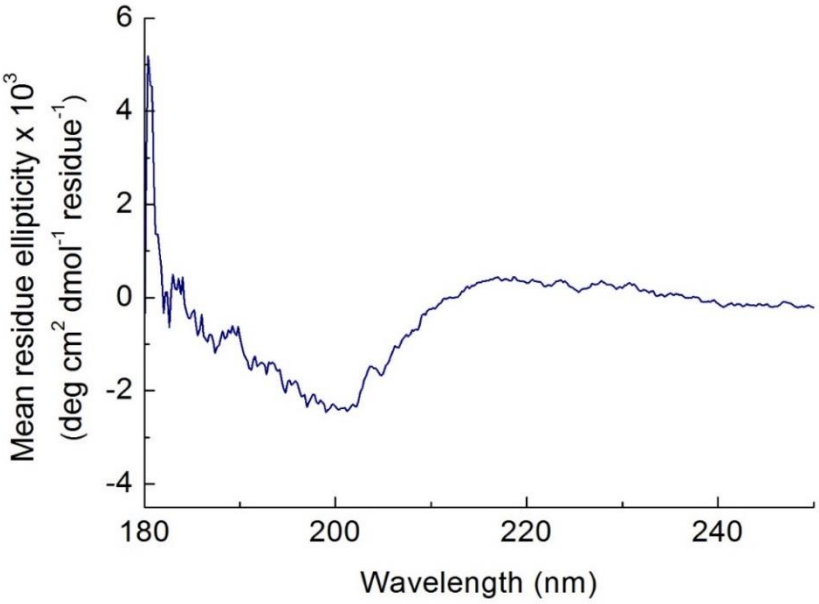

Figure 3.2. The calculated far-UV CD spectrum of D3-Ccs1 protein. This spectrum of D3-Ccs1 was calculated by subtracting the spectrum of D1/2-Ccs1 from that of WT-Ccs1 (both shown in Figure 3.1). This resulting spectrum resembles that for an unstructured peptide highlighting the lack of secondary structure in D3.

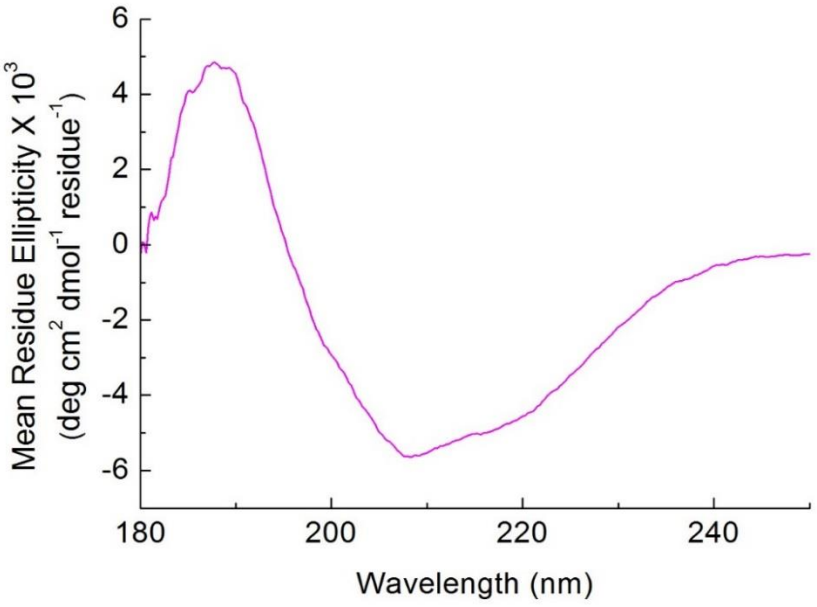

Figure 3.3. Far-UV CD spectrum of apo-Atx1 indicating the secondary structure of the protein. The data was obtained on an apo-Atx1 sample (0.50 mg/mL) in 100 mM potassium phosphate pH 8.0, 20^{o}C.

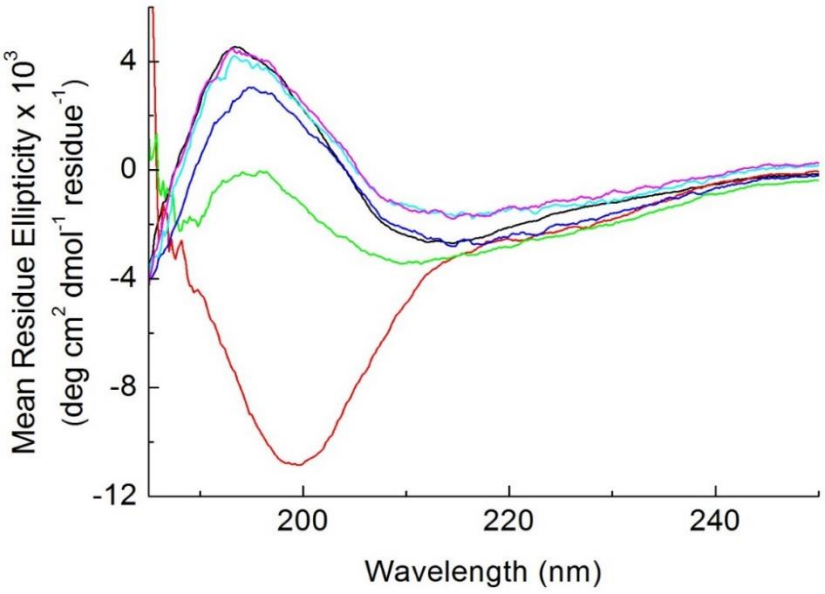

Figure 3.4. Far-UV CD spectra of Sod1 after purification and at various stages of the dialysis protocol to remove zinc. Purified E,Zn-Sod1 [binding 0.7 equivalents of Zn^{2+}] at pH 7.5 (black), E,E-Sod1 at pH 3.8 (red), E,E-Sod1 at pH 5.5 (green), E,E-Sod1 at pH 7.5 (navy), E,Zn-Sod1 [plus 1.0 equivalent of Zn^{2+}] at pH 7.5 (cyan) and Cu,Zn-Sod1 [plus 1.0 equivalent of Cu^{2+} and Zn^{2+}] at pH 7.5 (magenta). All protein concentrations were 0.50 mg/mL and spectra were measured at 20°C. Sod1 without Zn^{2+} bound becomes unfolded at pH 3.8 and refolds without the addition of Zn^{2+} at pH 7.5

Table 3.3. Gel filtration elution volumes and apparent molecular weights of apo and Cu^{1+}-bound WT and mutant Ccs1 proteins under anaerobic and aerobic conditions

Protein[a]	Cu^{1+} : protein ratio	Elution Volumes (mL)	Apparent mass[b] (kDa)	Oxygen condition
WT-Ccs1	0	10.2, 11.5	56, 32	Anaerobic
	0.5	10.2, 11.5	56, 32	
	1.0	10.1, 11.5	59, 32	
	1.5	10.1, 11.5	56, 32	
	2.0	11.5	32	
	0	10.1, 11.5	59, 32	Aerobic (with DTT)
	0.5	11.5	32	
	1.0	10.2, 11.5	56, 32	
	1.5	-	-	
	2.0	-	-	
C17S/C20S-Ccs1	0	10.0, 11.5	61, 32	Anaerobic
	0.5	10.0, 11.5	61, 32	
	1.0	10.0, 11.5	61, 32	
	0	10.4, 11.2	51, 37	Aerobic (with DTT)
	0.5	10.4, 11.1	51, 38	
	1.0	10.4, 11.2	51, 37	
C229S/C231S-Ccs1	0	10.0, 11.5	61, 32	Anaerobic
	0.5	10.0, 11.5	61, 32	
	1.0	10.0, 11.5	61, 32	
	0	11.5	32	Aerobic (with DTT)
	0.5	11.5	32	
	1.0	11.5	32	
D1/2-Ccs1	0	10.5, 12.0	49, 26	Anaerobic
	0.5	10.5, 12.0	49, 26	
	1.0	10.5, 12.0	49, 26	
	0	12.0	26	Aerobic (with DTT)
	0.5	12.0	26	
	1.0	12.0	26	

[a] Gel filtration performed at room temperature on a Superdex 75 10/300 GL column either under aerobic conditions using 20 mM Hepes at pH 7.5 plus 200 mM NaCl with 250 μM DTT or anaerobically using deoxygenated 20 mM Hepes at pH 7.5 plus 200 mM NaCl.
[b] Apparent masses were calculated from elution volumes and a column calibration performed with a low molecular weight calibration kit (Methods 2.7.2) and indicate the presence of monomeric and/or dimeric forms of the proteins.

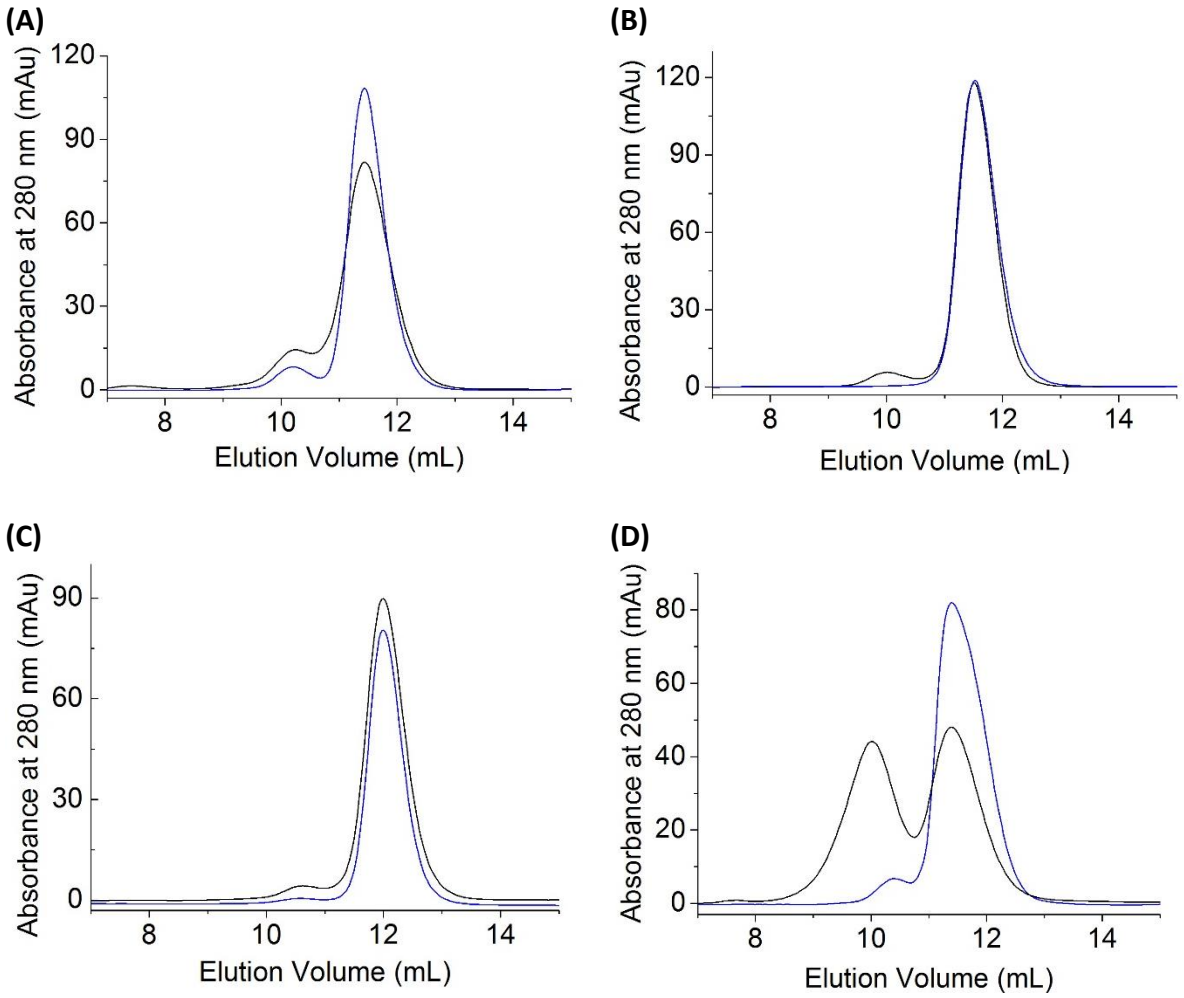

Figure 3.5. Gel filtration chromatograms of WT and mutant apo-Ccs1 proteins either under anaerobic conditions or in the presence of DTT. Plots of absorbance at 280 nm against elution volume for (A) apo-WT-Ccs1, (B) apo-C229S/C231S-Ccs1, (C) apo-D1/2-Ccs1 and (D) apo-C17S/C20S-Ccs1 in deoxygenated 20 mM Hepes at pH 7.5 plus 200 mM NaCl (black) or 20 mM Hepes at pH 7.5 plus 200 mM NaCl with 250 μM DTT (blue). Proteins (100 μM of 200 μL) were injected onto a Superdex 75 10/300 GL column at a flow rate of 0.8 mL/min at room temperature. For elution volumes and calculated apparent molecular weights see Table 3.3.

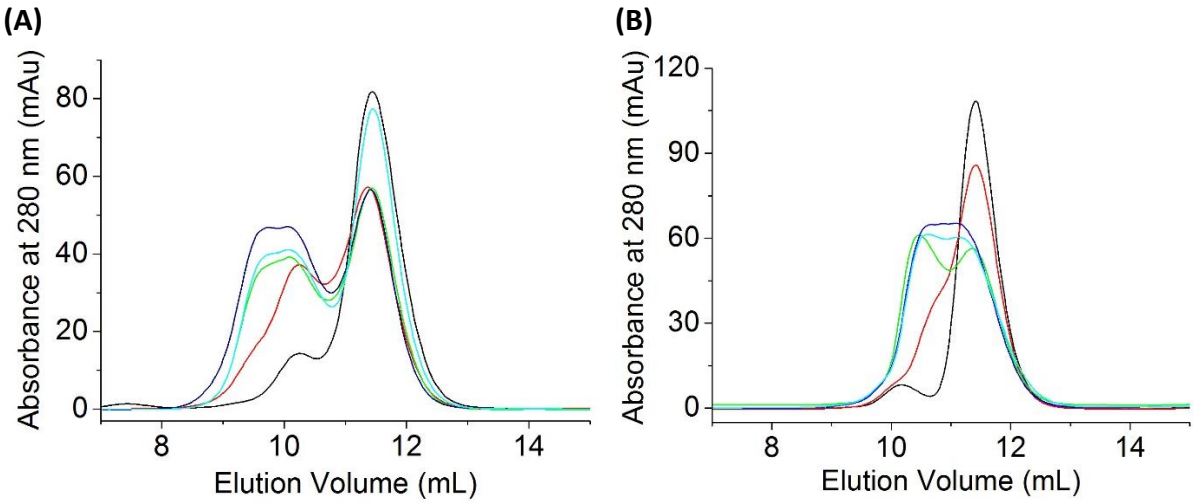

Figure 3.6. Gel filtration chromatograms of WT-Ccs1 protein with various equivalents of Cu^{1+} bound either under anaerobic conditions or in the presence of DTT. Plots of absorbance at 280 nm against elution volume for apo-WT-Ccs1 (black) and WT-Ccs1 in the presence of 0.5 equivalents Cu^{1+} (red), 1.0 equivalent Cu^{1+} (green), 1.5 equivalents Cu^{1+} (navy) and 2.0 equivalents Cu^{1+} (cyan) in (A) deoxygenated 20 mM Hepes pH 7.5 plus 200 mM NaCl or (B) 20 mM Hepes pH 7.5 plus 200 mM NaCl and 250 μM DTT. Proteins (100 μM of 200 μL) were injected onto a Superdex 75 10/300 GL column at a flow rate of 0.8 mL/min at room temperature. For elution volumes and calculated apparent molecular weights see Table 3.3.

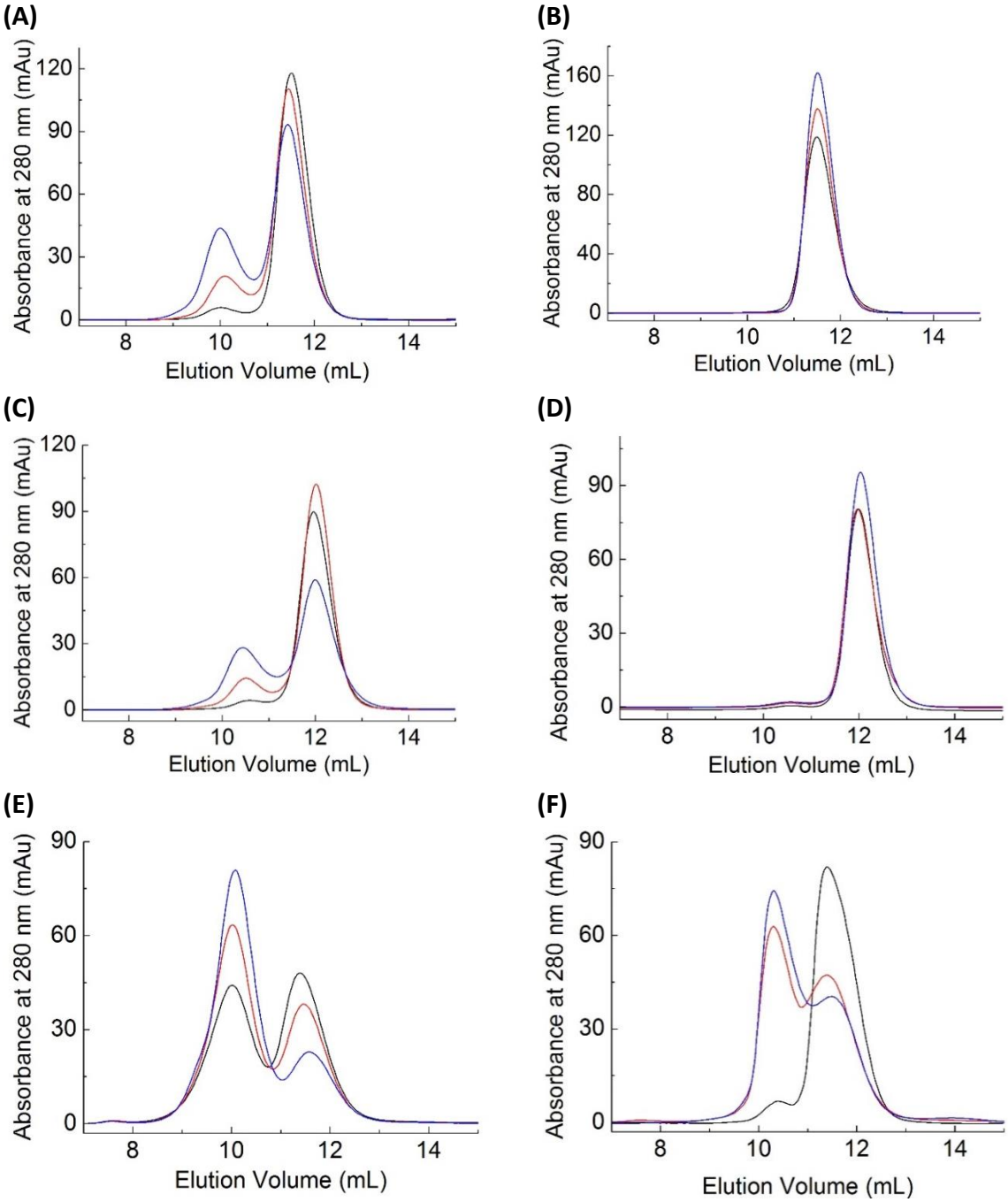

Figure 3.7. Gel filtration chromatograms of apo- and Cu^{1+}-bound Ccs1 variants either under anaerobic conditions or in the presence of DTT. Plots of absorbance at 280 nm against elution volume for C229S/C231-Ccs1 (A and B), D1/2-Ccs1 (C and D) and C17S/C229S-Ccs1 (E and F) as apo-protein (black) and in the presence of 0.5 Cu^{1+} (red) and 1.0 equivalent Cu^{1+} (blue) in deoxygenated 20 mM Hepes pH 7.5 plus 200 mM NaCl (A, C and E), or 20 mM Hepes pH 7.5 plus 200 mM NaCl and 250 μM DTT (B, D and F). Proteins (100 μM of 200 μL) were injected onto a Superdex 75 10/300 GL column at a flow rate of 0.8 mL/min at room temperature. For elution volumes and calculated apparent molecular weights see Table 3.3.

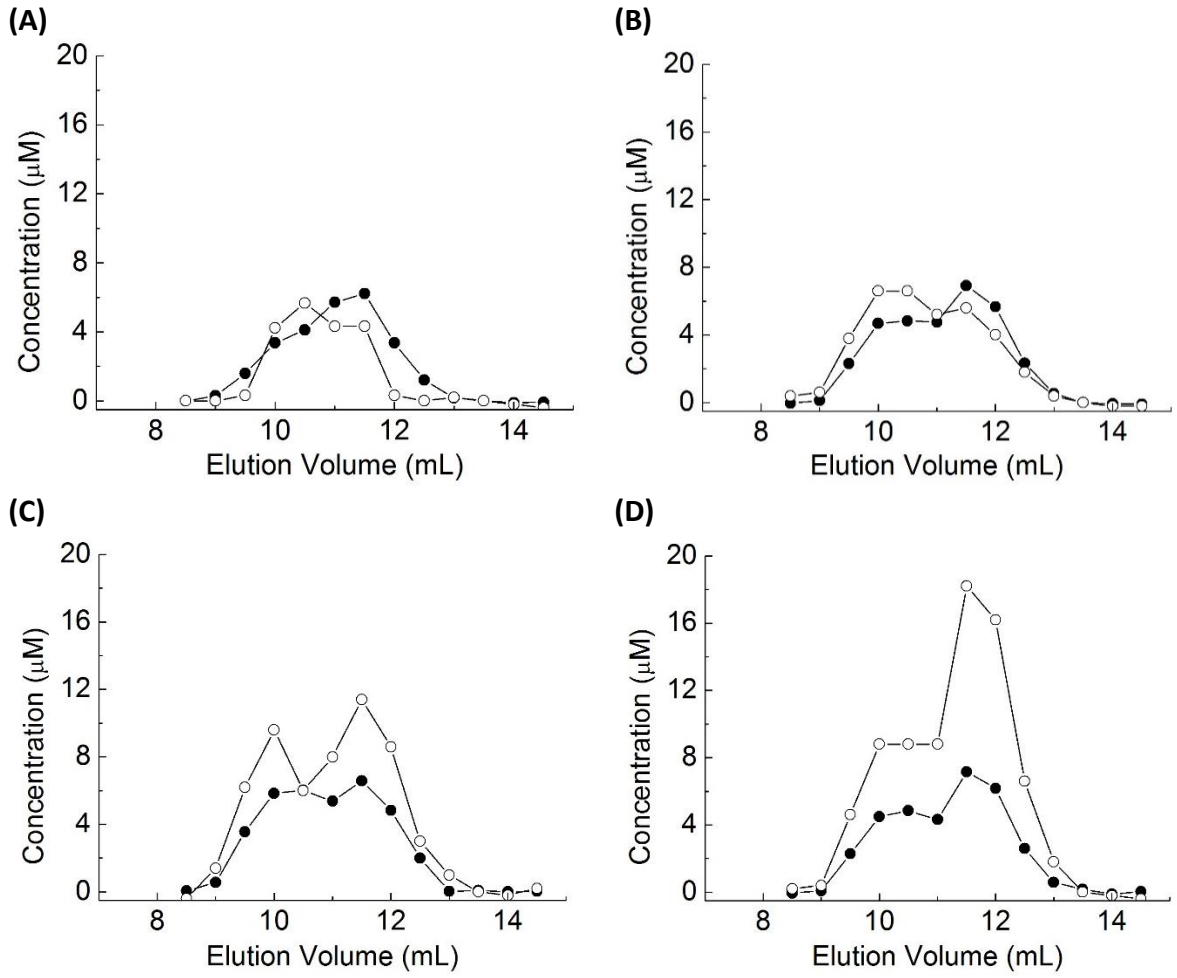

Figure 3.8. Distribution of WT-Ccs1 and Cu^{1+} in eluted fractions from a gel filtration column. Protein (●) and Cu^{1+} (○) content of fractions (500 µL) for WT-Ccs1 in the presence of (A) 0.5, (B) 1.0, (C) 1.5 and (D) 2.0 equivalents of Cu^{1+} in deoxygenated 20 mM Hepes pH 7.5 plus 200 mM NaCl. Proteins (100 µM of 200 µL) were injected onto a Superdex 75 10/300 GL column and eluted at a flow rate of 0.8 mL/min at room temperature. For elution volumes and calculated apparent molecular weights see Table 3.3. Cu^{1+} is associated with both monomeric and dimeric forms of WT-Ccs1.

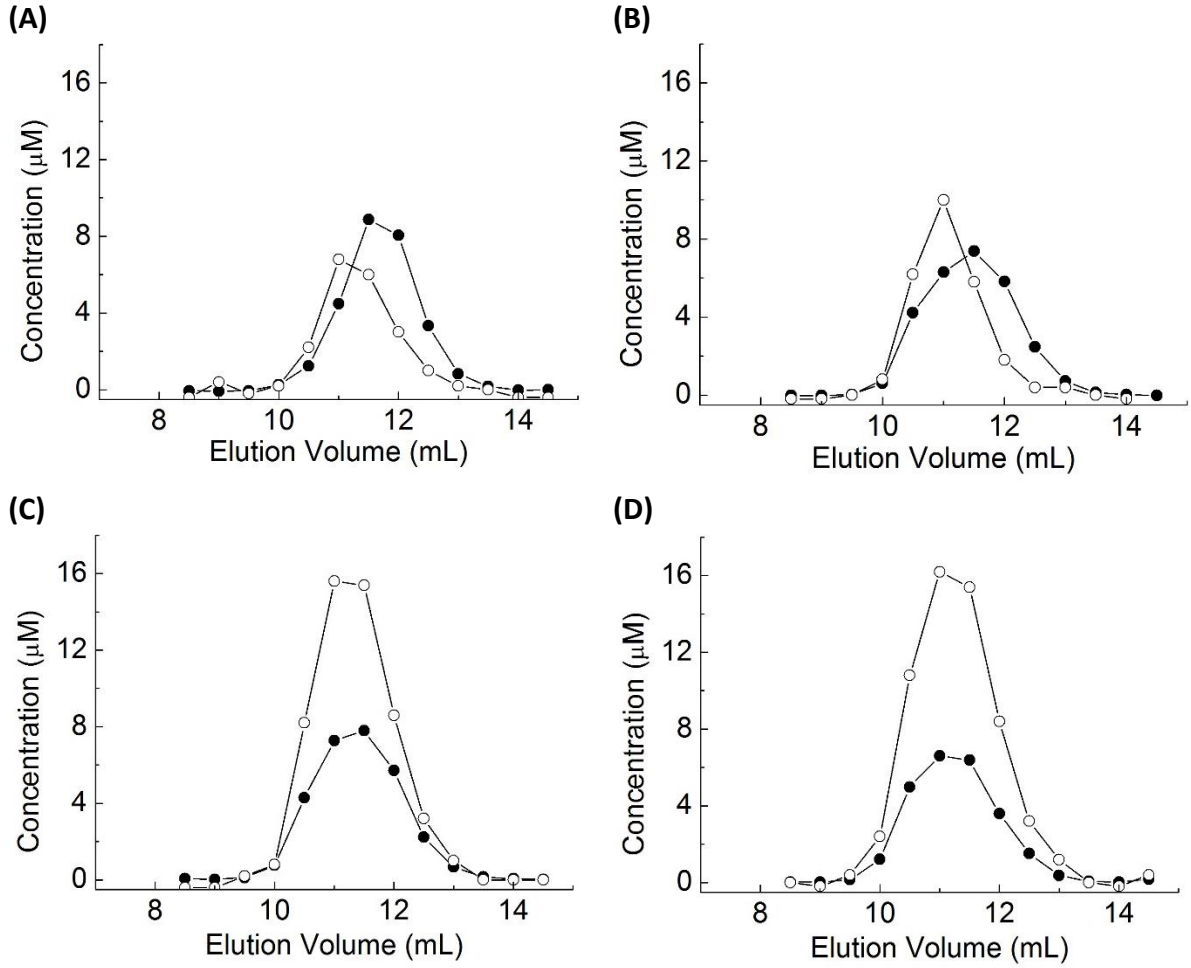

Figure 3.9. Distribution of WT-Ccs1 and Cu^{1+} in eluted fractions from a gel filtration column. Protein (●) and Cu^{1+} (○) content of fractions (500 µL) for WT-Ccs1 in the presence of (A) 0.5, (B) 1.0, (C) 1.5 and (D) 2.0 equivalents of Cu^{1+} in 20 mM Hepes pH 7.5 plus 200 mM NaCl with µM DTT. Proteins (100 µM of 200 µL) were injected onto a Superdex 75 10/300 GL column and eluted at a flow rate of 0.8 mL/min at room temperature. For elution volumes and calculated apparent molecular weights see Table 3.3. Cu^{1+} is associated with both monomeric and dimeric forms of WT-Ccs1.

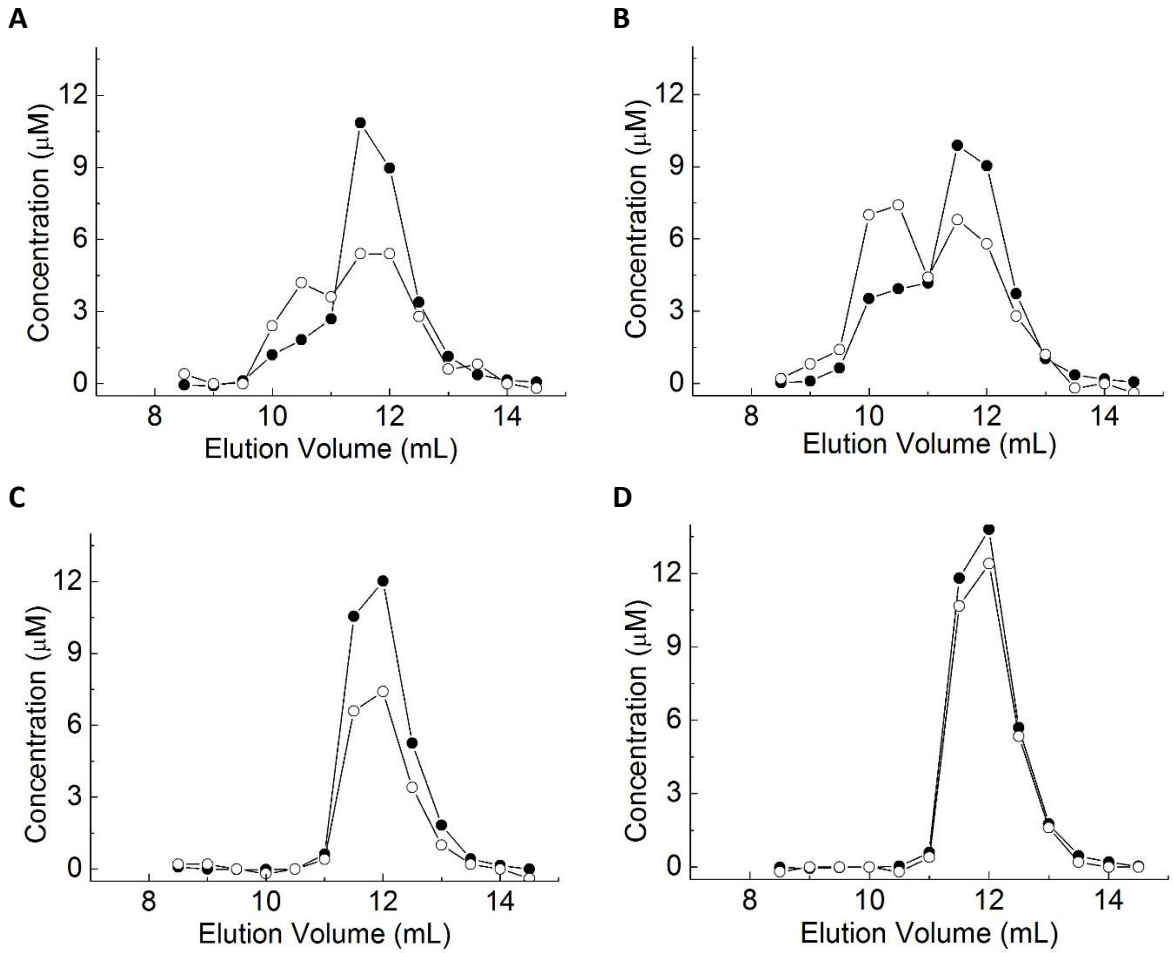

Figure 3.10. Distribution of C229/C231S-Ccs1 and Cu^{1+} concentrations in eluted fractions from a gel filtration column performed in deoxygenated buffer or the presence of DTT. This shows the oligomeric form and location of Cu^{1+}. Only monomeric C229S/C231S-Ccs1 is shown to be present in the presence of DTT . Protein (●) and Cu^{1+} (○) content of gel filtration fractions of C229S/C231S-Ccs1 in the presence of 0.5 (A and C) and 1.0 (B and D) equivalents Cu^{1+} in deoxygenated 20 mM Hepes pH 7.5 plus 200 mM NaCl (A and B) and the same buffer plus 250 µM DTT (C and D). Proteins (100 µM of 200 µL) were injected onto a Superdex 75 10/300 GL column and eluted at a flow rate of 0.8 mL/min at room temperature. For elution volumes and calculated apparent molecular weights see Table 3.3. Cu^{1+} is associated with both monomeric and dimeric forms of C229/C231S -Ccs1.

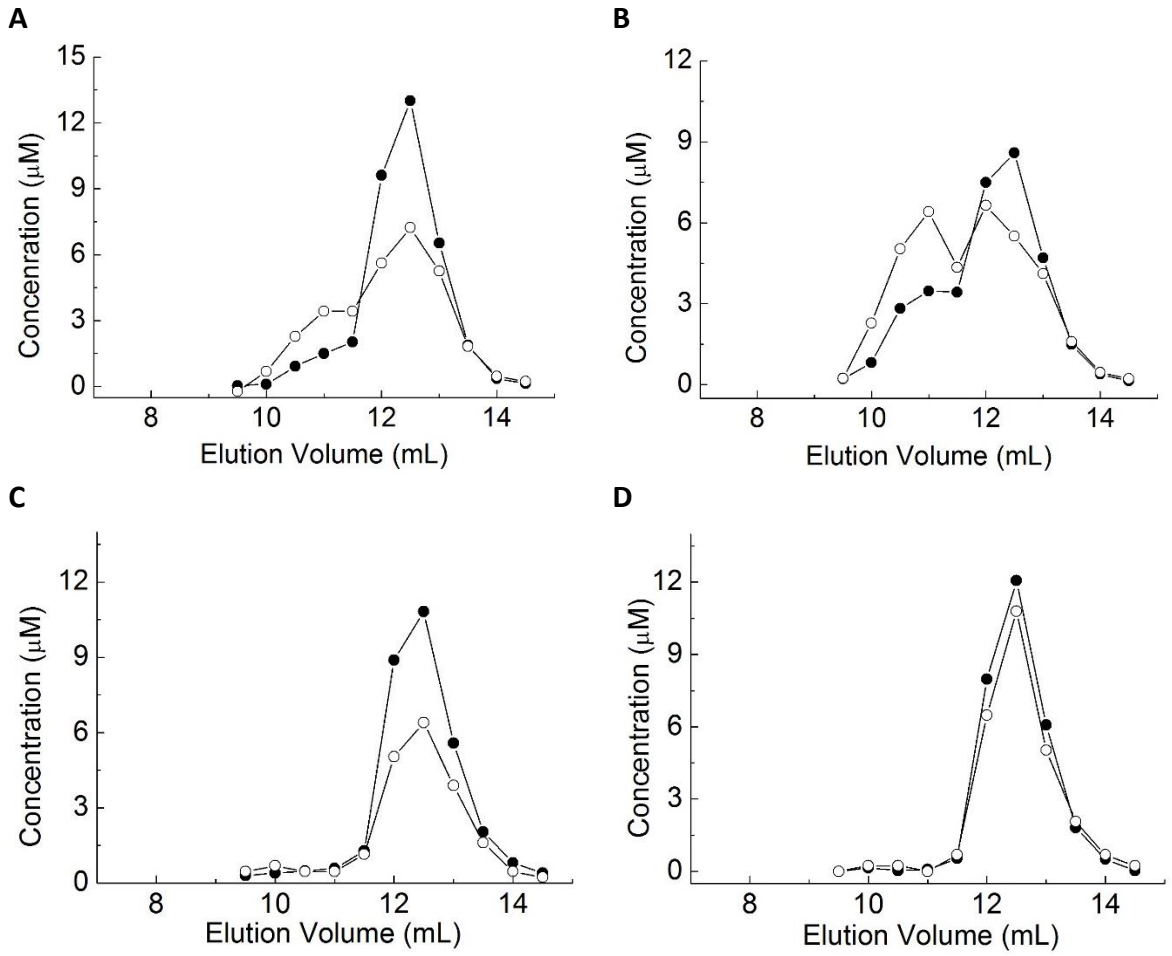

Figure 3.11. Distribution of D1/2-Ccs1 and Cu^{1+} concentrations in eluted fractions from a gel filtration column performed in deoxygenated buffer or the presence of DTT. This shows the oligomeric form and location of Cu^{1+}. Only monomeric D1/2-Ccs1 is shown to be present in the presence of DTT. Protein (●) and Cu^{1+} (○) content of gel filtration fractions of D1/2-Ccs1 in the presence of 0.5 (A and C) and 1.0 (B and D) equivalents Cu^{1+} in deoxygenated 20 mM Hepes pH 7.5 plus 200 mM NaCl (A and B) and the same buffer plus 250 μM DTT (C & D). Proteins (100 μM of 200 μL) were injected onto a Superdex 75 10/300 GL column and eluted at a flow rate of 0.8 mL/min at room temperature. For elution volumes and calculated apparent molecular weights see Table 3.3. Cu^{1+} is associated with both monomeric and dimeric forms of D1/2-Ccs1.

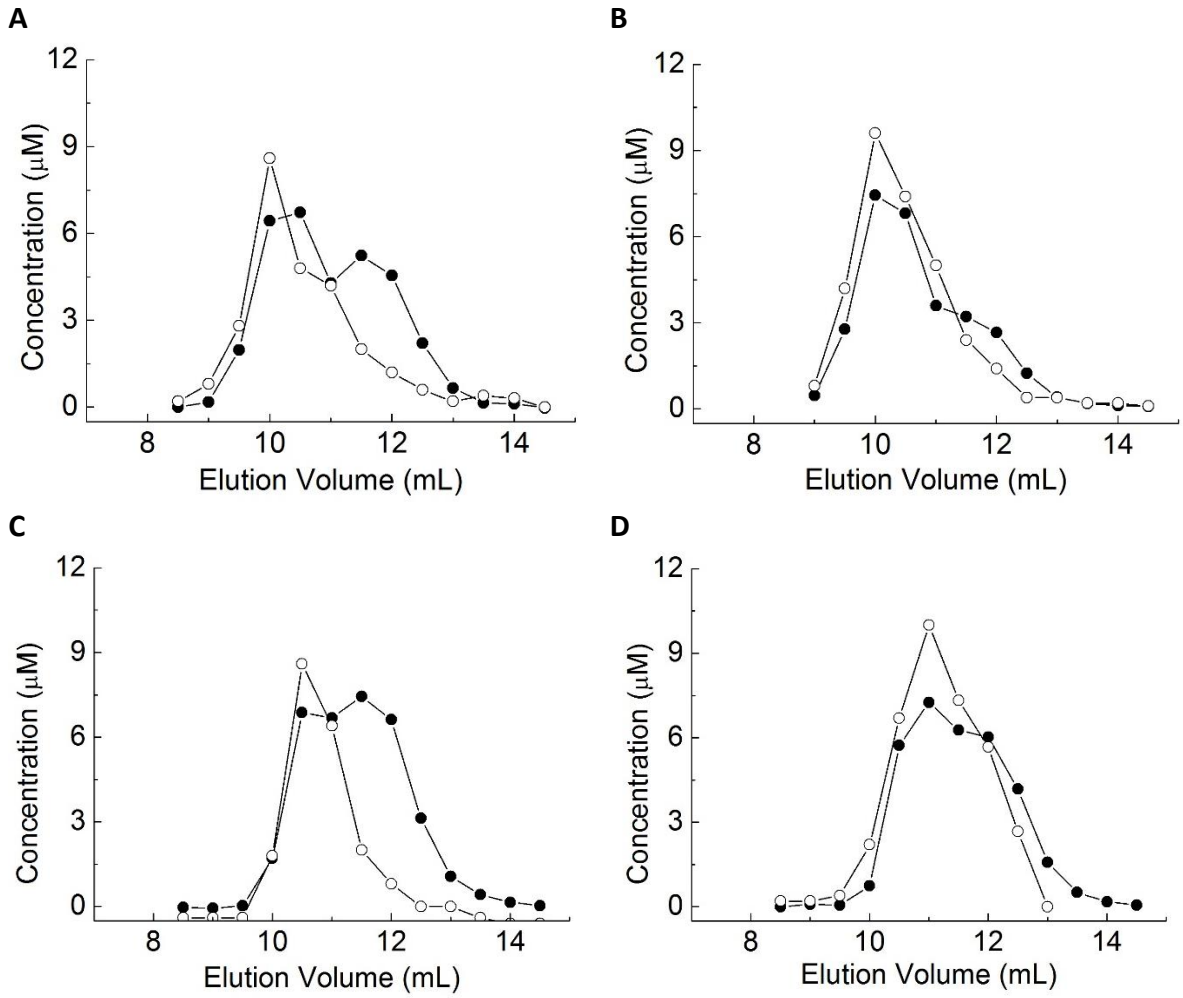

Figure 3.12. Distribution of C17/C20S-Ccs1 and Cu^{1+} concentrations in eluted fractions from a gel filtration column performed in deoxygenated buffer or the presence of DTT. This shows the oligomeric form and location of Cu^{1+}. Cu^{1+} is shown to be associated with both monomeric and dimeric C17S/C20S -Ccs1. Protein (●) and Cu^{1+} (○) content of gel filtration fractions of C17S/C20S-Ccs1 in the presence of 0.5 (A and C) and 1.0 (B and D) equivalents Cu^{1+} in deoxygenated 20 mM Hepes pH 7.5 plus 200 mM NaCl (A and B) and the same buffer plus 250 μM DTT (C and D). Proteins (100 μM of 200 μL) were injected onto a Superdex 75 10/300 GL column and eluted at a flow rate of 0.8 mL/min at room temperature. For elution volumes and calculated apparent molecular weights see Table 3.3. Cu^{1+} is associated with both monomeric and dimeric forms of C17/C20S-Ccs1.

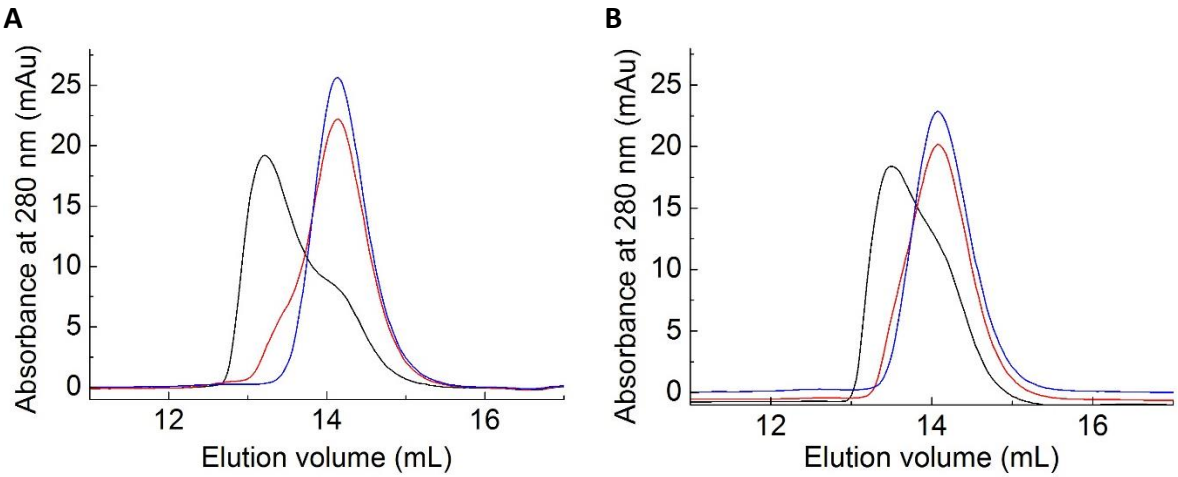

Figure 3.13. Gel-filtration chromatograms of Atx1 plus various equivalents of Cu^{1+} either under anaerobic conditions or in the presence of DTT. Plots of absorbance at 280 nm against elution volume for reduced apo-Atx1 (black) and Atx1 in the presence of 0.5 (red) and 1.0 equivalents Cu^{1+} (blue) in (A) deoxygenated 20 mM Hepes pH 7.5 plus 200 mM NaCl or (B) the same buffer plus 250 μM DTT. Proteins (200 μL of 100.0 μM) were injected onto a Superdex 75 10/300 GL column and eluted at a flow rate of 0.8 mL/min at room temperature. The peak eluting at ≈ 13.2 mL (16 kDa) corresponds to dimer and that eluting at ≈ 14.1 mL (11 kDa) to monomer.

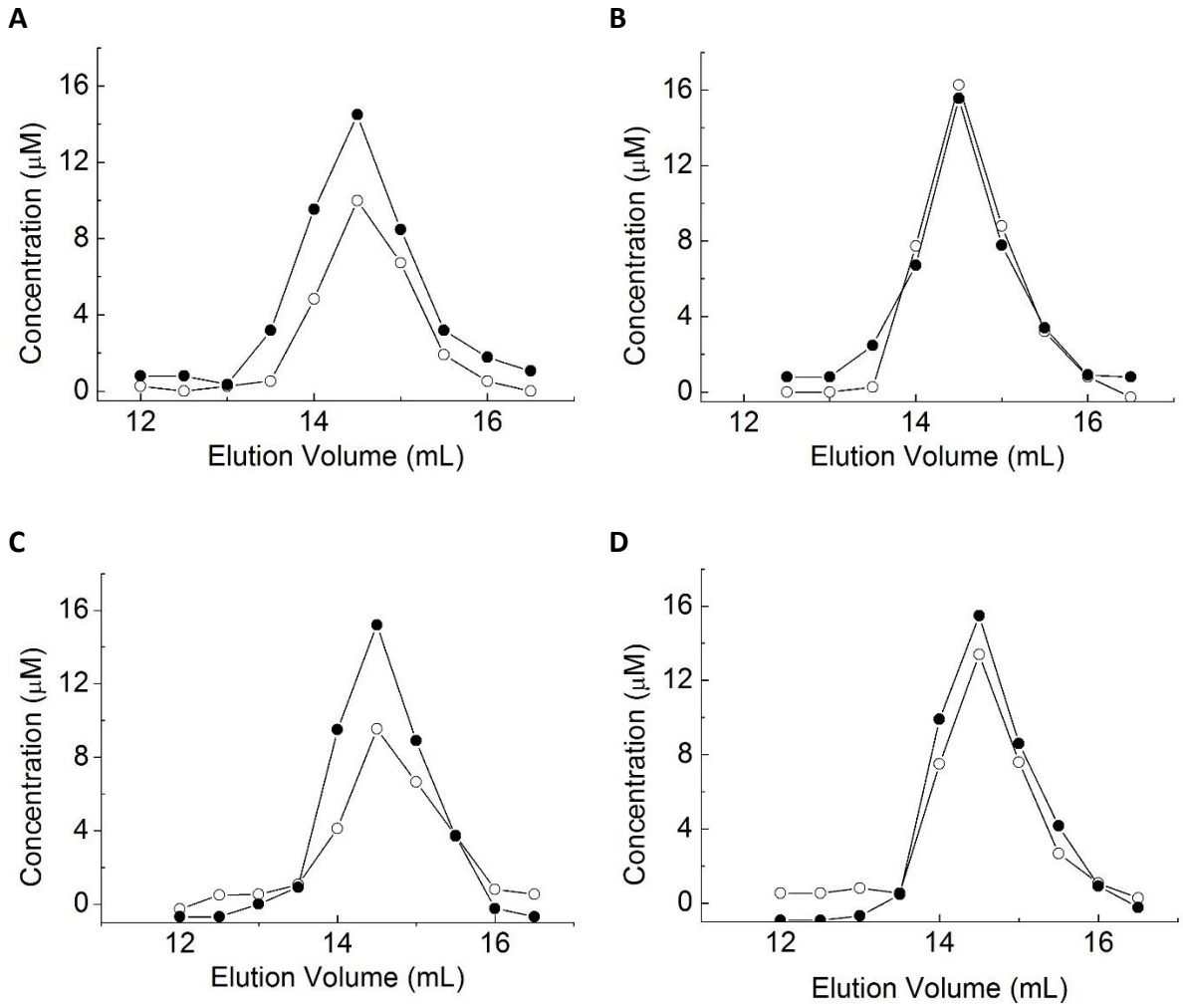

Figure 3.14. Distribution of Atx1 and Cu^{1+} in eluted fractions from a gel filtration column. Protein (●) and Cu^{1+} (○) content of fractions (500 µL) of Atx1 in the presence of 0.5 (A and C) and 1.0 (B and D) equivalents of Cu^{1+} in deoxygenated 20 mM Hepes pH 7.5 plus 200 mM NaCl (A and B) and the same buffer plus 250 µM DTT (C and D). Proteins (200 µL of 100.0 µM) were injected onto a Superdex 75 10/300 GL column and eluted at a flow rate of 0.8 mL/min at room temperature. The peak eluting at ≈ 13.2 mL (16 kDa) corresponds to dimer and that eluting at ≈ 14.1 mL (11 kDa) to monomer. Cu1+ is shown to be associated with monomeric Atx1.

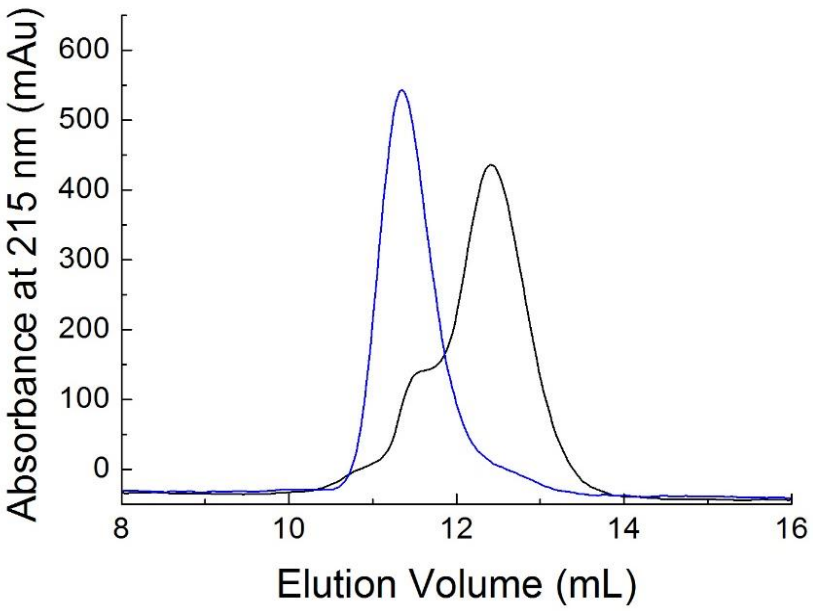

Figure 3.15. Gel-filtration chromatograms of purified Sod1 before and after incubation with DTT. Plots of absorbance at 215 nm against elution volume from a Superdex 75 10/300 GL column before (blue) and after (black) overnight incubation of E,E-Sod1 with DTT in 20 mM Hepes plus 200 mM NaCl (with 250 μM DTT for the latter sample). Proteins (200 μL of 100.0 μM) were eluted at a flow rate of 0.8 mL/min at room temperature. The peak eluting at ≈ 11.4 mL (34 kDa) corresponds to dimer and that eluting at ≈ 12.4 mL (22 kDa) to monomer.

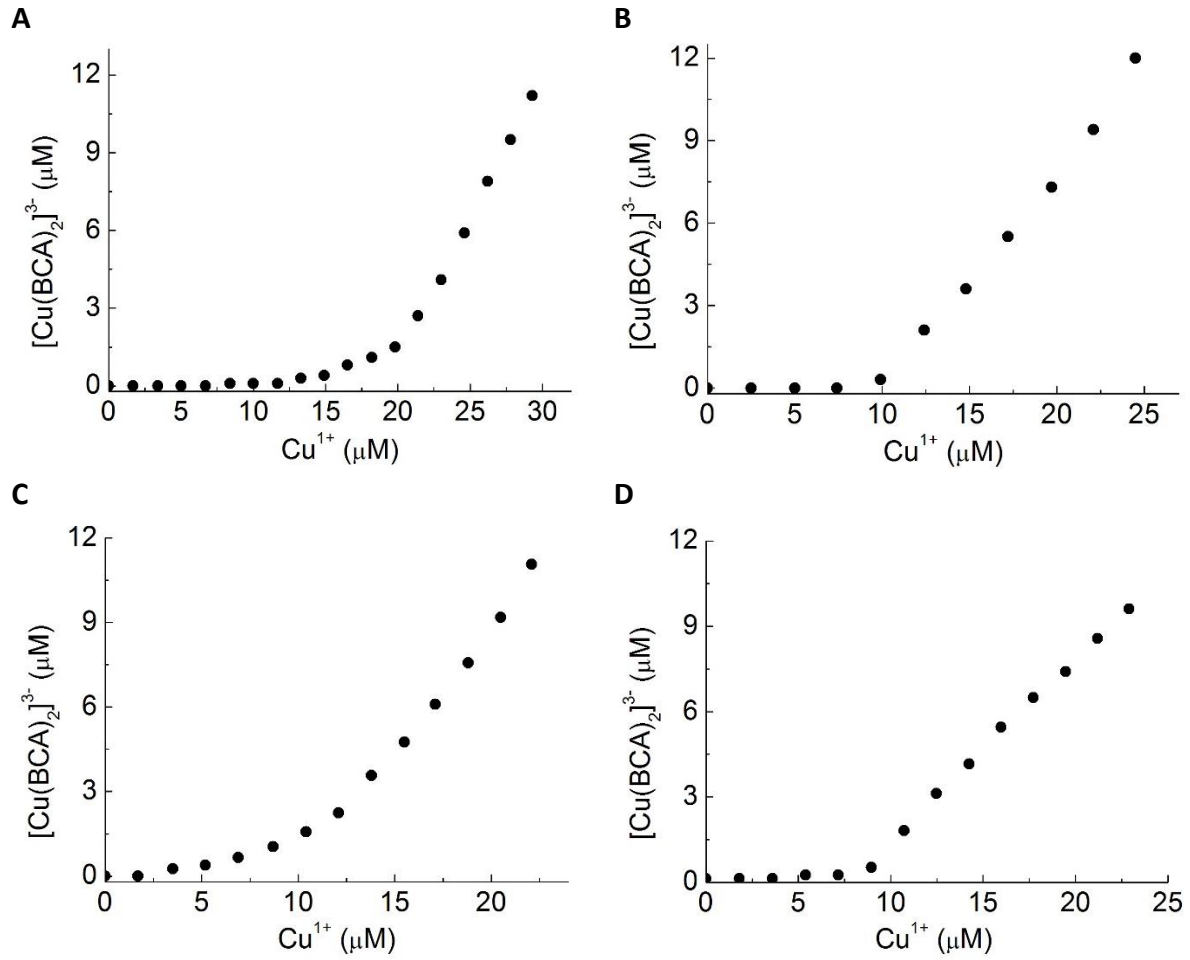

Figure 3.16. Titrations of Cu^{1+} into apo-Ccs1 proteins plus BCA to determine Cu^{1+}-binding stoichiometries. Plots of $[Cu(BCA)_2]^{3-}$ against Cu^{1+} concentration for reduced (A) apo-WT-Ccs1, (B) apo-C229S/C231S-Ccs1, (C) apo-C17S/C20S-Ccs1 and (D) apo-D1/2-Ccs1 (all at 10.0 μM) in the presence of 500 μM BCA in 20 mM Hepes pH 7.5 plus 200 mM NaCl. All solutions were prepared in an anaerobic chamber and titrations were performed at room temperature in anaerobic cuvettes with Cu^{1+} additions made using a gastight Hamilton syringe.

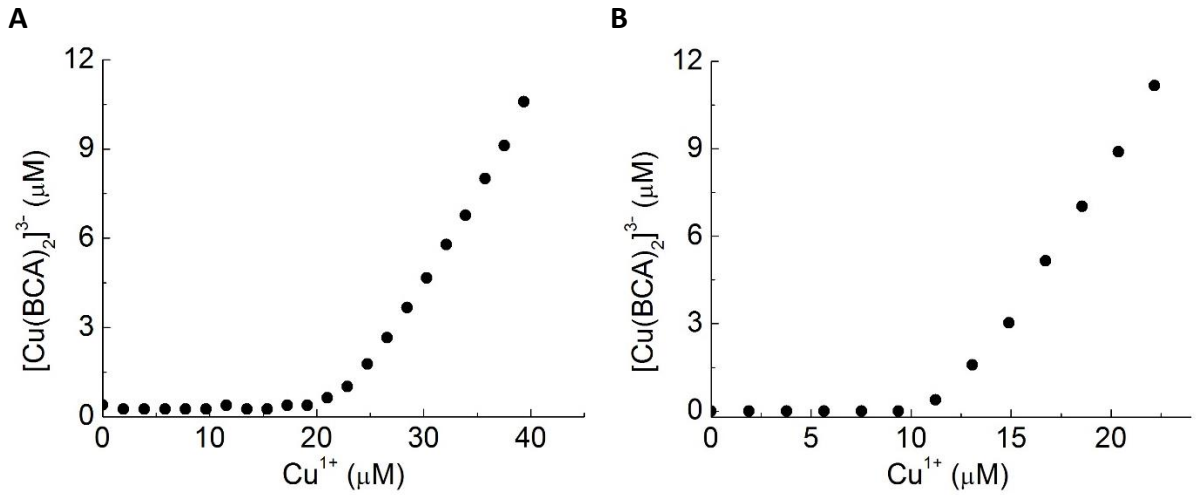

Figure 3.17. Titrations of Cu^{1+} into apo-Ccs1 proteins plus BCA to determine Cu^{1+}-binding stoichiometries. Plots of $[Cu(BCA)_2]^{3-}$ against Cu^{1+} concentration for reduced (A) apo-WT-Ccs1 and (B) apo-C17S/C20S-Ccs1 (both at 10.0 μM) in the presence of 150 μM BCA in 20 mM Hepes pH 7.5 plus 200 mM NaCl. All solutions were prepared in an anaerobic chamber and titrations were performed at room temperature in anaerobic cuvettes with Cu^{1+} additions made using a gastight Hamilton syringe.

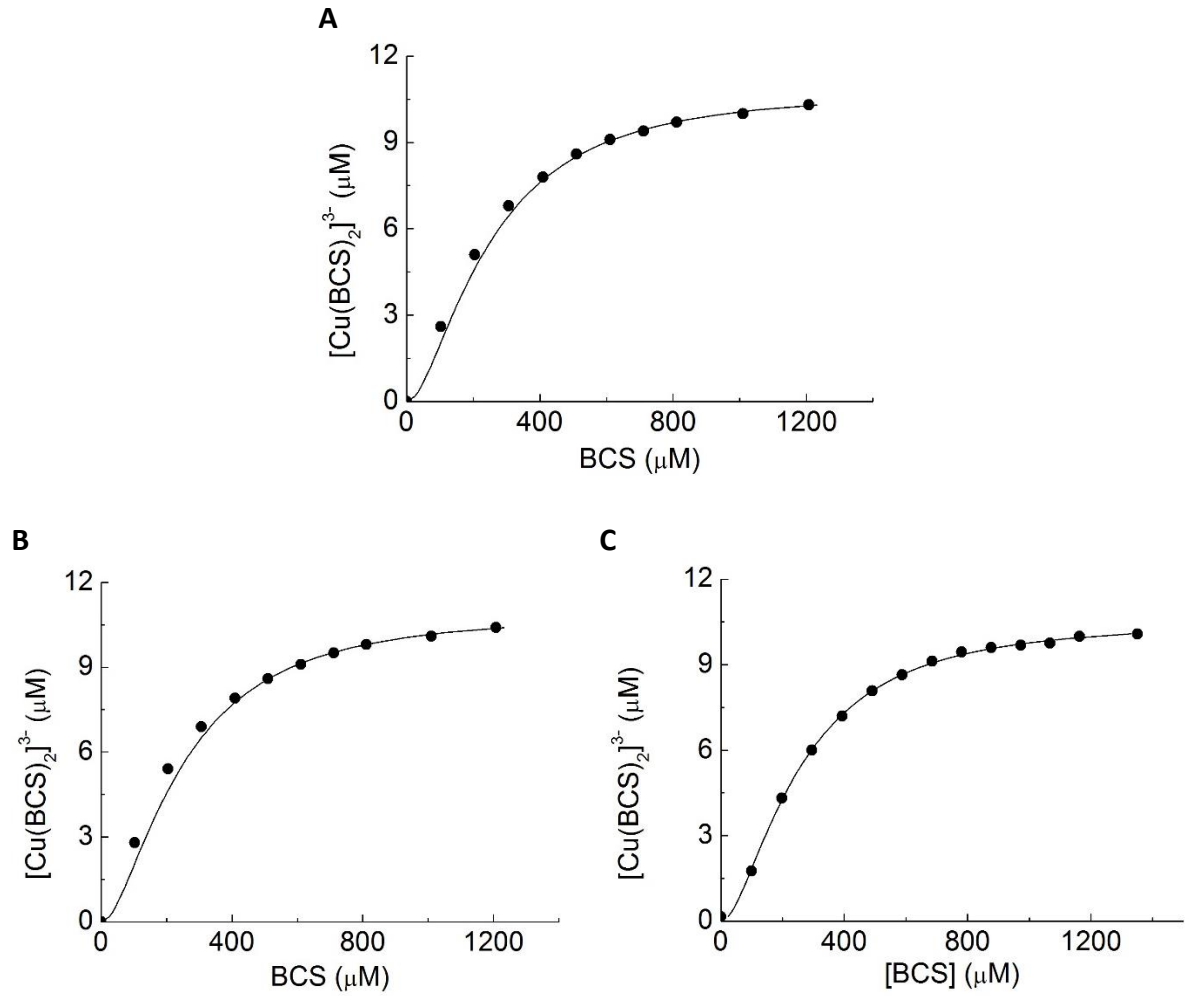

Figure 3.18. Titrations used to determine the Cu^{1+} affinities of Ccs1 proteins using BCS. Plots of $[Cu(BCS)_2]^{3-}$ against added BCS concentration for (A) WT-Ccs1, (B) C229S/C231S-Ccs1 and (C) D1/2-Ccs1 using apo-proteins (20 μM) plus 10 μM Cu^{1+} in 20 mM Hepes pH 7.5 plus 200 mM NaCl. Lines show fits of the data to Equation 2.1 (Methods 2.17.3). Using an overall stability constant (β_2) of 6.3 x 10^{20} M^{-2} gives K_b values of (A) (2.3 ± 0.1) x 10^{18} M^{-1}, (B) (2.3 ± 0.1) x 10^{18} M^{-1} and (C) (2.4 ± 0.2) x 10^{18} M^{-1}. All solutions were prepared in an anaerobic chamber and titrations were performed at room temperature in anaerobic cuvettes with Cu^{1+} additions made using a gastight Hamilton syringe.

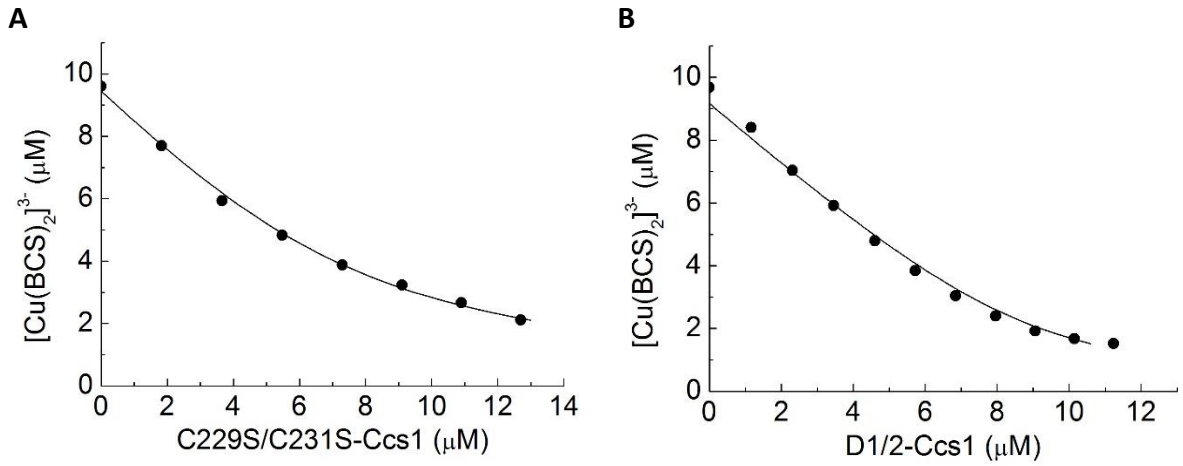

Figure 3.19. Titrations used to determine the Cu^{1+} affinities of Ccs1 proteins using BCS. Plots of $[Cu(BCS_2]^{3-}$ (10 μM) against added reduced apo-C229S/C231S-Ccs1 (A) and apo-D1/2-Ccs1 (B) in the presence of an excess 500 μM BCS in 20 mM Hepes pH 7.5 plus 200 mM NaCl. Lines show fit of the data to affinity Equation 2.2 (Methods 2.17.3). Using an overall stability constant (β_2) of 6.3 x 10^{20} M^{-2} gives K_b values of (A) (2.5 ± 0.2) x 10^{18} M^{-1} and (B) (3.2 ± 0.6) x 10^{18} M^{-1}. All solutions were prepared in an anaerobic chamber and titrations were performed at room temperature in anaerobic cuvettes with Cu^{1+} additions made using a gastight Hamilton syringe.

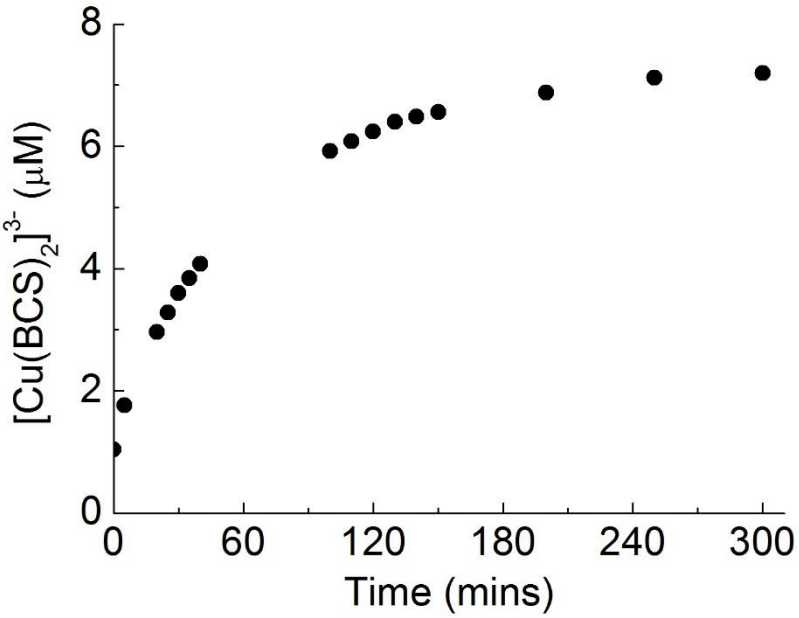

Figure 3.20. Plot showing the formation of $[Cu(BCS)_2]^{3-}$ due to the removal of Cu^{1+} from C17S/C20S-Ccs1 by BCS over time. The removal of Cu^{1+} from C17S/C20S-Ccs1 (20 μM) plus 10 μM Cu^{1+} by BCS (100 μM) in 20 mM Hepes pH 7.5 plus 200 mM NaCl. Protein, BCS and Cu^{1+} stock was prepared in an anaerobic chamber at room temperature. The sample was in an anaerobic cuvette that was returned to the chamber between measurements

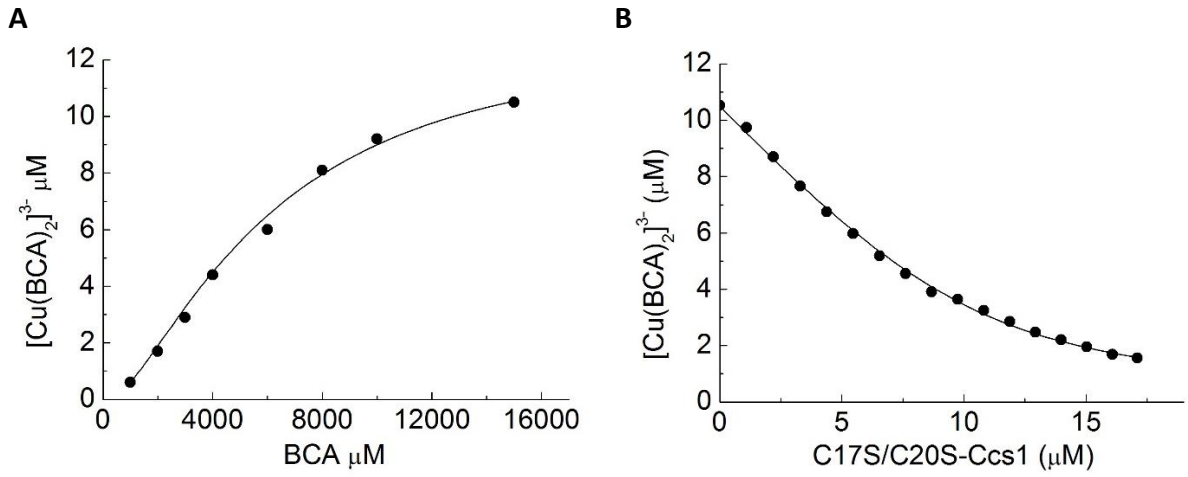

Figure 3.21. Titrations used to determine the Cu^{1+} affinity of C17S/C20S-Ccs1 using BCA. (A) A plot of $[Cu(BCA)_2]^{3-}$ against added BCA concentration for reduced apo-C17S/C20S-Ccs1 (20 μM) plus Cu^{1+} (10 μM) after incubating mixtures for 48 h. (B) A plot of $[Cu(BCA)_2]^{3-}$ against added reduced apo-C17S/C20S-Ccs1 concentration using 10 μM $[Cu(BCA)_2]^{3-}$ with an excess of 700 μM BCA. Both experiments were performed in 20 mM Hepes pH 7.5 plus 200 mM NaCl at room temperature. Lines show fits of the data to (A) Equation 2.1 and (B) Equation 2.2 (Methods 2.17.3), using a β_2 value for BCA of 5.0×10^{17} M^{-2} gives K_b values of (A) $(1.2 \pm 0.1) \times 10^{18}$ M^{-1} and (B) $(4.1 \pm 0.9) \times 10^{17}$ M^{-1}. All solutions were prepared in an anaerobic chamber and titrations were performed at room temperature in anaerobic cuvettes with additions made using a gastight Hamilton syringe.

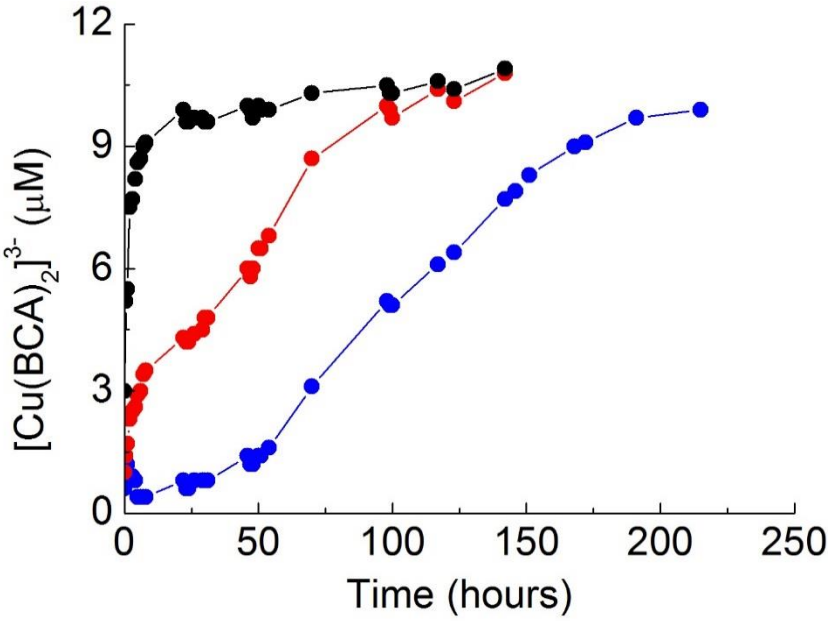

Figure 3.22. The removal of Cu^{1+} from C17S/C20S-Ccs1 by BCA over time. A plot showing the formation of $[Cu(BCA)_2]^{3-}$ (10 μM) against time for Cu^{1+}-C17S/C20S-Ccs1 (10 μM) plus an excess of apo-C17S/C20S-Ccs1 (10 μM) incubated with 1 (blue), 4 (red) and 15 (black) mM BCA in 20 mM Hepes pH 7.5 plus 200 mM NaCl. All solutions were prepared in an anaerobic chamber and the experiments performed at room temperature in anaerobic cuvettes that were returned to the chamber between most measurements.

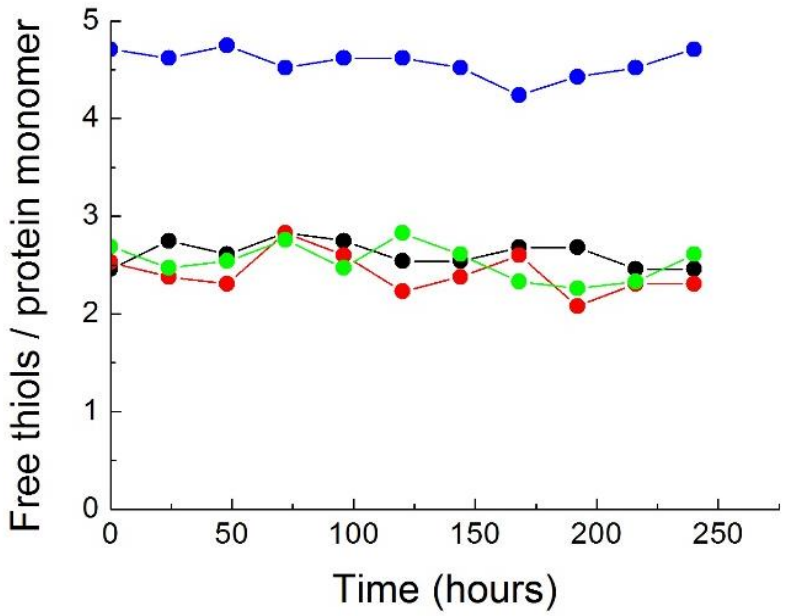

Figure 3.23. The stability of the thiols in reduced Ccs1 proteins over time under anaerobic conditions. Plots of thiol/protein monomer against time for apo-C17/C20S-Ccs1 (black), Cu^{1+}-C17/C20S-Ccs1 [0.5 equivalents of Cu^{1+}] (red), apo-C17/C20S-Ccs1 with 4 mM BCA (green) and apo-WT-Ccs1 with 4 mM BCA (blue) in 20 mM Hepes pH 7.5 plus 200 mM NaCl. All proteins (20 μM) were reduced prior to this experiment in an anaerobic chamber. The samples were in anaerobic cuvettes that were returned to the chamber between measurements at room temperature.

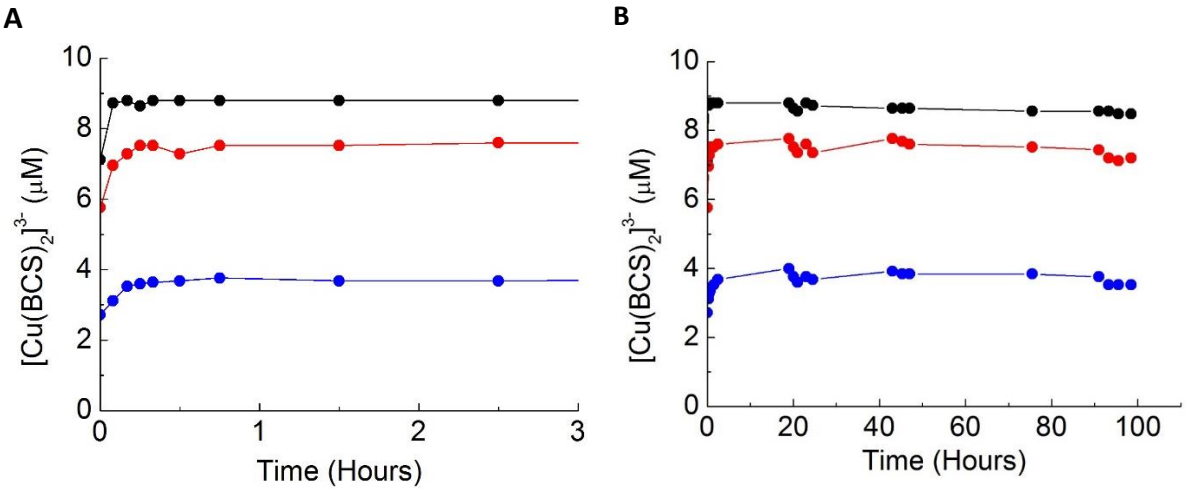

Figure 3.24. The removal of Cu^{1+} from WT-Ccs1 in the presence of BCS. Plots of the formation of $[Cu(BCS)_2]^{3-}$ against time for Cu^{1+}-WT-Ccs1 (10 μM) plus an excess apo-WT-Ccs1 (10 μM) incubated with 100 (blue), 300 (red) and 1200 (black) μM BCS in 20 mM Hepes pH 7.5 plus 200 mM NaCl. Data acquired at room temperature for up to 3 (A) and 100 (B) h are shown. All solutions were prepared in an anaerobic chamber and the experiments performed in anaerobic cuvettes that were returned to the chamber between most measurements.

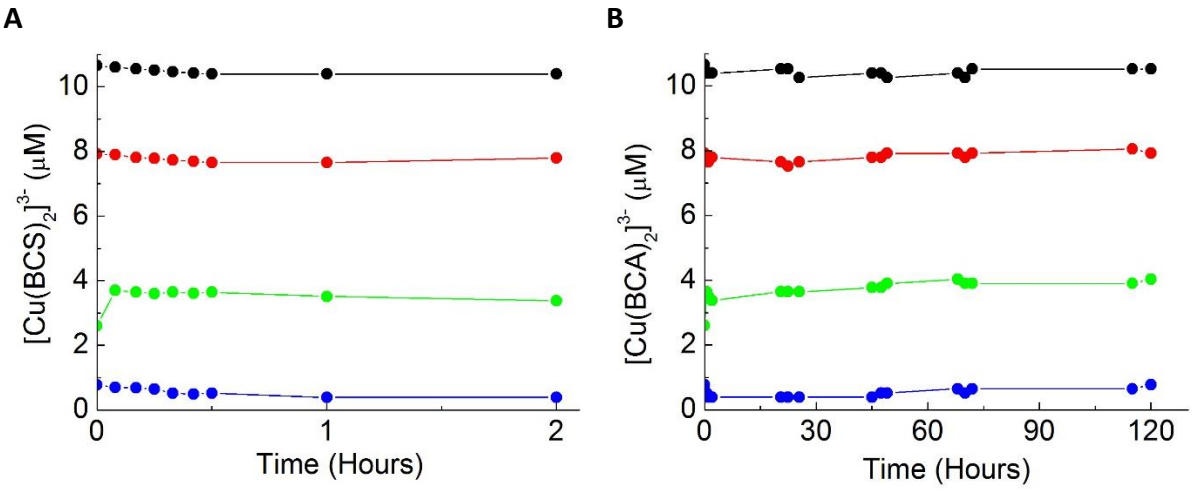

Figure 3.25. The stability of the mixtures formed upon adding apo-C17S/C20S-Ccs1 to $[Cu(BCA)_2]^{3-}$. Plots of $[Cu(BCA)_2]^{3-}$ against time for 10 μM $[Cu(BCA)_2]^{3-}$ plus an excess of BCA (700 μM) incubated with 0 (blue), 2 (green), 5 (red) and 10 (black) μM apo-C17S/C20S-Ccs1 in 20 mM Hepes pH 7.5 plus 200 mM NaCl. Data acquired at room temperature for up to 2 (A) and 120 (B) h are shown. All solutions were prepared in an anaerobic chamber and the experiments performed in anaerobic cuvettes that were returned to the chamber between most measurements.

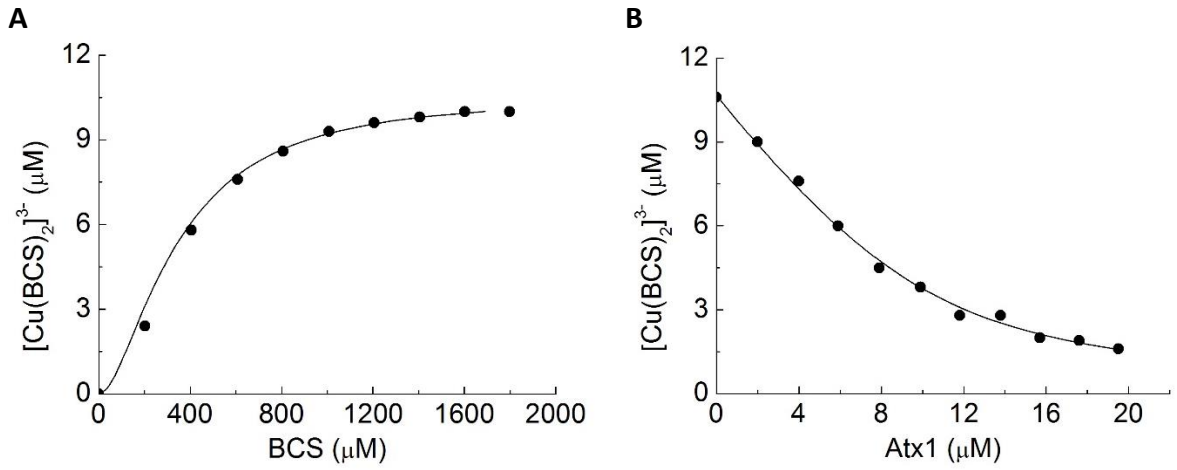

Figure 3.26. Titrations used to determine the Cu^{1+} affinity of Atx1 using BCS at pH 7.0. (A) A plot of $[Cu(BCS)_2]^{3-}$ against added BCS concentration using 20 μM reduced apo-Atx1 and 10 μM Cu^{1+}. (B) A plot of $[Cu(BCS)_2]^{3-}$ against added reduced apo-Atx1 concentration using 10 μM $[Cu(BCS)_2]^{3-}$ in the presence of an excess of BCS (100 μM) in 20 mM Hepes pH 7.0 plus 200 mM NaCl. Lines show the fit of the data to (A) Equation 2.1 and (B) Equation 2.2 (Methods 2.17.3), and using a β_2 of 6.3×10^{17} M^{-2} for $[Cu(BCS)_2]^{3-}$ gives K_b values of (A) $(4.1 \pm 0.4) \times 10^{18}$ M^{-1} and (B) $(4.3 \pm 0.3) \times 10^{18}$ M^{-1}. All solutions were prepared in an anaerobic chamber and titrations were performed at room temperature in anaerobic cuvettes with additions made using a gastight Hamilton syringe.

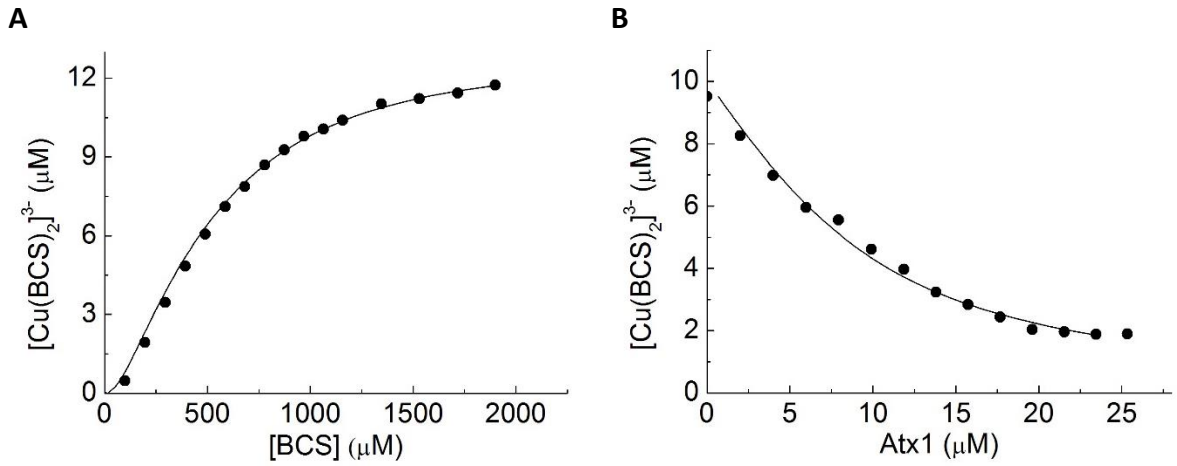

Figure 3.27. Titrations used to determine the Cu^{1+} affinity of Atx1 using BCS at pH 7.5. (A) A plot of $[Cu(BCS)_2]^{3-}$ against added BCS concentration for 20.0 µM reduced apo-Atx1 plus 10 µM Cu^{1+}. (B) A plot of $[Cu(BCS)_2]^{3-}$ against added reduced apo-Atx1 concentration using 10 µM $[Cu(BCS)_2]^{3-}$ with an excess of 100 µM BCS in 20 mM Hepes pH 7.5 plus 200 mM NaCl. Lines show the fit of the data to (A) Equation 2.1 and B) Equation 2.2 (Methods 2.17.3), and using a β_2 of 6.3 x 10^{20} M^{-2} for $[Cu(BCS)_2]^{3-}$ gives K_b values of (A) (1.1 ± 0.1) x 10^{19} M^{-1} and (B) (1.2 ± 0.7) x 10^{19} M^{-1}. All solutions were prepared in an anaerobic chamber and titrations were performed at room temperature in anaerobic cuvettes with additions made using a gastight Hamilton syringe.

Table 3.4. Summary of the average Cu^{1+} affinities (K_b values) for WT Ccs1 and variants as well as Atx1 from S. cerevisiae compared to values for human homologues.

Organism	Protein	pH	K_b (BCA) (M^{-1})[g]	K_b (BCS) (M^{-1})[g]
S. cerevisiae	WT-Ccs1[b,e]	7.5	-	$(2.6 \pm 1.1) \times 10^{18}$
S. cerevisiae	WT-Ccs1[a,e]	7.5	-	$(2.3 \pm 0.1) \times 10^{17}$
S. cerevisiae[103]	WT-Ccs1[a,]	7.5	-	$(2.4 \pm 0.5) \times 10^{17}$
H. sapiens[103]	WT-CCS[a,]	7.5	-	$(5.5 \pm 0.6) \times 10^{17}$
S. cerevisiae	D1/2-Ccs1[b,e]	7.5	-	$(2.7 \pm 1.0) \times 10^{18}$
S. cerevisiae	D1/2-Ccs1[a,e]	7.5	-	$(2.5 \pm 0.6) \times 10^{17}$
H. sapiens	D1-CCS[a,103]	7.5	-	$(5.5 \pm 3.5) \times 10^{17}$
S. cerevisiae	C229S/C231S-Ccs1[b,e]	7.5	-	$(2.6 \pm 0.5) \times 10^{18}$
S. cerevisiae	C229S/C231S-Ccs1[a,e]	7.5	-	$(2.3 \pm 0.1) \times 10^{17}$
H. sapiens[103]	C244S/C246S-CCS[a,]	7.5	-	$(4.6 \pm 1.0) \times 10^{17}$
S. cerevisiae	C17S/C20S-Ccs1[d,f]	7.5	$(4.1 \pm 0.9) \times 10^{17}$	-
S. cerevisiae	C17S/C20S-Ccs1[c,f]	7.5	$(4.4 \pm 0.8) \times 10^{16}$	-
H. sapiens[103]	C22S/C25S-CCS[c,]	7.5	$(2.7 \pm 1.4) \times 10^{16}$	-
S. cerevisiae	Atx1[b,e]	7.0	-	$(4.2 \pm 1.4) \times 10^{18}$
S. cerevisiae	Atx1[a,e]	7.0	-	$(4.6 \pm 0.5) \times 10^{17}$
H. sapiens[139]	HAH1[a,]	7.0	-	$(5.6) \times 10^{17}$
S. cerevisiae	Atx1[b,e]	7.5	-	$(1.2 \pm 0.7) \times 10^{19}$
S. cerevisiae	Atx1[a,e]	7.5	-	$(1.1 \pm 0.8) \times 10^{18}$

[a] Calculated using a $\log(\beta_{max})$ for $[Cu(BCS)_2]^{3-}$ of 19.9.[138]
[b] Calculated using a $\log(\beta_{max})$ for $[Cu(BCS)_2]^{3-}$ of 20.8.[144]
[c] Calculated using a $\log(\beta_{max})$ for $[Cu(BCA)_2]^{3-}$ of 17.3.[138]
[d] Calculated using a $\log(\beta_{max})$ for $[Cu(BCA)_2]^{3-}$ of 17.7.[144]
[e] Obtained from titrations of either BCS or BCA into Cu^{1+}-protein.
[f] Determined from titrations of apo-proteins into $[Cu(BCA)_2]^{3-}$.
[g] Average values from three independent determinations.

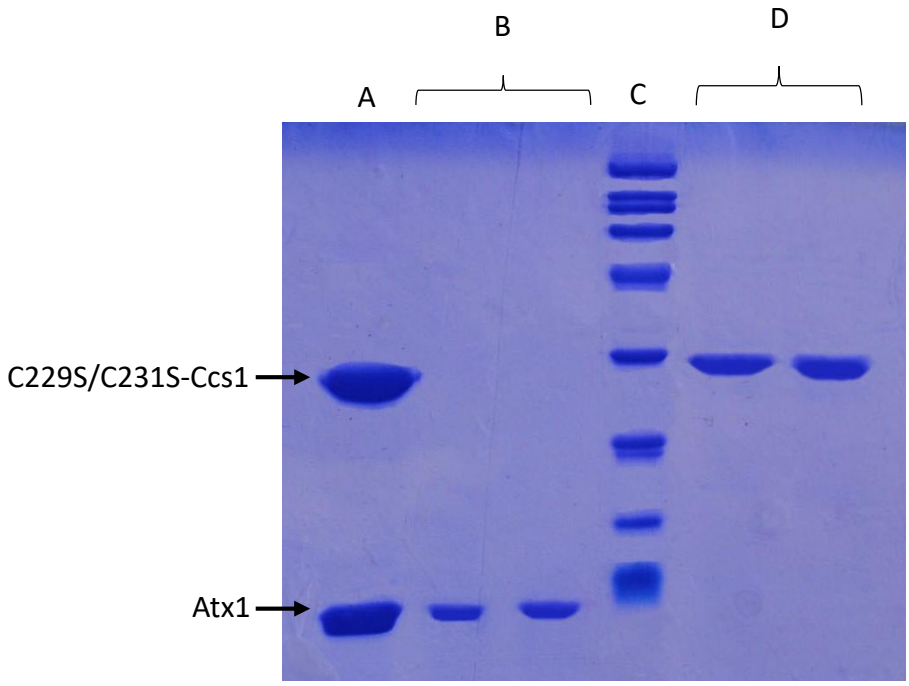

Figure 3.28. SDS-PAGE gel showing the separation of a mixture of Atx1 and C229S/C231S-Ccs1 by anion exchange chromatography. (A) The Cu^{1+}-Atx1 and apo-C229S/C231S-Ccs1 mixture, (B) fractions eluted from a HiTrap Q HP column with 20 mM Hepes pH 7.5 that contain Atx1, (C) molecular weight marker and (D) fractions eluted with 20 mM Hepes pH 7.5 plus 200 mM NaCl that contain C229S/C231S-Ccs1.

Table 3.5. Protein concentrations from Cu^{1+} exchange experiments between Atx1 and C229S/C231S-Ccs1, and exchange equilibrium constant (K_{ex} values) after incubation for 1 hr.

	Initial Concentrations (µM)				Equilibrium Concentrations (µM)[a]					
Proteins	Cu^{1+}-Atx1	Atx1	Cu^{1+}-C229S/C231S-Ccs1	C229S/C231S-Ccs1	Cu^{1+}-Atx1	Atx1	Cu^{1+}-C229S/C231S-Ccs1	C229S/C321S-Ccs1	K_{ex}	K_{theo}[b]
Cu^{1+}-Atx1 + apo-C229S/C231S-Ccs1	25	25	0	50	17	33	8	42	0.37	0.17
apo-Atx1 + Cu^{1+}-C229S/C231S-Ccs1	0	50	25	25	18	32	7	43	0.29	

[a] Concentrations corrected for dilutions

[b] Calculated using $K_{theo} = K_b^{(C229S/C231S\text{-}Ccs1)} / K_b^{(Atx1)}$ and the affinities (K_b values) of the partner proteins from Table 3.4.

Table 3.6. Protein concentrations from Cu^{1+} exchange experiments between Atx1 and C17S/C20S-Ccs1, and exchange equilibrium constant (K_{ex} values) after incubation for 1 hr.

	Initial Concentrations (µM)				Equilibrium Concentrations (µM)[a]					
Proteins	Cu^{1+}-Atx1	Atx1	Cu^{1+}-C17S/C20S-Ccs1	C17S/C20S-Ccs1	Cu^{1+}-Atx1	Atx1	Cu^{1+}-C17S/C20S-Ccs1	C17S/C20S-Ccs1	**K_{ex}**	**K_{theo}[b]**
Cu^{1+}-Atx1 + apo-C17S/C20S-Ccs1	25	25	0	50	20	30	5	45	0.17	0.03
apo-Atx1 + Cu^{1+}-C17S/C20S-Ccs1	0	50	25	25	17	33	8	42	0.37	

[a] Concentrations corrected for dilutions.

[b] Calculated using $K_{theo} = K_b^{(C17S/C20S\text{-}Ccs1)} / K_b^{(Atx1)}$ and the Cu1+ affinities (K_b values) of the partner proteins from Table 3.4.

Table 3.7. Protein concentrations from Cu^{1+} exchange experiments between Atx1 and C17S/C20S-Ccs1, and exchange equilibrium constant (K_{ex} values) after incubation for 24 h.

	Initial Concentrations (µM)				Equilibrium Concentrations (µM)[a]					
Proteins	Cu^{1+}-Atx1	Atx1	Cu^{1+}-C17S/C20S-Ccs1	C17S/C20S-Ccs1	Cu^{1+}-Atx1	Atx1	Cu^{1+}-C17S/C20S-Ccs1	C17S/C20S-Ccs1	**K_{ex}**	**K_{theo}[b]**
Cu^{1+}-Atx1 + apo-C17S/C20S-Ccs1	25	25	0	50	21	29	4	46	0.12	0.03
apo-Atx1 + Cu^{1+}-C17S/C20S-Ccs1	0	50	25	25	21	29	4	46	0.12	

[a] Concentrations corrected for dilutions.

[b] Calculated using $K_{theo} = K_b^{(C229S/C231S\text{-}Ccs1)} / K_b^{(Atx1)}$ and the Cu^{1+} affinities K_b values from Table 3.4.

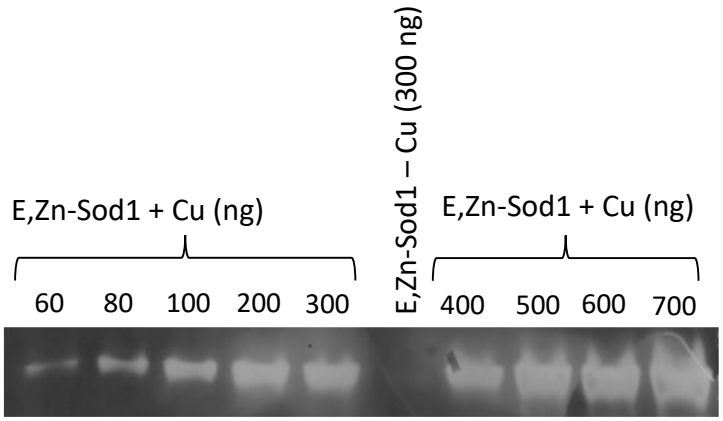

Figure 3.29. Visualisation of superoxide dismutase activity using an in-gel assay *(Methods 2.19)*. A native gel showing the activity of Cu,Zn-Sod1, and the absence of activity for E,Zn-Sod1 produced by the addition of Zn^{2+} to E,E-Sod1. For Cu,Zn-Sod1 the total amount of protein loaded was varied to determine the optimum amount for activity quantification. Active Sod1 is indicated by white bands in the image.

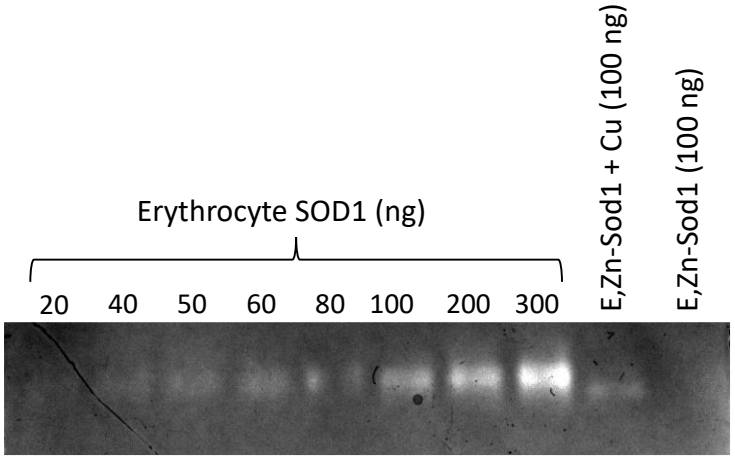

Figure 3.30. In-gel activity assay *(Methods 2.19)* of Cu,Zn-Sod1 and E,Zn-Sod1 compared to a standard protein. A native gel showing the superoxide dismutase activity of Cu,Zn-Sod1, and absence of activity of E,Zn-Sod1, as well as different total amounts of bovine erythrocyte SOD1 used as a standard. Active Sod1 is indicated by white bands in the image.

	A	B	C	D	E	F
E,Zn-Sod1^{SH}	+	+	-	-	-	-
$Cu^{2+}(NO_3)_2$	+	-	-	-	-	-
Cu^{1+} – WT-Ccs1	-	-	+	-	-	-
Cu^{1+} – C17S/C20S-Ccs1	-	-	-	+	-	-
Cu^{1+} – C229S/C231S-Ccs1	-	-	-	-	+	-
Cu^{1+} - D1/2-Ccs1	-	-	-	-	-	+

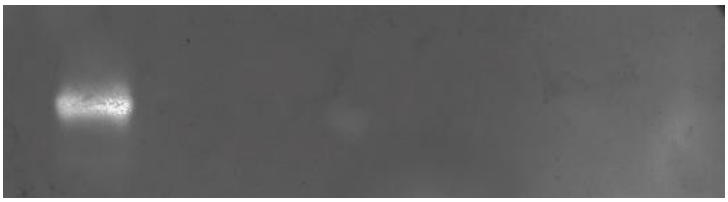

Figure 3.31. In-gel Cu,Zn-Sod1 activity assay *(Methods 2.19)* used to analyse the metalation of E,Zn-Sod1. A native gel showing Cu,Zn-Sod1 activity for a Zn-Sod1 sample (100 ng Sod1 loaded in gel lane A and B) incubated with (A) and without (B) a Cu^{2+} salt. Cu^{1+}-loaded forms of WT and variant Ccs1 proteins were loaded in gel lanes (C-F) without incubation with Sod1. Active Sod1 is indicated by white bands in the image. All solutions were prepared in an anaerobic chamber and all proteins were reduced prior to use. E,Zn-Sod1 and Cu,Zn-Sod1 were prepared by the addition of equal quantities of E,E-Sod1, $ZnSO_4$ and/or $Cu^{2+}(NO_3)_2$. Apo-Ccs1 proteins and Cu^{1+} (1 equivalent) were incubated anaerobically for 30 mins. The Reaction mixtures consisted of 5 µM E,Zn-Sod1, 5 µM Cu^{1+}-Ccs1, 100 µM EDTA and 100 µM BCS. Samples were exposed to air, incubated at 37 ^{o}C for 1 h and loaded onto a NATIVE-PAGE gel.

	A	B	C	D	E	F
E,Zn-Sod1^{SH}	+	+	+	+	+	+
$Cu^{2+}(NO_3)_2$	+	-	-	-	-	-
Cu^{1+} – WT-Ccs1	-	-	+	-	-	-
Cu^{1+} – C17S/C20S-Ccs1	-	-	-	+	-	-
Cu^{1+} – C229S/C231S-Ccs1	-	-		-	+	-
Cu^{1+} - D1/2-Ccs1	-	-	-	-	-	+

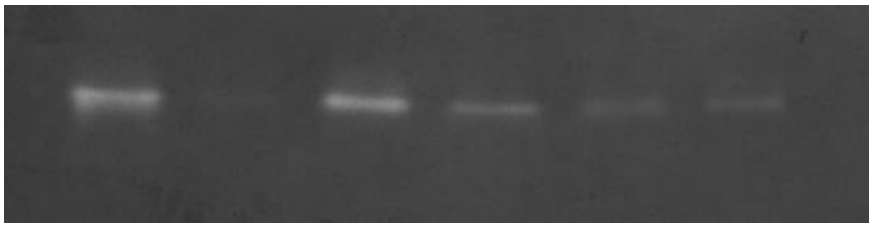

Figure 3.32. In-gel Cu,Zn-Sod1 activity assay *(Methods 2.19)* used to analyse the metalation of E,Zn-Sod1. A native gel showing Cu,Zn-Sod1 activity for Zn-Sod1 samples (100 ng Sod1 loaded in each gel lane) incubated with a Cu^{2+} salt and Cu^{1+}-loaded forms of WT and variant Ccs1 proteins. Active Sod1 is indicated by white bands in the image. All solutions were prepared in an anaerobic chamber and all proteins were reduced prior to use. E,Zn-Sod1 and Cu,Zn-Sod1 were prepared by the addition of equal quantities of E,E-Sod1, $ZnSO_4$ and/or $Cu^{2+}(NO_3)_2$. Apo-Ccs1 proteins and Cu^{1+} (1 equivalent) were incubated anaerobically for 30 mins prior to being mixed with E,Zn-Sod1. The Reaction mixtures consisted of 5 μM E,Zn-Sod1, 5 μM Cu^{1+}-Ccs1, 100 μM EDTA and 100 μM BCS. Once combined, samples were exposed to air, incubated at 37 ^{o}C for 1 h and loaded onto a NATIVE-PAGE gel.

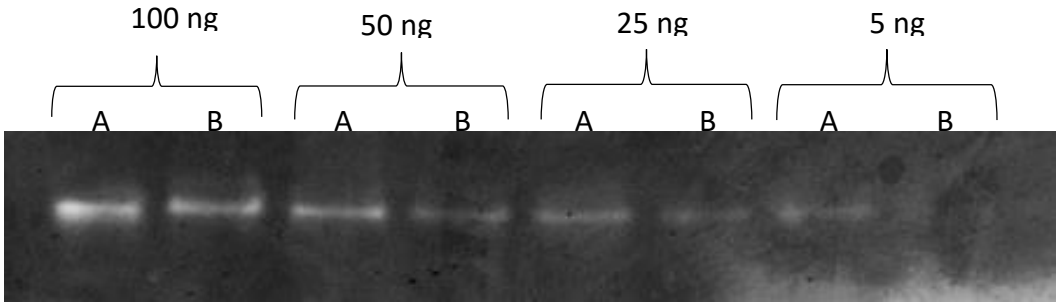

Figure 3.33. In-gel Cu,Zn-Sod1 activity assay *(Methods 2.19)* used to analyse the metalation of E,Zn-Sod1. A native gel showing Cu,Zn-Sod1 activity for Zn-Sod1 samples (stated amount of Sod1 loaded in each gel lane) incubated with Cu^{1+}-loaded forms of (A) WT-Ccs1 and (B) C17S/C20S-Ccs1 . Active Sod1 is indicated by white bands in the image. All solutions were prepared in an anaerobic chamber and all proteins were reduced prior to use. E,Zn-Sod1 was prepared by the addition of an equal quantity of E,E-Sod1 and $ZnSO_4$. Apo-Ccs1 proteins and Cu^{1+} (1 equivalent) were incubated anaerobically for 30 mins prior to being mixed with E,Zn-Sod1. The Reaction mixtures consisted of 5 µM E,Zn-Sod1, 5 µM Cu^{1+}-Ccs1, 100 µM EDTA and 100 µM BCS. Once combined, samples were exposed to air, incubated at 37 ^{o}C for 1 h and loaded onto a NATIVE-PAGE gel.

3.9 References

1. F. Frottin, A. Martinez, P. Peynot, S. Mitra, R. C. Holz, C. Giglione and T. Meinnel, *Molecular & Cellular Proteomics*, 2006, **5**, 2336-2349.
2. H. C. Gasteiger E., Gattiker A., Duvaud S., Wilkins M.R., Appel R.D., Bairoch A., *Protein Identification and Analysis Tools on the ExPASy Server*, Humana Press, 2005.
3. R. W. Woody, in *Methods in Enzymology*, Academic Press, 1995, vol. 246, pp. 34-71.
4. W. C. Johnson, *Proteins: Structure, Function, and Bioinformatics*, 1990, **7**, 205-214.
5. S. Allen, A. Badarau and C. Dennison, *Biochemistry*, 2012, **51**, 1439-1448.
6. S. M. Kelly, T. J. Jess and N. C. Price, *Biochimica et Biophysica Acta (BBA) - Proteins and Proteomics*, 2005, **1751**, 119-139.
7. J. L. Lopes, A. J. Miles, L. Whitmore and B. A. Wallace, *Protein science : a publication of the Protein Society*, 2014, **23**, 1765-1772.
8. I. Gokce, R. W. Woody, G. Anderluh and J. H. Lakey, *Journal of the American Chemical Society*, 2005, **127**, 9700-9701.
9. S. Allen, A. Badarau and C. Dennison, *Dalton Transactions*, 2013, **42**, 3233-3239.
10. A. Badarau and C. Dennison, *Proceedings of the National Academy of Sciences*, 2011, **108**, 13007-13012.
11. R. A. Pufahl, C. P. Singer, K. L. Peariso, S. J. Lin, P. J. Schmidt, C. J. Fahrni, V. C. Culotta, J. E. Penner-Hahn and T. V. O'Halloran, *Science*, 1997, **278**, 853-856.
12. A. Hörnberg, D. T. Logan, S. L. Marklund and M. Oliveberg, *Journal of Molecular Biology*, 2007, **365**, 333-342.
13. P. A. Doucette, L. J. Whitson, X. Cao, V. Schirf, B. Demeler, J. S. Valentine, J. C. Hansen and P. J. Hart, *Journal of Biological Chemistry*, 2004, **279**, 54558-54566.
14. F. Arnesano, L. Banci, I. Bertini, M. Martinelli, Y. Furukawa and T. V. O'Halloran, *Journal of Biological Chemistry*, 2004, **279**, 47998-48003.
15. A. Badarau and C. Dennison, *Journal of the American Chemical Society*, 2011, **133**, 2983-2988.
16. Z. Xiao, J. Brose, S. Schimo, S. M. Ackland, S. La Fontaine and A. G. Wedd, *Journal of Biological Chemistry*, 2011, **286**, 11047-11055.
17. P. Bagchi, M. T. Morgan, J. Bacsa and C. J. Fahrni, *Journal of the American Chemical Society*, 2013, **135**, 18549-18559.

Chapter 4: Discussion

Copper is essential for eukaryotic cells to function optimally and is employed for a variety of purposes such as involvement in the key machinery of energy production.[59-61, 154] Interestingly, the redox characteristic of copper that is exploited by many biological systems is also highly damaging to cellular components and copper can cause a variety of toxic issues for cells.[15, 16] To overcome this difficulty, a complex network of copper trafficking pathways has evolved within eukaryotic cells to strictly control the transport of copper to its required locations, whilst also limiting its exposure and damage to organelles.

Copper chaperones are integral machinery in the copper trafficking pathways and not only sequester copper to prevent damage, but also deliver copper to specific targets such as copper-requiring proteins. This process of copper transfer from chaperone to target protein can also act as a crucial step in the activation or maturation of these proteins and is therefore required for correct functioning. If the delivery of copper is interrupted or the transfer is erroneous, this can have an adverse knock-on effect further downstream of the pathway or the function of the target protein can be lost or subverted. Deviations in the function of some of the key proteins in the cellular copper network are associated with human diseases. These include Menkes and Wilson's disease (see section 8.1.3 of Introduction) and amyotrophic lateral sclerosis (ALS) (see section 1.6.5 of Introduction). The biological importance of the copper chaperones has motivated the study of these integral components and associated pathways in order to further understand the intricacies of the cellular copper networks, clarify the source of any modifications to the correct functioning of key proteins and identify any potential therapeutic targets. For example, the identification of new therapeutic targets is highly desirable for the treatment and early diagnosis of ALS. Currently, there is only one drug licensed to treat ALS in the UK[155] and the effect on the survival outcome has been shown in randomised clinical trials to improve by 2-3 months.[156]

The complexities of the copper trafficking networks can make it challenging to study a particular process in isolation due to subsidiary pathways. This has been shown to exist in the case of SOD1 activation in humans due to a CCS-independent activation pathway that does not exist in *S. cerevisiae* (see section 1.11 of the Introduction). Therefore, in order to study the activation of this protein by its metallochaperone, the yeast network presents the ideal system of study. Not only would any measured change to the mechanism of activation

not be concealed by alternate sources of Ccs1-independent activation in yeast, the dependence on Ccs1 only may cause differences in the activation mechanism as compared to the human system thereby identifying key steps in the process.

Ccs1 contains seven Cys residues, four of which are located in D1, including two involved in the CXXC copper-binding motif, and another two that form a disulfide bridge. One cysteine is located in D2, and two more are in the CXC copper-binding motif of D3 *(Figure 4.2)*.[92] The detection of only 4.7 ± 0.4 free thiols for Ccs1-WT after reduction of the protein with DTT suggests that the protein is highly sensitive to oxidation and the formation of disulphide bonds, and some cysteine residues are not solvent exposed. This value is also consistent with the previous range of 4.5 - 5.0 free thiols determined for Ccs1.[103] The mutants C17S/C20S-Ccs1, C229S/C231S-Ccs1 and D1/2-Ccs1 gave 2.7 ± 0.5, 3.0 ± 0.5 and 2.9 ± 0.1 thiols per monomer respectively. The measurement of two thiols less for each of the Ccs1 mutants is expected since they all feature the loss of two Cys residues.

The requirement of a reducing DTT treatment in order to detect the free thiols of Ccs1 indicates that oxidation of the Cys residues of Ccs1 occurs in the presence of oxygen. Oxidation may cause the formation of intra- or inter-molecular disulfide bonds, causing a loss of ability to bind copper and the formation of oligomers. To avoid possible oxygen-induced oligomerization and maintain the reduced thiol state of the Ccs1 Cys residues, samples were prepared in anaerobic chamber and gel filtration chromatography was performed in buffer degassed and bubbled with nitrogen *(Method 2.7.2)*. Under these anaerobic conditions, gel filtration data shows that in the absence of Cu^{1+}, WT-Ccs1 is predominantly monomeric with 11 % of the protein forming a dimer *(Figure 3.5 A)*. This is distinct from human CCS1 which is shown to be a dimer in the apo-form by gel filtration performed at pH 6.5.[103] A reducing environment decreased the proportion of dimer observed for apo-WT-Ccs1 to 8 % although dimerization was not eliminated *(Figure 3.5 A)*. C229S/C231S-Ccs1 and D1/2-Ccs1 also appear as predominantly monomeric with only 4 and 3 % dimer formed respectively in the absence of Cu^{1+} and DTT *(Figure 3.5 B & C)*. The presence of DTT eliminated the dimeric form in both cases and only monomer is observed. Interestingly, C17S/C20S-Ccs1 appears more prone to dimerization since, in the absence of Cu^{1+} and DTT, an equal amount of dimer and monomer are observed *(Figure 3.5 D)*. Experiments under reducing conditions greatly reduced the amount of apo-C17S/C20S-Ccs1

dimer from 49 to 5 %. The decrease in the amount of dimer in the apo-proteins by DTT indicates that this is most probably due to the formation of intermolecular disulfide bridges. The higher proportion of dimer observed for C17S/C20S-Ccs1 compared to the other Ccs1 proteins suggests that the D3 CXC motif is primarily involved in intermolecular disulfide formation. Oxidation may not be the only influence, although the Cys residues of D1 are solvent exposed *(Figure 4.1)*, they are fixed in position by the secondary structure of Ccs1. Alternatively, the irregular structure of D3 may afford flexibility which enables its CXC motif to come into contact with other D3 sites more readily than those of D1. Also, the pK_a values of Cys residues are tuned by their surrounding environment and can influence the nucleophilicity of the thiolate group.[157] The fixed position of the D1 Cys residues compared to the ability of D3 to move provides different environments that may alter the pK_a values of the Cu^{1+}-binding Cys residues. The pK_a values of the Cys residues in D3 may be higher than at D3 than D1, causing disulfide formation to occur more readily at D3.

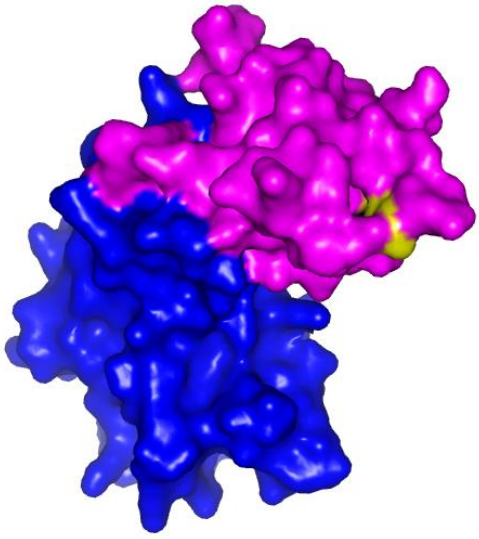

Figure 4.1. The surface structure of the Ccs1 protein. Crystal structure of *S. cerevisiae* Ccs1 in which only D1 (magenta) and D2 (blue) are observed. The metal-binding Cys residues of D1 are shown in yellow and are solvent exposed. Image created using PyMol v1.3 from the PDB file 1QUP.[92]

Upon the addition of Cu^{1+}, the gel filtration data of WT-Ccs1 shows that the proportion of dimer increases *(Figure 3.6 A).* It has been reported previously that in the presence of Cu^{1+}, Ccs1 forms a mixture of monomer and dimer.[103, 104, 158] In the presence of Cu^{1+}, human CCS1 is found in dimeric and tetrameric forms.[103] Gel filtration experiments in buffer containing DTT provides a reducing environment and eliminates the formation of dimers due to oxidation which would have otherwise been attributed to the presence of Cu^{1+} *(Figure 3.6 B)* . A concentration of 250 µM DTT was utilised as this is sufficiently low that competition with the Ccs1 proteins for Cu^{1+} is not an issue. The affinity of DTT for Cu^{1+} has been estimated as $K_b = 10^{15.3}$ M^{-1} at pH 7.3,[138] which is three orders of magnitude lower than the affinity of WT-Ccs1 measured here, $(2.6 \pm 1.1) \times 10^{18}$ M^{-1}.

The formation of dimeric WT-Ccs1 is not affected by the presence of DTT, indicating that dimerization is not due to intermolecular disulfide formation and is related to the binding of Cu^{1+}. Analysis of the eluted fractions from the gel filtration column to measure protein and Cu^{1+} concentrations can determine whether Cu^{1+} is associated with monomeric or dimeric protein. Cu^{1+} is found to associate with both the monomeric and dimeric forms of WT-Ccs1 *(Figure 3.8)* although at greater than 1 equivalent, Cu^{1+} preferentially binds to the monomeric protein *(Figure 3.8 D)*. In the presence of DTT, the WT-Ccs1 monomer/dimer peaks are not resolved, however Cu^{1+} appears to be located at elution volumes associated with the dimeric protein up to a Cu^{1+} concentration of one equivalent *(Figure 3.9 A & B)*. At Cu^{1+} concentrations higher than one equivalent, the protein and Cu^{1+} content is not resolved and it is impossible to distinguish between monomer and dimer *(Figure 3.9 C & D)*.

Similar to WT-Ccs1, C229S/C231S-Ccs1 and D1/2-Ccs1 also show an increase in the proportion of dimer as Cu^{1+} is added. Dimerization of C229S/C231S-Ccs1 increases from 4 to 16 and 34 % dimer for apo-protein, 0.5 and 1.0 equivalent of Cu^{1+} respectively *(Figure 3.7 A).* In addition, dimerization of D1/2-Ccs1 increases from 4 to 13 and 33 % dimer for apo-protein, 0.5 and 1.0 equivalent of Cu^{1+} respectively *(Figure 3.7 C).* Also, Cu^{1+} associates with both dimer and monomer *(Figure 3.10 A & B, Figure 3.11 A & B)*. Dimerization of Cu^{1+}-C229S/C231S-Ccs1 and Cu^{1+}-D1/2-Ccs1 is completely eliminated in the presence of DTT *(Figure 3.7 B & D)* and Cu^{1+} is found associated with the monomer *(Figure 3.10 C & D, Figure 3.11 C & D)*. The elimination of the dimer by DTT suggests that dimerization is disulfide linked through D1, however dimeric protein is still able to bind Cu^{1+}. An increase in dimer

concentration upon the addition of Cu^{1+} is also observed with C17S/C20S-Ccs1. Dimerization of C17S/C20S-Ccs1 increases from 49 to 61 and 77 % dimer for apo-protein, 0.5 and 1.0 equivalent of Cu^{1+} respectively *(Figure 3.7 E),* and this is not eliminated by the presence of DTT *(Figure 3.7 F)*. There is an overall reduction (5, 49 and 59 % dimer for apo-protein, 0.5 and 1.0 equivalent of Cu^{1+} respectively) but dimeric Cu^{1+}-C17S/C20S-Ccs1 remains a major form. This suggests that dimerization through D3 is not linked to disulfide formation and is related to the presence of Cu^{1+}. C17S/C20S-Ccs1 is found to preferentially bind Cu^{1+} in the dimeric form *(Figure 3.12)*. This is not affected by a reducing environment and could be due to an overall higher proportion of the dimeric protein.

The gel filtration data shows that Ccs1 is able to form dimers through disulfide linking of both the Cys residues of the D1 and D3 site, and the dimeric protein is able to bind Cu^{1+}. Dimerization through D1 appears to occur by disulfide bridges only, whereas D3 dimerization occurs through Cu^{1+} binding. The appearance of homodimers in the crystal structures of both yeast Ccs1[92] and human CCS[98] and complementary residues along the D2-D2 interface implicated D2 as a site of dimerization similar to dimerization observed with SOD1. However, if D2-D2 interactions were producing the dimerization observed for Cu^{1+}-C17S/C20S-Ccs1 in the presence of DTT, this would also be seen with Cu^{1+}-C229S/C231S-Ccs1 and Cu^{1+}-D1/2-Ccs1 as they also contain D2, but dimerization is absent. Dimerization of human CCS was found to include multinuclear copper clusters which occurs through D3 only.[134, 159] If dimerization does occur at D3 as a copper cluster, this could have mechanistic implications since D3 of yeast Ccs1 is regarded to be the location of copper transfer to Sod1[104] whereas this is D1 in human CCS.[83]

Overexpressed D2/3-Ccs1 was shown to consist of unfolded protein by far-UV CD spectroscopy *(Figure 3.1)* and the measured molecular weight is 191 Da less (60 Da less from N-terminal methionine) than the expected value *(Table 3.1)* which is not easily explained. This was highly unexpected since D2 of Ccs1 and Sod1 share a similar structure, and recombinant Sod1 is folded (Figure 3.4). Purified D1/2-Ccs1 is shown to have a very similar structure to WT-Ccs1 *(Figure 3.1)* by far-UV CD spectroscopy. This was achieved by incubation of *E. coli* at 16 ^{o}C rather than 37 ^{o}C to avoid the production of insoluble protein (Method 2.10.2). The amino acid sequence of D2/3-Ccs1 consisted of residue 72 to 249, which includes the seven residues that link D1 and D2. This was based on the fact that in

the crystal structure[92] of Ccs1 there is a hydrogen bond between residues 72 and 220 *(Figure 4.2)* which may provide stability to the secondary structure of the protein. Previously, a Ccs1 mutant lacking D1 was cloned from residue 75 and was able to activate Sod1 successfully, suggesting that the protein folded correctly, although no in vitro characterization of the purified protein was reported.[104] Why D2/3-Ccs1 does not fold correctly could be due to unknown consequences of including the linking residues.

Stoichiometry titrations show that in the presence of the competitive ligand BCA at 500 μM, C229S/C231S-Ccs1 and D1/2-Ccs1 bind ≈ 1 equivalent of Cu^{1+} whilst WT-Ccs1 binds more than one equivalent Cu^{1+} *(Figure 3.16)*. C17S/C20S-Ccs1 shows weak competition with BCS for Cu^{1+} and an accurate binding stoichiometry determination is not possible. Upon reduction of BCA to 150 μM, C17S/C20S-Ccs1 is found to bind ≈ 1 equivalent of Cu^{1+} *(Figure 3.17 B)*. Similarly, reduction of the BCA concentration also shows that WT-Ccs1 binds ≈ 2 equivalents of Cu^{1+} *(Figure 3.17 A)*. This is expected since WT-Ccs1 features two potential Cu^{1+} binding sites and each of the Ccs1 variants features the loss of one of these sites. The ability of the Ccs1 mutants to bind Cu^{1+} indicates that the loss of the cysteine residues at one of the Cu^{1+} binding sites, or the loss of D3 in D1/2-Ccs1, does not affect Cu^{1+} binding by the remaining site, and that Cu^{1+} is bound independently. This data suggests a weaker affinity of D3 for Cu^{1+} than that of D1 since a lower BCA concentration is needed for effective competition for Cu^{1+} with C17S/C20S-Ccs1 than with C229S/C231S-Ccs1 and D1/2-Ccs1.

Competition titrations with BCS were performed to measure the affinity (K_b value) of the proteins for Cu^{1+}. Titrations with WT-Ccs1, C229S/C231S-Ccs1 and D1/2-Ccs1 in the presence of 0.5 equivalents of Cu^{1+} provided K_b values of $(2.6 \pm 1.1) \times 10^{18}$ M^{-1}, $(2.6 \pm 0.5) \times 10^{18}$ M^{-1} and $(2.7 \pm 1.0) \times 10^{18}$ respectively *(Table 3.4)*. Experiments involving titrations of BCS into Cu^{1+}-protein *(Figure 3.18)* and titrations of apo-protein into $[Cu(BCS)_2]^{3-}$ *(Figure 3.19)* gave consistent affinity values. This indicates that equilibrium was reached and the affinity values measured are accurate. These values are essentially the same for all three proteins and suggests that the Cu^{1+} is bound by the same site in all proteins. This can only be the copper binding motif of D1 since C229S/C231S-Ccs1 and D1/2-Ccs1 only contain this copper binding site.

Measurement of the copper binding site in D3 by use of the C17S/C20S-Ccs1 mutant proved more difficult. A relatively small concentration of BCS removed a large proportion of Cu^{1+} from C17S/C20S-Ccs1 providing insufficient competition for affinity titrations *(Figure 3.20)*. This had also been observed for the equivalent human mutant (C244S/C246S-CCS), therefore experiments with BCA were performed due to the lower affinity for Cu^{1+} than BCS by 2.6 orders of magnitude, making it more suitable for effective competition with the D3 site.[138] Affinity experiments with human C244S/C246S-CCS involving additions of BCA to Cu^{1+}-protein also required much longer experiment time-frames (48 hrs). This approach, applied to C17S/C20S-Ccs1, resulted in prolonged removal of Cu^{1+} from the protein by BCA after the 48 hr experiment time-frame *(Figure 3.22)*. This suggests that a lower concentration of BCA is required to effectively complete with C17S/C20S-Ccs1 for Cu^{1+}, indicating that the affinity of the Cu^{1+}-binding site of D3 is weaker than the human site. Interestingly, the stability of affinity titrations involving additions of apo-C17S/C20S-Ccs1 into $[Cu(BCA)_2]^{3-}$ over time indicated that equilibrium was achieved within the time-frame of these experiments *(Figure 3.25)*. These provided a measurement of the affinity as $(4.1 \pm 0.9) \times 10^{17}\ M^{-1}$.

The affinity measurements are consistent with the implication from the stoichiometry titrations that the Cu^{1+}-binding site of D3 is weaker than that of D1. The affinity of C229S/C231-Ccs1 is 3 times higher than that of C17S/C20S-Ccs1. This trend agrees with the higher affinity of D1 than D3 measured for human CCS. Plots of the affinity data using previous BCS/BCA β_{max} values provides affinity values for WT-Ccs1, C229S/C231S-Ccs1 and C17S/C20S-Ccs1 which are comparable to previously calculated literature values for the human proteins *(Table 3.4)*.[103] Comparison of the yeast and human proteins containing the D1 site only shows that the affinity of the D1 copper-binding site of Ccs1 is half the value of the equivalent site for Cu^{1+} in the human protein. Interestingly, the proteins containing the D3 site only show that the affinity of the D3 copper-binding site of Ccs1 is ≈ twice the value of the equivalent site for Cu^{1+} in the human protein. This highlights that although the affinity for Cu^{1+} of the D1 site of Ccs1 is higher than that of D3, this difference is not as pronounced as the equivalent domains in human CCS. These results are not able to confirm the hypothesis that the mechanism of copper transfer between Ccs1 and Sod1 is fundamentally different from that of the human system.

The higher affinity of D1 for Cu^{1+} than D3 further complicates the hypothesis of a difference between the human and yeast mechanism for Sod1 activation *(Figure 4.3)*. The higher affinity of D1 agrees with the site of Cu^{1+} transfer to SOD1 in humans having been established as D1, and D3 essential for the formation of the disulfide bond.[82, 83] However, this is in contradiction with D3 of yeast Ccs1 being found to be critical for copper transfer in yeast.[104] Due to the flexibility of D3 it has been proposed that D3 is able to obtain copper from D1.[75, 105, 106] Therefore the role of D1 would be expected to involve Cu^{1+} acquisition and transfer to D3 for insertion into SOD1, however the increased affinity of D1 for Cu^{1+} compared to D3 would make this thermodynamically unfavourable. Copper transfer occurring at D1 in humans makes it hard to justify that with a similarly higher affinity of Ccs1 D1 than D3, copper transfer actually occurs through D3. However, there are differences in the two systems of humans and yeast. There are structural differences between the proteins, with human CCS possessing the zinc-binding loop and electrostatic channel loop of SOD[98] whereas in yeast Ccs1 this is absent.[92] Also, the oligomerisation of the human and yeast proteins are different. Human CCS adopts a dimeric form as apo-protein and a tetramer in the presence of Cu^{1+},[159] whereas yeast Ccs1 exists primarily as a monomer in the apo-form and dimerizes upon the addition of Cu^{1+}. In yeast, activation of Sod1 is dependent on Ccs1,[133] whereas in humans SOD1 can be activated independently of CCS1.[132, 133, 160] Also, some organisms express CCS of which the D1 copper binding motif is missing and is still able to activate SOD under copper abundant conditions.[95, 160] These differences of the human and yeast copper chaperones may actually demand a different mechanism of Sod1 activation between the two systems. Until further evidence towards the mechanism of action is provided, the similarities or differences of CCS1 and Ccs1 will remain unclear.

Sod1 contains two cysteines, both of which are located at the active site.[74] The detection of 1.8 ± 0.2 free thiols per monomer for Sod1 after reduction of the protein with DTT shows that the cysteines are solvent exposed and can be reduced.

Purified E,Zn-Sod1 was shown by analytical gel filtration to be dimeric in the presence of DTT and monomeric protein was only observed after incubation with DTT overnight *(Figure 3.15)*. This agrees with previous experiments in which the major determinant of Sod1 dimerization was found to be the thiol status, with E,Zn-$Sod1^{SH}$ largely existing as a monomer and E,Zn-$SOD1^{S\text{-}S}$ as a dimer.[85] In humans, it has been determined that

dimerization of hSOD1 requires not only the reduction of the disulfide, but also at least partial loss of the catalytic metals.[80, 152, 153] The disulfide between Cys_{57} and Cys_{146} covalently anchors the conformation of an interface loop which is reoriented upon reduction of the disulfide, thereby disturbing the dimer interface. Addition of the catalytic metals copper and zinc restores the loop conformation and the dimer interface. It is interesting that the human E,Zn-SOD1^{SH} protein form favours the dimeric state, whereas the yeast E,Z-Sod1^{SH} protein form prefers the monomeric state. This difference in the behaviour of human and yeast proteins has been hypothesized to be associated to two proline residues located near the disulfide which are present in the human protein but not in the yeast protein. These proline residues have already been linked to the CCS-independent activation pathways which show differences between the human and yeast proteins.[133]

The purified Sod1 protein was shown to be activated by incubation with metal salts and Sod1 activity was successfully visualised by means of an NBT assay *(Figure 3.29)*. Only the fully metallated Cu,Zn-Sod1$^{S\text{-}S}$ displayed activation, and partial metalation by zinc only (E,Zn-Sod1$^{S\text{-}S}$) was unable to perform any catalytic activity. Cu^{1+}-loaded Ccs1 proteins do not provide a positive activity band in the NBT assay, therefore positive activity bands are only produced as a result of a fully active Sod1. Sod1 activity is observed after incubation with all Cu^{1+}-Ccs1 variants *(Figure 3.32)*. WT-Ccs1 provides a level of Sod1 activation similar to that observed from Sod1 fully-metallated by metal salts, whereas the Ccs1 mutants all provide lower activation levels. However, Cu^{1+}-C17S/C20S-Ccs1 shows a greater level of Sod1 activation than Cu^{1+}-C229S/C231S-Ccs1 and Cu^{1+}-D1/2-Ccs1, which show equal levels of Sod1 activation.

The observation of Sod1 activity from incubation with Cu^{1+}-C17S/C20S-Ccs1, at a lower level to WT-Ccs1 is consistent with previous *in vivo* data.[104] However, the low level of activation observed after incubation with Cu^{1+}-Ccs1 mutants containing the D1 copper-binding site only (C229S/C231S-Ccs1 and D1/2-Ccs1) is unexpected. Previously, a D1/2-Ccs1 mutant was unable to activate Sod1 *in vivo* and D1 was designated as being necessary under copper limiting conditions only.[104] These experiments involved the expression of specific mutants in yeast strains with a deleted Ccs1 gene. Furthermore, there are issues inherent in the NBT assay. Activity of Sod1 is only achieved upon the maturation of Sod1 to a fully mature protein of the form Cu,Zn-Sod1$^{S\text{-}S}$ which includes acquisition of copper and zinc, and the

formation of the disulfide. The NBT assay only provides a positive response to complete activation and does not distinguish whether disulfide formation or copper transfer alone has occurred.

The observation of apo-Atx1 dimers in the presence of a reducing environment indicates that dimerization does not occur through intermolecular disulfide bridges, and indicates an alternative interaction. One possibility is a similar recognition process as the electrostatic forces between Atx1 and Ccc2a, as Ccc2a shares a similar structure to Atx1,[110] two Atx1 monomers may assemble in a similar manner. However, the addition of Cu^{1+} shifts the oligomeric state of Atx1 to a monomer suggesting that dimerization is linked to interactions of the protein with Cu^{1+}. It has been reported previously that the predominant form of Atx1 is a monomer regardless of the presence of Cu^{1+},[31] which conflicts with the results shown here, although dimerization of Atx1 has been shown with the incorporation of excess GSH.[53]

The affinities measured for Atx1 were replotted using a previous BCS β_{max} value providing affinity values which are comparable to previously calculated literature values for the yeast and human proteins *(Table 3.4)*. The affinity values match those previously reported,[140, 141] however, the use of the current BCS β_{max} value provide affinities $\approx$ an order of magnitude higher than those using the previous value. The two differing approaches used here to measure the affinity of Atx1 for Cu^{1+} are consistent, which indicates that equilibrium was reached and confirms the validity of these methods. The increase in the K_b value (> 3-fold) from pH 7.0 to 7.5 is most probably due to protonation of the Cysteine residues within the copper binding motif which has been shown extensively within the analogous human pathway.[139] The dependence of Cu^{1+} affinities on pH has been determined as a result of competition between H^+ and Cu^{1+} for the cysteine residues of the copper binding motifs.[139, 161]

The calculation of protein affinities is important in understanding the thermodynamics of Cu^{1+} distribution amongst copper-trafficking pathways within cells, and the transfer of copper between partner proteins. It has been suggested that relative affinities drives Cu^{1+} along particular routes to target proteins.[137] However, this thermodynamic driving force was found to be unfavourable at pH < 7.0,[139] and also not true in the prokaryote *Synechocystis* which designates the affinity of proteins as not the determining factor in copper trafficking.[147]

It has been suggested that with the similar affinities of Ccs1 and Atx1, along with similar protein levels,[17, 162] that thermodynamically these metallo-chaperones may be able to compete for copper. Due to the higher affinity of Atx1 to both Ccs1 domains, the K_{theo} values calculated suggest that the majority of Cu^{1+} will be bound at equilibrium to Atx1. The K_{theo} values also indicate that this reaction quotient will be more pronounced with C17S/C20S-Ccs1 than C229S/C231S-Ccs1 due to the lower affinity of D3 compared with D1.

Exchange experiments have shown that Cu^{1+} transfer between Atx1 and Ccs1 does occur *in vitro* and supports the hypothesis that Ccs1 and Atx1 can compete for copper. Interestingly, this transfer can take place at both the copper binding sites of D1 and D3-Ccs1, although exchange to D3 is very limited. These exchange experiments validate the trend seen with the affinity values, that D1 has a higher affinity for Cu^{1+} than D3 since the K_{ex} value for exchange with C17S/C20S-Ccs1 is lower than that with C229S/C231S-Ccs1. The product distribution between Atx1 and C17S/C20S-Ccs1 in both directions required more time than with C229S/C231S-Ccs1 to equilibrate. Incubation for 24 hrs provided consistent K_{ex} values for exchange in both directions indicating that equilibrium had been reached. C17S/C20S-Ccs1 has shown similar requirements for longer experiment times when measuring the affinity, which demonstrates that this is a characteristic of the binding site in D3-Ccs1 rather than an issue with Atx1.

The exchange of Cu^{1+} between Atx1 and Ccs1 suggests that the distribution of copper along a particular route could be selected depending on the affinities and concentrations of proteins present at the copper pool. This would indicate that copper is not collected directly from Ctr1 because distribution would depend on preferential interactions at the chaperone-transporter interface and not interactions between Ccs1 and Atx1. Also, *in vivo* studies in S. cerevisiae have indicated that Ccs1 and Atx1 do not collect copper directly from metal transporters,[163] however, Ctr1 is able to transfer Cu^{1+} to Atx1 *in vitro*.[130] Nonetheless, even if proteins initially collected copper from Ctr1 or separate locations, the process of exchange could be a downstream method for allocating copper along a particular route.

The results presented in this work have provided a quantitative ability to compare the human CCS and yeast Ccs1 proteins through the copper affinity values of the copper-binding sites and can be used to make informed mechanistic implications. These measured values can also be applied to other areas of the copper transport network and contribute to the

understanding of the thermodynamic distribution of copper amongst the cellular trafficking pathways. Additionally, differences in the affinity values for copper between the human and yeast protein have been confirmed and quantified which supports the hypothesis that the mechanisms of action differ. The differences in the proposed mechanisms of activation between the human and yeast systems are juxtaposed in *Figure 4.3*. Although this work has shown a difference between the copper affinities of the human and yeast proteins, the spread of the affinities between the two protein domains is shown to be similar, which complicates the ability to explain why the mechanism of copper transfer between the two systems is different. The evidence provided here as visualised by the NBT assay showing that D3 of Ccs1 is able to activate Sod1 to the same level as the wild-type protein indicates a fundamental difference between the human and yeast proteins. This supports the proposed mechanism of Sod1 activation in yeast. However, the observed ability of D1 of Ccs1 to also activate Sod1 to a lesser extent has called into question either the validity of the NBT assay method or highlighted an issue with applying *in vitro* experiments to the *in vivo* environment. This result contradicts a previous literature experiment and future work investigating the reliability of the assay method is required. Definitive confirmation of whether D1 of Ccs1 is able to activate Sod1 is critical in order to confirm the fundamental differences between the human and yeast mechanisms. Experimental methodology that is able to distinguish the steps of activation; copper transfer and disulphide formation, should be explored going forward. The elucidation of the role each domain of the yeast Ccs1 plays in these steps would better inform the suggested mechanism in yeast.

Determination of the affinity value for Atx1 has provided a quantitative ability to compare the value measured for Ccs1 and develop the discussion in regards to the hypothesis of whether these two proteins can compete for copper. The exchange of copper between Ccs1 and Atx1 has been shown to occur *in vitro* and is consistent with the expected ability denoted by the affinity values. These results suggest that copper metallochaperones from separate copper trafficking pathways should be able to compete for and exchange copper in a cellular environment. These findings also contribute to the overall considerations of how cells may allocate and distribute copper along the complex transport pathways. The logical step forward is to investigate these isolated *in vitro* results in the cellular environment to determine if this ability to exchange copper is physiologically relevant. Also, the ability of

Atx1 and Ccs1 to exchange copper raises the question of whether other metallochaperones are also able to exchange copper. Similar exchange experiments with proteins from other copper trafficking pathways, such as the delivery of copper into the mitochondria, would indicate whether this metal exchange ability is a general method to distribute copper within yeast cells or is limited to Atx1 and Ccs1. Furthermore, confirmation that Atx1 and Ccs1 are able to exchange copper does not establish whether these proteins are exposed to the same copper pool within the cell and ultimately compete for copper. Future work to identify the sources of copper for Atx1 and Ccs1 will confirm if competition between these copper chaperones occurs within yeast cells.

```
C17S/C20S-Ccs1        MTTNDTYEATYAIPMHSENSVNDIKACLKNVPGINSLNFDIEQQIMSVESSVAPSTIINT    60
D2/3-Ccs1             ------------------------------------------------------------    0
C229S/C231S-Ccs1      MTTNDTYEATYAIPMHCENCVNDIKACLKNVPGINSLNFDIEQQIMSVESSVAPSTIINT    60
WT-Ccs1               MTTNDTYEATYAIPMHCENCVNDIKACLKNVPGINSLNFDIEQQIMSVESSVAPSTIINT    60
D1/2-Ccs1             MTTNDTYEATYAIPMHCENCVNDIKACLKNVPGINSLNFDIEQQIMSVESSVAPSTIINT    60

C17S/C20S-Ccs1        LRNCGKDAIIRGAGKPNSSAVAILETFQKYTIDQKKDTAVRGLARIVQVGENKTLFDITV    120
D2/3-Ccs1             -----------GAGKPNSSAVAILETFQKYTIDQKKDTAVRGLARIVQVGENKTLFDITV    49
C229S/C231S-Ccs1      LRNCGKDAIIRGAGKPNSSAVAILETFQKYTIDQKKDTAVRGLARIVQVGENKTLFDITV    120
WT-Ccs1               LRNCGKDAIIRGAGKPNSSAVAILETFQKYTIDQKKDTAVRGLARIVQVGENKTLFDITV    120
D1/2-Ccs1             LRNCGKDAIIRGAGKPNSSAVAILETFQKYTIDQKKDTAVRGLARIVQVGENKTLFDITV    120

C17S/C20S-Ccs1        NGVPEAGNYHASIHEKGDVSKGVESTGKVWHKFDEPIECFNESDLGKNLYSGKTFLSAPL    180
D2/3-Ccs1             NGVPEAGNYHASIHEKGDVSKGVESTGKVWHKFDEPIECFNESDLGKNLYSGKTFLSAPL    109
C229S/C231S-Ccs1      NGVPEAGNYHASIHEKGDVSKGVESTGKVWHKFDEPIECFNESDLGKNLYSGKTFLSAPL    180
WT-Ccs1               NGVPEAGNYHASIHEKGDVSKGVESTGKVWHKFDEPIECFNESDLGKNLYSGKTFLSAPL    180
D1/2-Ccs1             NGVPEAGNYHASIHEKGDVSKGVESTGKVWHKFDEPIECFNESDLGKNLYSGKTFLSAPL    180

C17S/C20S-Ccs1        PTWQLIGRSFVISKSLNHPENEPSSVKDYSFLGVIARSAGVWENNKQVCACTGKTVWEER    240
D2/3-Ccs1             PTWQLIGRSFVISKSLNHPENEPSSVKDYSFLGVIARSAGVWENNKQVCACTGKTVWEER    169
C229S/C231S-Ccs1      PTWQLIGRSFVISKSLNHPENEPSSVKDYSFLGVIARSAGVWENNKQVSASTGKTVWEER    240
WT-Ccs1               PTWQLIGRSFVISKSLNHPENEPSSVKDYSFLGVIARSAGVWENNKQVCACTGKTVWEER    240
D1/2-Ccs1             PTWQLIGRSFVISKSLNHPENEPSSVKDYSFLGVIARSAGVW------------------    222

C17S/C20S-Ccs1        KDALANNIK       249
D2/3-Ccs1             KDALANNIK       178
C229S/C231S-Ccs1      KDALANNIK       249
WT-Ccs1               KDALANNIK       249
D1/2-Ccs1             ---------       222
```

Figure 4.2 Sequence alignment of the WT and Ccs1 variants used throughout this thesis. The Cu^{1+}-binding Cys residues are highlighted in yellow and the remaining Cys residues are highlighted in blue. Two residues that are hydrogen-bonded in the crystal structure[92] are highlighted in magenta. Protein sequences sourced from UniProt[100] and aligned with Clustal Omega.[27, 101]

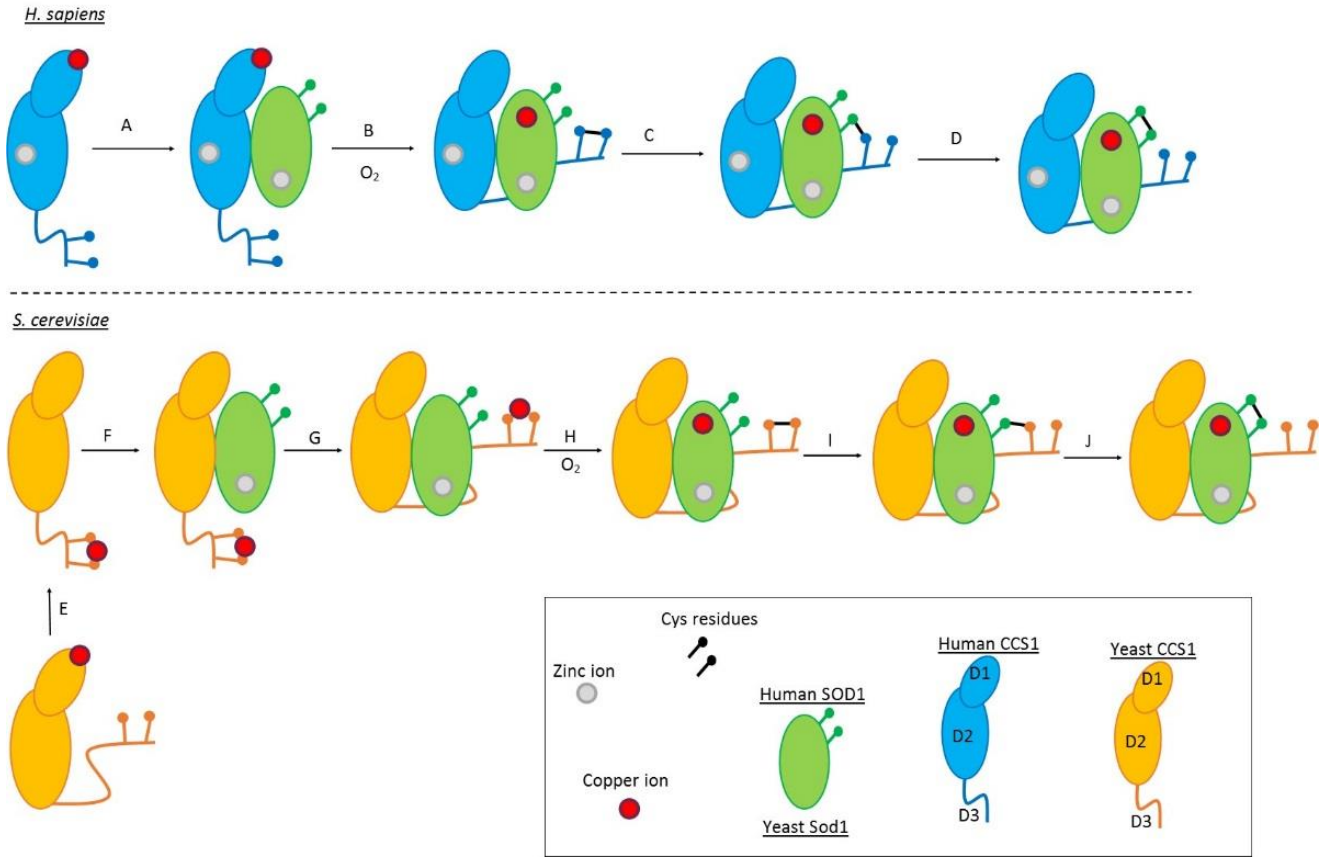

Figure 4.3. A comparison of the activation of Cu,Zn-superoxide dismutase by the protein's Cu^{1+}-metallochaperones in yeast and humans. In the *H. sapiens* Cu^{1+}-CCS1 in which Cu^{1+} is bound at D1, forms a heterodimeric complex with E,Zn-SOD1 (A). D1 of CCS1 transfers Cu^{1+} to SOD1 and disulfide formation within the CXC motif occurs and D3 is orientated towards the SOD1 active site (B). Finally, disulphide isomerisation from D3 of CCS1 to SOD1 occurs (C and D). In *S. cerevisiae*, Cu^{1+} is possibly first recruited by the CXXC motif of Ccs1 D1 and transferred to the CXC motif of D3 (E). Cu^{1+}-Ccs1 forms a heterodimeric complex with Sod1 (F). D3 of Ccs1 orientates towards the Sod1 active site (G). D3 of Ccs1 transfers Cu^{1+} to Sod1 and disulphide formation occurs within the CXC motif of D3 in Ccs1 (H). Finally, disulfide isomerisation from D3 of CCS1 to SOD1 occurs (I and J). . The *H. sapien* scheme is adapted from reference [83] and the *S. cerevisiae* scheme is adapted from reference [75]. Images created in Microsoft Publisher.

4.1 References

1. H. C. Gasteiger E., Gattiker A., Duvaud S., Wilkins M.R., Appel R.D., Bairoch A., *Protein Identification and Analysis Tools on the ExPASy Server*, Humana Press, 2005.
2. W. C. Johnson, *Proteins: Structure, Function, and Bioinformatics*, 1990, **7**, 205-214.
3. J. F. Monty, R. M. Llanos, J. F. Mercer and D. R. Kramer, *The Journal of nutrition*, 2005, **135**, 2762-2766.
4. D. S. Shin, M. DiDonato, D. P. Barondeau, G. L. Hura, C. Hitomi, J. A. Berglund, E. D. Getzoff, S. C. Cary and J. A. Tainer, *Journal of Molecular Biology*, 2009, **385**, 1534-1555.
5. Maud E. S. Achard, Sian L. Stafford, Nilesh J. Bokil, J. Chartres, Paul V. Bernhardt, Mark A. Schembri, Matthew J. Sweet and Alastair G. McEwan, *Biochemical Journal*, 2012, **444**, 51-57.
6. C. White, J. Lee, T. Kambe, K. Fritsche and M. J. Petris, *Journal of Biological Chemistry*, 2009, **284**, 33949-33956.
7. D. Wagner, J. Maser, B. Lai, Z. Cai, C. E. Barry, K. Höner zu Bentrup, D. G. Russell and L. E. Bermudez, *The Journal of Immunology*, 2005, **174**, 1491-1500.
8. F. D'Amico, E. Skarmoutsou, S. Sanfilippo and J. Camakaris, *Acta histochemica*, 2005, **107**, 373-378.
9. M. J. Petris, D. Strausak and J. F. Mercer, *Human molecular genetics*, 2000, **9**, 2845-2851.
10. T. C. Steveson, G. D. Ciccotosto, X. M. Ma, G. P. Mueller, R. E. Mains and B. A. Eipper, *Endocrinology*, 2003, **144**, 188-200.
11. J. A. Tainer, E. D. Getzoff, J. S. Richardson and D. C. Richardson, *Nature*, 1983, **306**, 284.
12. F. Haber and J. Weiss, *Naturwissenschaften*, 1932, **20**, 948-950.
13. H. J. H. Fenton, *Journal of the Chemical Society, Transactions*, 1894, **65**, 899-910.
14. H. Irving and R. J. P. Williams, *Journal of the Chemical Society (Resumed)*, 1953, **0**, 3192-3210.
15. L. Macomber and J. A. Imlay, *Proceedings of the National Academy of Sciences*, 2009, **106**, 8344-8349.
16. S. Tottey, K. J. Waldron, S. J. Firbank, B. Reale, C. Bessant, K. Sato, T. R. Cheek, J. Gray, M. J. Banfield, C. Dennison and N. J. Robinson, *Nature*, 2008, **455**, 1138-1142.
17. T. D. Rae, P. J. Schmidt, R. A. Pufahl, V. C. Culotta and T. V. O'Halloran, *Science*, 1999, **284**, 805-808.
18. N. S. Kosower and E. M. Kosower, in *International Review of Cytology*, eds. G. H. Bourne, J. F. Danielli and K. W. Jeon, Academic Press, 1978, vol. 54, pp. 109-160.
19. C. S. Sevier and C. A. Kaiser, *Nature Reviews Molecular Cell Biology*, 2002, **3**, 836.
20. M. E. Reardon-Robinson and H. Ton-That, *Journal of Bacteriology*, 2016, **198**, 746-754.
21. C. Seung-Gu, C. Ki-Doo, J. Seung-Hwan and S. Hang-Cheol, *Mol. Cells*, 2003, **16**, 323-330.
22. J. Wypych, M. Li, A. Guo, Z. Zhang, T. Martinez, M. J. Allen, S. Fodor, D. N. Kelner, G. C. Flynn, Y. D. Liu, P. V. Bondarenko, M. S. Ricci, T. M. Dillon and A. Balland, *The Journal of Biological Chemistry*, 2008, **283**, 16194-16205.
23. T. Fukuhara, K. Kobayashi, Y. Kanayama, S. Enomoto, T. Kondo, N. Tsunekawa, M. Nemoto, N. Ogasawara, K. Inagaki and T. Tamura, *Bioscience, biotechnology, and biochemistry*, 2016, **80**, 600-609.
24. R. Wimmer, T. Herrmann, M. Solioz and K. Wuthrich, *J Biol Chem*, 1999, **274**, 22597-22603.
25. D. A. Capdevila, K. A. Edmonds and D. P. Giedroc, *Essays in biochemistry*, 2017, **61**, 177-200.
26. A. K. Wernimont, D. L. Huffman, A. L. Lamb, T. V. O'Halloran and A. C. Rosenzweig, *Nat Struct Biol*, 2000, **7**, 766-771.
27. M. Goujon, H. McWilliam, W. Li, F. Valentin, S. Squizzato, J. Paern and R. Lopez, *Nucleic Acids Research*, 2010, **38**, W695-W699.
28. R. Hassett, D. R. Dix, D. J. Eide and D. J. Kosman, *Biochemical Journal*, 2000, **351**, 477-484.
29. E. Georgatsou, L. A. Mavrogiannis, G. S. Fragiadakis and D. Alexandraki, *Journal of Biological Chemistry*, 1997, **272**, 13786-13792.

30. R. Hassett and D. J. Kosman, *Journal of Biological Chemistry*, 1995, **270**, 128-134.
31. R. A. Pufahl, C. P. Singer, K. L. Peariso, S. J. Lin, P. J. Schmidt, C. J. Fahrni, V. C. Culotta, J. E. Penner-Hahn and T. V. O'Halloran, *Science*, 1997, **278**, 853-856.
32. C. Askwith, D. Eide, A. Van Ho, P. S. Bernard, L. Li, S. Davis-Kaplan, D. M. Sipe and J. Kaplan, *Cell*, 1994, **76**, 403-410.
33. A. B. Maxfield, D. N. Heaton and D. R. Winge, *Journal of Biological Chemistry*, 2004, **279**, 5072-5080.
34. S. C. Leary, P. A. Cobine, B. A. Kaufman, G.-H. Guercin, A. Mattman, J. Palaty, G. Lockitch, D. R. Winge, P. Rustin, R. Horvath and E. A. Shoubridge, *Cell Metabolism*, 2007, **5**, 9-20.
35. V. C. Culotta, L. W. J. Klomp, J. Strain, R. L. B. Casareno, B. Krems and J. D. Gitlin, *Journal of Biological Chemistry*, 1997, **272**, 23469-23472.
36. J. L. Lopes, A. J. Miles, L. Whitmore and B. A. Wallace, *Protein science : a publication of the Protein Society*, 2014, **23**, 1765-1772.
37. V. C. Culotta, W. R. Howard and X. F. Liu, *Journal of Biological Chemistry*, 1994, **269**, 25295-25302.
38. S. S. Narula, D. R. Winge and I. M. Armitage, *Biochemistry*, 1993, **32**, 6773-6787.
39. L. T. Jensen, W. R. Howard, J. J. Strain, D. R. Winge and V. C. Culotta, *Journal of Biological Chemistry*, 1996, **271**, 18514-18519.
40. M. S. Cyert and C. C. Philpott, *Genetics*, 2013, **193**, 677-713.
41. E. M. Rees, J. Lee and D. J. Thiele, *Journal of Biological Chemistry*, 2004, **279**, 54221-54229.
42. D. H. Hamer, D. J. Thiele and J. E. Lemontt, *Science*, 1985, **228**, 685-690.
43. E. B. Gralla, D. J. Thiele, P. Silar and J. S. Valentine, *Proc Natl Acad Sci U S A*, 1991, **88**, 8558-8562.
44. C. T. Dameron, D. R. Winge, G. N. George, M. Sansone, S. Hu and D. Hamer, *Proceedings of the National Academy of Sciences of the United States of America*, 1991, **88**, 6127-6131.
45. A. Dobi, C. T. Dameron, S. Hu, D. Hamer and D. R. Winge, *J Biol Chem*, 1995, **270**, 10171-10178.
46. L. T. Jensen and D. R. Winge, *European Molecular Biology Organization Journal*, 1998, **17**, 5400-5408.
47. M. M. Pena, K. A. Koch and D. J. Thiele, *Mol Cell Biol*, 1998, **18**, 2514-2523.
48. Y. Yamaguchi-Iwai, M. Serpe, D. Haile, W. Yang, D. J. Kosman, R. D. Klausner and A. Dancis, *J Biol Chem*, 1997, **272**, 17711-17718.
49. S. Labbe, Z. Zhu and D. J. Thiele, *J Biol Chem*, 1997, **272**, 15951-15958.
50. Z. Zhu, S. Labbe, M. M. Pena and D. J. Thiele, *J Biol Chem*, 1998, **273**, 1277-1280.
51. J. Yonkovich, R. McKenndry, X. Shi and Z. Zhu, *J Biol Chem*, 2002, **277**, 23981-23984.
52. C. E. Ooi, E. Rabinovich, A. Dancis, J. S. Bonifacino and R. D. Klausner, *The EMBO Journal*, 1996, **15**, 3515-3523.
53. Y. Yamaguchi-Iwai, M. Serpe, D. Haile, W. Yang, D. J. Kosman, R. D. Klausner and A. Dancis, *Journal of Biological Chemistry*, 1997, **272**, 17711-17718.
54. S. Labbé, Z. Zhu and D. J. Thiele, *Journal of Biological Chemistry*, 1997, **272**, 15951-15958.
55. A. Joshi, M. Serpe and D. J. Kosman, *Journal of Biological Chemistry*, 1999, **274**, 218-226.
56. M. Yukawa, K. Amano, M. Suzuki-Yasumoto and M. Terai, *Archives of environmental health*, 1980, **35**, 36-44.
57. L. Rossi, M. F. Lombardo, M. R. Ciriolo and G. Rotilio, *Neurochemical Research*, 2004, **29**, 493-504.
58. T. Tsukihara, H. Aoyama, E. Yamashita, T. Tomizaki, H. Yamaguchi, K. Shinzawa-Itoh, R. Nakashima, R. Yaono and S. Yoshikawa, *Science*, 1996, **272**, 1136-1144.
59. J. S. Ingwall, *ATP and the Heart*, Springer US, 2012.
60. H. Suga, *Physiological Reviews*, 1990, **70**, 247-277.
61. C. L. Gibbs, *Physiological Reviews*, 1978, **58**, 174-254.
62. S. A. Molloy and J. H. Kaplan, *Journal of Biological Chemistry*, 2009, **284**, 29704-29713.

63. K. Terada, Y. Kawarada, N. Miura, O. Yasui, K. Koyama and T. Sugiyama, *Biochimica et Biophysica Acta (BBA) - Molecular Basis of Disease*, 1995, **1270**, 58-62.
64. M. Sato and J. D. Gitlin, *Journal of Biological Chemistry*, 1991, **266**, 5128-5134.
65. I. Hamza, M. Schaefer, L. W. J. Klomp and J. D. Gitlin, *Proceedings of the National Academy of Sciences*, 1999, **96**, 13363-13368.
66. C. Oswald, U. Krause-Buchholz and G. Rödel, *Journal of Molecular Biology*, 2009, **389**, 470-479.
67. R. Rakhit and A. Chakrabartty, *Biochimica et Biophysica Acta (BBA) - Molecular Basis of Disease*, 2006, **1762**, 1025-1037.
68. Y. Furukawa and T. V. O'Halloran, *Antioxidants & redox signaling*, 2006, **8**, 847-867.
69. J. F. Turrens, *Bioscience Reports*, 1997, **17**, 3-8.
70. N. L. Ogihara, H. E. Parge, P. J. Hart, M. S. Weiss, J. J. Goto, B. R. Crane, J. Tsang, K. Slater, J. A. Roe, J. S. Valentine, D. Eisenberg and J. A. Tainer, *Biochemistry*, 1996, **35**, 2316-2321.
71. I. Bertini, M. Piccioli, M. S. Viezzoli, C. Y. Chiu and G. T. Mullenbach, *European Biophysics Journal*, 1994, **23**, 167-176.
72. H. X. Deng, A. Hentati, J. A. Tainer, Z. Iqbal, A. Cayabyab, W. Y. Hung, E. D. Getzoff, P. Hu, B. Herzfeldt, R. P. Roos and a. et, *Science*, 1993, **261**, 1047-1051.
73. L. M. Murphy, R. W. Strange and S. S. Hasnain, *Structure*, 1997, **5**, 371-379.
74. K. Djinovic, G. Gatti, A. Coda, L. Antolini, G. Pelosi, A. Desideri, M. Falconi, F. Marmocchi, G. Rotilio and M. Bolognesi, *Journal of Molecular Biology*, 1992, **225**, 791-809.
75. A. L. Lamb, A. S. Torres, T. V. O'Halloran and A. C. Rosenzweig, *Nature Structural & Molecular Biology*, 2001, **8**, 751-755.
76. E. M. Fielden, P. B. Roberts, R. C. Bray, D. J. Lowe, G. N. Mautner, G. Rotilio and L. Calabrese, *Biochem J*, 1974, **139**, 49-60.
77. D. Klug-Roth, I. Fridovich and J. Rabani, *Journal of the American Chemical Society*, 1973, **95**, 2786-2790.
78. J. Rabani, D. Klug and I. Fridovich, *Israel Journal of Chemistry*, 1972, **10**, 1095-1106.
79. V. V. Smirnov and J. P. Roth, *Journal of the American Chemical Society*, 2006, **128**, 16424-16425.
80. F. Arnesano, L. Banci, I. Bertini, M. Martinelli, Y. Furukawa and T. V. O'Halloran, *Journal of Biological Chemistry*, 2004, **279**, 47998-48003.
81. L. Banci, L. Barbieri, I. Bertini, F. Cantini and E. Luchinat, *PLoS ONE*, 2011, **6**, e23561.
82. L. Banci, L. Barbieri, I. Bertini, E. Luchinat, E. Secci, Y. Zhao and A. R. Aricescu, *Nature Chemical Biology*, 2013, **9**, 297-299.
83. L. Banci, I. Bertini, F. Cantini, T. Kozyreva, C. Massagni, P. Palumaa, J. T. Rubino and K. Zovo, *Proceedings of the National Academy of Sciences*, 2012, **109**, 13555-13560.
84. C. Hwang, A. J. Sinskey and H. F. Lodish, *Science*, 1992, **257**, 1496-1502.
85. Y. Furukawa, A. S. Torres and T. V. O'Halloran, *European Molecular Biology Organization Journal*, 2004, **23**, 2872-2881.
86. L. J. Haverkamp, V. Appel and S. H. Appel, *Brain : a journal of neurology*, 1995, **118 (Pt 3)**, 707-719.
87. D. R. Rosen, T. Siddique, D. Patterson, D. A. Figlewicz, P. Sapp, A. Hentati, D. Donaldson, J. Goto, J. P. O'Regan, H. X. Deng and et al., *Nature*, 1993, **362**, 59-62.
88. H. X. Deng, A. Hentati, J. A. Tainer, Z. Iqbal, A. Cayabyab, W. Y. Hung, E. D. Getzoff, P. Hu, B. Herzfeldt, R. P. Roos and et al., *Science*, 1993, **261**, 1047-1051.
89. L. I. Bruijn, M. K. Houseweart, S. Kato, K. L. Anderson, S. D. Anderson, E. Ohama, A. G. Reaume, R. W. Scott and D. W. Cleveland, *Science*, 1998, **281**, 1851-1854.
90. E. J. Yoon, H. J. Park, G. Y. Kim, H. M. Cho, J. H. Choi, H. Y. Park, J. Y. Jang, H. S. Rhim and S. M. Kang, *Experimental & molecular medicine*, 2009, **41**, 611-617.
91. S. A. Ezzi, M. Urushitani and J. P. Julien, *J Neurochem*, 2007, **102**, 170-178.

92. A. L. Lamb, A. K. Wernimont, R. A. Pufahl, V. C. Culotta, T. V. O'Halloran and A. C. Rosenzweig, *Nature Structural & Molecular Biology*, 1999, **6**, 724-729.
93. T. Endo, T. Fujii, K. Sato, N. Taniguchi and J. Fujii, *Biochemical and Biophysical Research Communications*, 2000, **276**, 999-1004.
94. P. J. Schmidt, C. Kunst and V. C. Culotta, *Journal of Biological Chemistry*, 2000, **275**, 33771-33776.
95. K. Kirby, L. T. Jensen, J. Binnington, A. J. Hilliker, J. Ulloa, V. C. Culotta and J. P. Phillips, *Journal of Biological Chemistry*, 2008, **283**, 35393-35401.
96. J. Laliberté, L. J. Whitson, J. Beaudoin, S. P. Holloway, P. J. Hart and S. Labbé, *Journal of Biological Chemistry*, 2004, **279**, 28744-28755.
97. F. Arnesano, L. Banci, I. Bertini, D. L. Huffman and T. V. O'Halloran, *Biochemistry*, 2001, **40**, 1528-1539.
98. A. L. Lamb, A. K. Wernimont, R. A. Pufahl, T. V. O'Halloran and A. C. Rosenzweig, *Biochemistry*, 2000, **39**, 1589-1595.
99. K. Djinovic, G. Gatti, A. Coda, L. Antolini, G. Pelosi, A. Desideri, M. Falconi, F. Marmocchi, G. Rolilio and M. Bolognesi, *Acta crystallographica. Section B, Structural science*, 1991, **47 (Pt 6)**, 918-927.
100. The UniProt Consortium, *Nucleic Acids Research*, 2017, **45**, D158-D169.
101. F. Sievers, A. Wilm, D. Dineen, T. J. Gibson, K. Karplus, W. Li, R. Lopez, H. McWilliam, M. Remmert, J. Söding, J. D. Thompson and D. G. Higgins, *Molecular Systems Biology*, 2011, **7**.
102. A. L. Caruano-Yzermans, T. B. Bartnikas and J. D. Gitlin, *Journal of Biological Chemistry*, 2006, **281**, 13581-13587.
103. S. Allen, A. Badarau and C. Dennison, *Biochemistry*, 2012, **51**, 1439-1448.
104. P. J. Schmidt, T. D. Rae, R. A. Pufahl, T. Hamma, J. Strain, T. V. O'Halloran and V. C. Culotta, *Journal of Biological Chemistry*, 1999, **274**, 23719-23725.
105. A. C. Rosenzweig, *Accounts of Chemical Research*, 2000, **34**, 119-128.
106. T. D. Rae, A. S. Torres, R. A. Pufahl and T. V. O'Halloran, *Journal of Biological Chemistry*, 2001, **276**, 5166-5176.
107. G. S. A. Wright, S. S. Hasnain and J. G. Grossmann, *Biochemical Journal*, 2011, **439**, 39-44.
108. A. C. Rosenzweig, D. L. Huffman, M. Y. Hou, A. K. Wernimont, R. A. Pufahl and T. V. O'Halloran, *Structure*, 1999, **7**, 605-617.
109. D. Fu, T. J. Beeler and T. M. Dunn, *Yeast*, 1995, **11**, 283-292.
110. L. Banci, I. Bertini, S. Ciofi-Baffoni, D. L. Huffman and T. V. O'Halloran, *Journal of Biological Chemistry*, 2001, **276**, 8415-8426.
111. F. Arnesano, L. Banci, I. Bertini, S. Ciofi-Baffoni, E. Molteni, D. L. Huffman and T. V. O'Halloran, *Genome Research*, 2002, **12**, 255-271.
112. M. E. Portnoy, A. C. Rosenzweig, T. Rae, D. L. Huffman, T. V. O'Halloran and V. C. Culotta, *Journal of Biological Chemistry*, 1999, **274**, 15041-15045.
113. A. K. Wernimont, D. L. Huffman, A. L. Lamb, T. V. O'Halloran and A. C. Rosenzweig, *Nature Structural Molecular Biology*, 2000, **7**, 766-771.
114. D. L. Huffman and T. V. O'Halloran, *Journal of Biological Chemistry*, 2000, **275**, 18611-18614.
115. C. Vulpe, B. Levinson, S. Whitney, S. Packman and J. Gitschier, *Nature Genetics*, 1993, **3**, 7-13.
116. L. B. Moller, M. Mogensen and N. Horn, *Biochimie*, 2009, **91**, 1273-1277.
117. J. H. Menkes, M. Alter, G. K. Steigleder, D. R. Weakley and J. H. Sung, *Pediatrics*, 1962, **29**, 764-779.
118. S. G. Kaler, *Advances in pediatrics*, 1994, **41**, 263-304.
119. P. C. Bull, G. R. Thomas, J. M. Rommens, J. R. Forbes and D. W. Cox, *Nature Genetics*, 1993, **5**, 327-337.
120. A. Ala, A. P. Walker, K. Ashkan, J. S. Dooley and M. L. Schilsky, *The Lancet*, 2007, **369**, 397-408.

121. S. Chillappagari, M. Miethke, H. Trip, O. P. Kuipers and M. A. Marahiel, *Journal of Bacteriology*, 2009, **191**, 2362-2370.
122. A. El Ghazouani, A. Baslé, S. J. Firbank, C. W. Knapp, J. Gray, D. W. Graham and C. Dennison, *Inorganic Chemistry*, 2011, **50**, 1378-1391.
123. H. J. Kim, D. W. Graham, A. A. DiSpirito, M. A. Alterman, N. Galeva, C. K. Larive, D. Asunskis and P. M. A. Sherwood, *Science*, 2004, **305**, 1612-1615.
124. F. W. Outten, D. L. Huffman, J. A. Hale and T. V. O'Halloran, *Journal of Biological Chemistry*, 2001, **276**, 30670-30677.
125. C. Rensing, B. Fan, R. Sharma, B. Mitra and B. P. Rosen, *Proceedings of the National Academy of Sciences*, 2000, **97**, 652-656.
126. G. Grass and C. Rensing, *Biochemical and Biophysical Research Communications*, 2001, **286**, 902-908.
127. J. V. Stoyanov, J. L. Hobman and N. L. Brown, *Molecular Microbiology*, 2001, **39**, 502-512.
128. L. Banci, I. Bertini, R. Del Conte, J. Markey and F. J. Ruiz-Dueñas, *Biochemistry*, 2001, **40**, 15660-15668.
129. P. A. Cobine, L. D. Ojeda, K. M. Rigby and D. R. Winge, *Journal of Biological Chemistry*, 2004, **279**, 14447-14455.
130. Z. Xiao and A. G. Wedd, *Chemical Communications*, 2002, **0**, 588-589.
131. L. T. Jensen and V. C. Culotta, *Journal of Biological Chemistry*, 2005, **280**, 41373-41379.
132. J. M. Leitch, L. T. Jensen, S. D. Bouldin, C. E. Outten, P. J. Hart and V. C. Culotta, *Journal of Biological Chemistry*, 2009, **284**, 21863-21871.
133. M. C. Carroll, J. B. Girouard, J. L. Ulloa, J. R. Subramaniam, P. C. Wong, J. S. Valentine and V. C. Culotta, *Proceedings of the National Academy of Sciences of the United States of America*, 2004, **101**, 5964-5969.
134. J. P. Stasser, G. S. Siluvai, A. N. Barry and N. J. Blackburn, *Biochemistry*, 2007, **46**, 11845-11856.
135. J. P. Stasser, J. F. Eisses, A. N. Barry, J. H. Kaplan and N. J. Blackburn, *Biochemistry*, 2005, **44**, 3143-3152.
136. Z. Xiao and A. G. Wedd, *Natural Product Reports*, 2010, **27**, 768-789.
137. L. Banci, I. Bertini, S. Ciofi-Baffoni, T. Kozyreva, K. Zovo and P. Palumaa, *Nature*, 2010, **465**, 645-648.
138. Z. Xiao, J. Brose, S. Schimo, S. M. Ackland, S. La Fontaine and A. G. Wedd, *Journal of Biological Chemistry*, 2011, **286**, 11047-11055.
139. A. Badarau and C. Dennison, *Journal of the American Chemical Society*, 2011, **133**, 2983-2988.
140. S. Allen, A. Badarau and C. Dennison, *Dalton Transactions*, 2013, **42**, 3233-3239.
141. Z. Xiao, F. Loughlin, G. N. George, G. J. Howlett and A. G. Wedd, *Journal of the American Chemical Society*, 2004, **126**, 3081-3090.
142. A. Kr zel, W. Lesniak, M. Jezowska-Bojczuk, P. Mlynarz, J. Brasun, H. Kozlowski and W. Bal, *J Inorg Biochem*, 2001, **84**, 77-88.
143. Z. Xiao, P. S. Donnelly, M. Zimmermann and A. G. Wedd, *Inorganic Chemistry*, 2008, **47**, 4338-4347.
144. P. Bagchi, M. T. Morgan, J. Bacsa and C. J. Fahrni, *Journal of the American Chemical Society*, 2013, **135**, 18549-18559.
145. C. T. Chung, S. L. Niemela and R. H. Miller, *Proceedings of the National Academy of Sciences*, 1989, **86**, 2172-2175.
146. P. W. Riddles, R. L. Blakeley and B. Zerner, *Analytical Biochemistry*, 1979, **94**, 75-81.
147. A. Badarau and C. Dennison, *Proceedings of the National Academy of Sciences*, 2011, **108**, 13007-13012.
148. F. Frottin, A. Martinez, P. Peynot, S. Mitra, R. C. Holz, C. Giglione and T. Meinnel, *Molecular & Cellular Proteomics*, 2006, **5**, 2336-2349.

149. R. W. Woody, in *Methods in Enzymology*, Academic Press, 1995, vol. 246, pp. 34-71.
150. S. M. Kelly, T. J. Jess and N. C. Price, *Biochimica et Biophysica Acta (BBA) - Proteins and Proteomics*, 2005, **1751**, 119-139.
151. I. Gokce, R. W. Woody, G. Anderluh and J. H. Lakey, *Journal of the American Chemical Society*, 2005, **127**, 9700-9701.
152. A. Hörnberg, D. T. Logan, S. L. Marklund and M. Oliveberg, *Journal of Molecular Biology*, 2007, **365**, 333-342.
153. P. A. Doucette, L. J. Whitson, X. Cao, V. Schirf, B. Demeler, J. S. Valentine, J. C. Hansen and P. J. Hart, *Journal of Biological Chemistry*, 2004, **279**, 54558-54566.
154. T. Tsukihara, H. Aoyama, E. Yamashita, T. Tomizaki, H. Yamaguchi, K. Shinzawa-Itoh, R. Nakashima, R. Yaono and S. Yoshikawa, *Science*, 1996, **272**, 1136-1144.
155. N. I. f. H. a. C. Excellence, 2001, TA20.
156. R. G. Miller, J. D. Mitchell and D. H. Moore, *Cochrane Database of Systematic Reviews*, 2012, DOI: 10.1002/14651858.CD001447.pub3.
157. A.-S. Yang, M. R. Gunner, R. Sampogna, K. Sharp and B. Honig, *Proteins: Structure, Function, and Bioinformatics*, 1993, **15**, 252-265.
158. A. S. Torres, V. Petri, T. D. Rae and T. V. O'Halloran, *Journal of Biological Chemistry*, 2001, **276**, 38410-38416.
159. J. F. Eisses, J. P. Stasser, M. Ralle, J. H. Kaplan and N. J. Blackburn, *Biochemistry*, 2000, **39**, 7337-7342.
160. J. M. Leitch, P. J. Yick and V. C. Culotta, *The Journal of biological chemistry*, 2009, **284**, 24679-24683.
161. L. Zhou, C. Singleton and Nick E. Le Brun, *Biochemical Journal*, 2008, **413**, 459-465.
162. M. E. Portnoy, A. C. Rosenzweig, T. Rae, D. L. Huffman, T. V. O'Halloran and V. C. Culotta, *J Biol Chem*, 1999, **274**, 15041-15045.
163. M. E. Portnoy, P. J. Schmidt, R. S. Rogers and V. C. Culotta, *Molecular genetics and genomics : MGG*, 2001, **265**, 873-882.